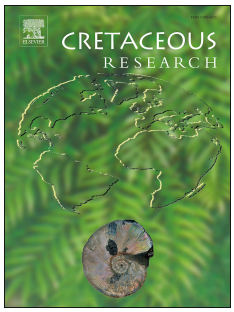

Patterns of planktonic foraminiferal extinctions and eclipses during Oceanic Anoxic Event 2 at Eastbourne (SE England) and other mid-low latitude locations

Francesca Falzoni, Maria Rose Petrizzo

PII: S0195-6671(20)30279-2

DOI: https://doi.org/10.1016/j.cretres.2020.104593

Reference: YCRES 104593

To appear in: *Cretaceous Research*

Received Date: 25 March 2020

Revised Date: 21 July 2020

Accepted Date: 26 July 2020

Please cite this article as: Falzoni, F., Petrizzo, M.R., Patterns of planktonic foraminiferal extinctions and eclipses during Oceanic Anoxic Event 2 at Eastbourne (SE England) and other mid-low latitude locations, *Cretaceous Research*, https://doi.org/10.1016/j.cretres.2020.104593.

Patterns of planktonic foraminiferal extinctions and eclipses during Oceanic Anoxic Event 2 at Eastbourne (SE England) and other mid-low latitude locations

Francesca Falzoni[a]*, Maria Rose Petrizzo[a]

[a]Dipartimento di Scienze della Terra "A. Desio", via Mangiagalli 34, 20133 Milano, Italy

*corresponding author: F. Falzoni

E-mail: F. Falzoni (francesca.falzoni1@gmail.com), M.R. Petrizzo (mrose.petrizzo@unimi.it)

Abstract

The latest Cenomanian Oceanic Anoxic Event (OAE) 2 represents one of the most extreme perturbations of the global carbon cycle. Planktonic foraminiferal events, variations in the taxonomic composition of assemblages (e.g., appearances, extinctions, temporary crisis of certain taxa) and their correlation with changes in the physico-chemical properties of surface waters are essential to reconstructing the consequences of OAE 2 on this group of calcareous microfossils.

We present the results of a high-resolution biostratigraphic and taxonomic study of planktonic foraminifera performed at Eastbourne (SE England), representing the most expanded, complete and well-calibrated OAE 2 record in Europe.

In this stratigraphic section, we identify a sequence of step-wise extinctions (i.e., *Thalmanninella* and *Rotalipora* species, and "*Globigerinelloides*" *bentonensis*) that are followed by an eclipse (temporary disappearance) of planispiral taxa and of hedbergellids

with clavate chambers. These events are consistently found in approximately coeval stratigraphic intervals across low to mid-latitudes, suggesting that they were controlled by wide-scale environmental perturbations. Moreover, this study suggests that the extinction of rotaliporids might have been influenced by climate changes (i.e., warming for *Thalmanninella* and cooling during the Plenus Cold Event for *Rotalipora*) at the onset of OAE 2, whereas the eclipse of planispiral taxa and hedbergellids with clavate chambers during the second half of OAE 2 was likely related to enhanced productivity and mixing of surface waters potentially associated to warming after the PCE for planispirals.

Finally, we identify two short-range species (*Muricohedbergella kyphoma* and *Praeglobotruncana plenusiensis* n. sp.) that co-occur with boreal macrofossils at Eastbourne and might represent the first evidence for a planktonic foraminiferal PCE fauna. The long ranging species *Praeglobotrucana gungardensis* n. sp. is described as new.

Keywords: planktonic foraminifera; Oceanic Anoxic Event 2; Cenomanian–Turonian Boundary Interval; Plenus Cold Event; extinctions; eclipses.

1. Introduction

The latest Cenomanian-earliest Turonian Oceanic Anoxic Event 2 is a perturbation of the global carbon cycle evidenced by a synchronous positive $\delta^{13}C$ excursion of marine and terrestrial records and resulting from the burial of large amounts of organic matter in deep-sea and hemipelagic settings (e.g., Schlanger and Jenkyns, 1976; Scholle and Arthur, 1980; Schlanger et al., 1987; Jenkyns, 2010; Jenkyns et al., 2017).

Previous studies have suggested that intense submarine volcanic activity likely related to the emplacement of the Caribbean Large Igneous Province injected greenhouse gases and biolimiting metals in marine ecosystems leading to the onset of the Cenomanian–Turonian thermal maximum and enhancement of ocean fertility (e.g., Larson, 1991; Kuypers et al., 2002; Leckie et al., 2002; Erba, 2004; Pancost et al., 2004; Kuroda et al., 2007; Turgeon and Creaser, 2008; Barclay et al., 2010). These environmental perturbations certainly influenced the evolutionary history of planktonic organisms (e.g., Erbacher et al., 1996; Leckie et al., 2002; Erba, 2004; Pearce et al., 2009).

Planktonic foraminifera underwent a turnover across the Cenomanian–Turonian boundary interval with the isochronous extinction of several single-keeled rotaliporids at the onset of OAE 2 and the more gradational evolution and diversification of partially (*Praeglobotruncana*), double- and single-keeled (*Dicarinella* and *Marginotruncana*) taxa (e.g., Premoli Silva and Sliter, 1995, 1999; Hart, 1999), resulting in a biostratigraphically-relevant sequence of events that can be used to improve the resolution of the current biostratigraphic schemes and the accuracy of correlations. Moreover, planktonic foraminifera are often absent in the organic-rich layers deposited during OAE 2, or they are indicative of reduced thermal stratification and increased sea-surface productivity (Leckie, 1985, 1987; Leary et al., 1989; Lamolda et al., 1997; Leckie et al., 1998, 2002; Huber et al., 1999; Nederbragt and Fiorentino, 1999; Paul et al., 1999; Keller et al., 2001, 2008; Keller and Pardo, 2004; Caron et al., 2006; Coccioni et al., 2006; Grosheny et al., 2006, 2013; Kalanat and Vaziri-Moghaddam, 2019, among many others).

The Eastbourne section at Gun Gardens (SE England) encompasses the most expanded record of the Cenomanian–Turonian transition of the English Chalk and it has been proposed as the European reference section for the C/T boundary due to the completeness of its stratigraphic record and richness in the micro- and macrofossil content (Paul et al., 1999). Planktonic foraminifera have been the subject of several studies (Paul

et al., 1999; Keller et al., 2001; Hart et al., 2002; Tsikos et al., 2004). However, significant discrepancies still exist in the stratigraphic position of primary and secondary markers including the lowest occurrence (LO) of *Helvetoglobotruncana helvetica*, the secondary marker for the base of the Turonian Stage (Kennedy et al., 2005).

The record at Eastbourne is herein restudied at high-resolution with the aim of reconstructing the sequence of planktonic foraminiferal events and their response to the environmental perturbations related to OAE 2 within a highly-resolved bio- and chemostratigraphic record (after Paul et al., 1999; Tsikos et al., 2004; Gale et al., 2005; Jarvis et al., 2006; Pearce et al., 2009; Linnert et al., 2011). Innovation of the present study includes: 1) an implemented methodology to process lithified chalky samples with acetic acid (after Lirer, 2000) that improves species determinations and 2) the application of the most recent revisions of the taxonomy and phylogeny of Cenomanian–Turonian planktonic foraminifera (e.g., Hasegawa, 1999; González-Donoso et al., 2007; Desmares et al., 2007, 2008, 2020; Huber and Petrizzo, 2014; Haynes et al., 2015; Petrizzo et al., 2015; Falzoni et al., 2016a; Huber et al., 2017).

The synchronicity and reliability for correlation of the planktonic foraminiferal events identified during this study were presented in Falzoni et al. (2018). Here we discuss the stratigraphic ranges of relevant taxa and their potential relationship with the environmental changes that occurred during OAE 2. Moreover, we highlight the occurrence of poorly documented morphotypes that seem particularly promising for paleoenvironmental reconstructions.

The sequence of planktonic foraminiferal events identified at Eastbourne is compared to that documented across other complete OAE 2 records at low to mid-latitudes (Pont d'Issole: Grosheny et al., 2006; Clot Chevalier: Falzoni et al., 2016a, SE France; Ganuza, Spain: Lamolda et al., 1997; Tarfaya, Core S57, Morocco: Tsikos et al., 2004, Falzoni et al., 2018 and this study; Lar Anticline, Iran: Kalanat and Vaziri-Moghaddam, 2019; Pueblo,

Colorado: Leckie, 1985, Leckie et al. 1998; Keller and Pardo, 2004; Caron et al., 2006; Desmares et al., 2007, 2008; Elderbak and Leckie, 2016) (Fig. 1) with the aim to understand if planktonic foraminifera experienced common and synchronous variations in the taxonomic composition of assemblages and if these variations resulted from local or wider scale environmental perturbations.

2. Materials and methods

Several studies were dedicated to the stratigraphy of southern England and a detailed litho-, bio- and chemostratigraphic framework is available for the Cenomanian–Turonian Boundary Interval (e.g., Jefferies, 1962,1963; Gale et al., 1993, 2000, 2005; Lamolda et al., 1994; Paul et al., 1999; Keller et al., 2001; Hart et al., 2002; Tsikos et al., 2004; Jarvis et al., 2006, 2011; Pearce et al., 2009; Linnert et al., 2011; Falzoni et al., 2018).

The examined section at Gun Gardens is 27 m-thick and consists of 6 m of greyish rhythmically bedded chalks assigned to the Grey Chalk Mbr. (Fig. 2). A strongly burrowed omission surface (Sub-Plenus erosion surface; Jefferies, 1962, 1963) separates the Grey Chalk from the overlying Plenus Marl Mbr. and corresponds to a major sea-level fall and sequence boundary (Gale, 1996; Wilmsen, 2003; Pearce et al., 2009). The Plenus Marl Mbr. is a distinctive greenish marly unit pinched in between the two thick carbonate-rich successions of the Grey Chalk Mbr. and White Chalk Fm. and crops out at Gun Gardens with the maximum thickness (8 m) found in the Anglo-Paris Basin (Gale et al., 2005). Jefferies (1962, 1963) distinguished 8 beds within the Plenus Marl, based on their lithological features and paleontological content. The name of the member derives from the boreal belemnite *Praeactinocamax plenus* that was found from the top of Bed 3 to Bed 8, but with maximum abundance in Bed 4 (Gale and Christensen, 1996; Paul et al., 1999; Gale et al., 2000). Plenus Marl Beds 7 and 8 are lithologically transitional to the overlying

Ballard Cliff Mbr., a 4.5 m-thick white calcisphere-rich nodular chalk intercalated with thin marly layers (Gale et al., 2005). The overlying Holywell Mbr. is a pure white chalk intercalated with thin marly layers.

A total of 97 samples were studied for planktonic foraminifera with a resolution of 20 to 40 cm. Rock samples from the Plenus Marl were processed with a solution of peroxide water to obtain washed residues. Rock samples from the Grey Chalk, Ballard Cliff and Holywell Members were processed with acetic acid following the methodology by Lirer (2000) (see Falzoni et al., 2016a for detailed procedure). All size fractions >38 μm were carefully screened for the identification of planktonic foraminifera, in order to detect rare and small-sized species.

Planktonic foraminiferal type specimens illustrated in this study were obtained from the database for Mesozoic Planktonic Foraminifera "PF@mikrotax" available at http://www.mikrotax.org/pforams/index.html (see Huber et al., 2016). The type specimens of *Pseudoclavihedbergella simplicissima* (Magné and Sigal, 1954) and *Whiteinella paradubia* (Sigal, 1952) were photographed by using a stereomicroscope equipped with a digital camera and an ESEM at the Muséum National d'Histoire Naturelle in Paris (France). Following the policy of the museum, holotypes were exclusively photographed using the stereomicroscope to decrease the likelihood to damage or lose primary types. Other specimens illustrated in this study were photographed using the SEM at the Department of Earth Sciences of the University of Milan (Italy).

The taxonomic concepts applied for the identification of species follow their original descriptions and illustrations and the database "PF@mikrotax" (see Huber et al., 2016) and Falzoni et al. (2016a), unless specified otherwise. The taxonomy of noteworthy species is discussed in the Systematic Taxonomy section. Other species are listed in the Taxonomic Appendix with a brief explanation of the species concept applied in this study.

The relative abundances of planktonic foraminiferal species identified at Eastbourne are included in Appendix A. Supplementary data.

3. Overview of previous studies

3.1 Planktonic foraminiferal zones

The extinction of the late Cenomanian marker species *R. cushmani* in the Gun Gardens section is identified at 11.4 m (within Plenus Marl Bed 4) and defines the top of the nominate zone (Fig. 2). The overlying stratigraphic interval is entirely assigned to the uppermost Cenomanian–lowermost Turonian *Whiteinella archaeocretacea* Zone based on the absence of *Rotalipora cushmani* and *Helvetoglobotruncana helvetica* and following the tropical biozonation by Robaszynski and Caron (1995). This zonal assignment is in agreement with previous studies by Paul et al. (1999) and Tsikos et al. (2004). However, the occurrence of *H. helvetica* in the English Chalk is reported from few cm to several m above the C/T boundary (e.g., Jarvis et al., 1988; Hart and Leary, 1989; Keller et al., 2001; Hart et al., 2002) as defined by ammonite and chemostratigraphy (e.g., Gale et al., 1993; Kennedy et al., 2005; Jarvis et al., 2006). Such discrepancies likely result from inconsistencies in the taxonomic concepts applied by different authors, from its very rare occurrence at the base of its stratigraphic distribution, and from the poor preservation of planktonic foraminifera in some intervals of the White Chalk Fm. or from a combination of these causes (see Huber and Petrizzo, 2014 and Falzoni et al., 2018 for further details).

3.2 Identification of peak C on the $\delta^{13}C$ profile

The striking similarities in the shape of the carbon isotope excursion observed in different sections across the C/T boundary enable the identification of three positive peaks

that have been usually named A, B and C (after Jarvis et al., 2006), although different criteria and nomenclatures have been adopted over the years (see Falzoni et al., 2018 for a brief overview). Peaks are usually objectively recognizable when constrained by biostratigraphic datums, and when the carbon isotope record is highly resolved and diagenetic alteration did not affect the primary signal. At Eastbourne, however, peak C has been placed either at the top of the Ballard Cliff (Voigt et al., 2008) or at the base of the Holywell Mbr. (Jarvis et al., 2006). The graphic correlation (depth-depth plot) between the GSSP section for the base of the Turonian Stage at Pueblo (Colorado; Kennedy et al., 2005) and Eastbourne provides a higher correlation coefficient when considering peak C at the top of the Ballard Cliff Mbr. according to Voigt et al. (2008) (see Falzoni et al., 2018) and this option has been adopted in this study.

3.3 The Cenomanian–Turonian climate and the Plenus Cold Event (PCE)

The climate evolution during the middle–Late Cretaceous is relatively well constrained. The Cenomanian was likely characterized by increasing sea-surface temperatures that reached maximum values during the early Turonian (e.g., Pearce et al., 2009; MacLeod et al., 2013; O'Brien et al., 2017; Huber et al., 2018). In this interval, estimated pCO_2 levels were about 1300 ppmv (Sinninghe Damsté et al., 2008) and surface-ocean temperatures reached ~36 ℃ in the tropical and equatorial latitudinal belts (Forster et al., 2007; MacLeod et al., 2013) or were even higher (O'Brien et al., 2017).

The rising temperature trend was only interrupted by a transient cooling episode in the latest Cenomanian. The first evidence for a cold snap arose with the identification of a macrofossil fauna (i.e., belemnites including the species *Praeactinocamax plenus*, brachiopods, bivalves, serpulids) with strong boreal affinities in Bed 2 and 4 to 8 of the Plenus Marl (Jefferies, 1962, 1963) at Eastbourne and nearby sections (e.g., Dover). The macrofossil fauna is particularly abundant and diverse in Bed 4 suggesting that the

maximum cooling was reached during its deposition (Jefferies, 1962; Gale and Christensen, 1996; Paul et al., 1999). Gale and Christensen (1996) found *P. plenus* in correlative beds of the Vocontian Basin indicating that cooling reached further south into the subtropics and named this episode “Plenus Cold Event”.

The southward migration of endemic boreal macrofossil species (e.g., Jefferies, 1962, 1963; Jeans et al., 1991; Gale and Christensen, 1996; Paul et al., 1999; Wilmsen et al., 2010) is associated with additional biotic evidences for cooling, including the equatorward migration of boreal dinoflagellate cysts (van Helmond et al., 2016), a decreased frequency of stomata on plant leaves (Barclay et al., 2010), and the proliferation of a cold and less humid savanna-type vegetation (Heimhofer et al., 2018). Oxygen isotopes measured on bulk carbonates and macrofossil shells, $\Delta\delta^{13}C_{carb\text{-}org}$ and TEX_{86} values (e.g., Paul et al., 1999; Tsikos et al., 2004; Voigt et al., 2006, 2008; Forster et al., 2007; Sinninghe Damsté et al., 2010; Jarvis et al., 2011; Elderbak and Leckie, 2016; Jenkyns et al., 2017; Kuhnt et al., 2017; Gale et al., 2019; O’Connor et al., 2020) provide robust evidence for cooling, increasing latitudinal temperature gradients and decreasing atmosphere pCO_2 levels in several North European Basins, in the Western Interior Seaway (WIS) and in the north to equatorial Atlantic Ocean, although the timing and magnitude of cooling might have been controlled by local factors (O’Connor et al., 2020). Moreover, changes in the sea-surface circulation patterns and an increased diversity of benthic foraminifera are documented in the same stratigraphic interval in the WIS (i.e., “Benthonic Zone”: Eicher and Worstell, 1970; Eicher and Diner, 1985; Leckie, 1985; Elderbak and Leckie, 2016; Eldrett et al., 2017; Boudinot et al., 2020).

No evidence for cooling is currently available for the Southern Hemisphere, where, however, the record of the Cenomanian–Turonian boundary interval is often incomplete and/or compromised by diagenetic alteration (e.g., Falkland Plateau: Huber, 1992; Kerguelen Plateau: Petrizzo, 2001; Exmouth Plateau: Falzoni et al., 2016b; Tanzania:

Jiménez Berrocoso et al., 2015). For this reason, a reliable reconstruction of the timing, magnitude and extent of cooling during the PCE requires further study.

4. Results

4.1 Assemblage composition and planktonic foraminiferal events

Planktonic foraminiferal specimens are generally moderately to well-preserved in the Grey Chalk and Plenus Marl. Several specimens show little evidence for recrystallization of the wall texture, but all have calcite infilling. The preservation decreases in the lower part of the Ballard Cliff Mbr., where foraminifera show a strongly recrystallized wall, increases in the upper part of the Ballard Cliff and remains quite good in the Holywell Mbr. (Fig. 2).

Planktonic foraminiferal assemblages show a relatively similar composition in the Grey Chalk and Plenus Marl, where the large-sized (>125 μm) assemblages are dominated by hedbergellids (muricate and with radially elongated chambers), whiteinellids, and by *R. cushmani* up to its extinction level, while *Praeglobotruncana*, *Dicarinella,* and *Marginotruncana* are generally rare to frequent, but they occasionally show a moderate increase in abundance (Fig. 2). *Thalmanninella* and "*Globigerinelloides"* always represent a minor component of the assemblage. The small size fraction (<125 μm) is mostly composed of hedbergellids (muricate and non-muricate), biserial, triserial, and planispiral taxa, but other small-sized microfossils occur abundantly, including calcispheres and inoceramid prisms.

Planktonic foraminifera are less diverse in the White Chalk and the assemblages are dominated by whiteinellids and muricate hedbergellids. *Praeglobotruncana*, *Dicarinella,* and *Marginotruncana* are generally rare to very rare and most species show a

discontinuous stratigraphic distribution (Fig. 2). Hedbergellids and biserial taxa occur frequently to commonly in the small-size fraction (<125 μm), although calcispheres and inoceramid prisms represent the dominant component of the small-sized assemblage.

Four biostratigraphically relevant events (lowest occurrences, LOs) are recognized in the Grey Chalk Mbr., as listed below in stratigraphic order from bottom to top: the LOs of *Marginotruncana* cf. *sigali* at 0.8 m, *Dicarinella* cf. *primitiva* at 1.6 m, *Dicarinella canaliculata* at 3.2 m, and *Dicarinella marianosi* (= *Dicarinella elata* in Falzoni et al., 2018; see Huber et al., 2017) at 4.0 m (Fig. 2).

Eight biostratigraphic events are identified in the Plenus Marl. The extinctions (highest occurrences, HOs) of *Thalmanninella* species are recognized in Bed 1 as follows: *Thalmanninella* cf. *brotzeni* and *Thalmanninella brotzeni* (at 7.2 m), *Thalmanninella* cf. *greenhornensis* (at 7.6 m), *Thalmanninella deeckei* and *Thalmanninella greenhornensis* (at 8.2 m). The LO of *Praeglobotruncana oraviensis* is identified in the lower part of Bed 2 (at 8.8 m). This event is followed by the extinction of 3 species of the genus *Rotalipora* as follows: *Rotalipora montsalvensis* in the upper part of Bed 2 (at 9.2 m), *Rotalipora praemontsalvensis* in Bed 3 (at 10.0 m), and *R. cushmani* in the middle of Bed 4 (at 11.4 m). The HO of the planispiral species "*Globigerinelloides" bentonensis* is observed in Bed 7 (at 13.0 m) (Fig. 2).

Only one biostratigraphic event is identified in the White Chalk, i.e., the LO of *Dicarinella falsohelvetica* at 17.5 m (Fig. 2).

5. Discussion

5.1 Diversification of *Praeglobotruncana*, *Dicarinella* and *Marginotruncana*

The lowermost stratigraphic interval (0 to 6 m) at Eastbourne is characterized by a series of important lowest occurrences that suggests a pulse in the diversification of keeled taxa having raised (genus *Marginotruncana*) or depressed (genus *Dicarinella*) umbilical sutures (Fig. 2).

The LOs of *Marginotruncana* cf. *sigali* and of *Dicarinella* cf. *primitiva* were identified in the lowermost Turonian assemblages of the Vocontian Basin (Falzoni et al., 2016a), thus their occurrence in the Grey Chalk Mbr. at Eastbourne allows extension of their stratigraphic distributions to the upper Cenomanian *R. cushmani* Zone and below the onset of the $\delta^{13}C$ excursion (Fig. 2). The LOs of *Dicarinella canaliculata* and *Dicarinella marianosi* have been documented in different stratigraphic intervals across the C/T boundary at low to mid-latitudes and their appearance was regarded as diachronous and/or ecologically controlled (Falzoni et al., 2018). Their discontinuous stratigraphic distribution and rare occurrence at Eastbourne support this hypothesis.

Praeglobotruncana oraviensis was previously documented from lower Turonian assemblages (Scheibnerova, 1960; Falzoni et al., 2016a), thus its occurrence in the uppermost *R. cushmani* Zone at Eastbourne (Fig. 2) led to the extension of its stratigraphic distribution to the upper Cenomanian in agreement with the Crimea-Caucasus record, where the LO of *P. oraviensis* and the HO of *R. cushmani* are observed in the same sample (Kopaevich and Vishnevskaya, 2016). Desmares et al. (2020) reported specimens identified as *Praeglobotruncana* aff. *oraviensis* from the middle Cenomanian of the Anglo-Paris Basin that were interpreted as possible earlier representatives of this species. The unavailability of SEM images of *P. oraviensis* type specimens prevents a full comparison of shell features. However, the specimens illustrated by Desmares et al. (2020) differ from the drawing of the holotype of *P. oraviensis* by having a smaller umbilical area, a lower trochospire, and a less lobate equatorial periphery, and from the lower Turonian specimens of the Vocontian Basin (Falzoni et al., 2016a) and those identified in this study

by their weakly raised inner whorl. Nevertheless, a phyletic relationship between the specimens of *Praeglobotruncana* aff. *oraviensis* illustrated by Desmares et al. (2020) and *P. oraviensis* cannot be ruled out, because the reconstruction of the ancestor-descendant relationship among *Praeglobotruncana* species is complicated by the unavailability of continuous observations from mid- to upper Cenomanian sequences and by their morphologic plasticity in this stratigraphic interval.

The LO of *Dicarinella falsohelvetica* is the uppermost biostratigraphic event identified at Eastbourne (Fig. 2). This species was described from a coeval stratigraphic interval (*Neocardioceras juddii* ammonite Zone) in a French section (Mézières-sur-Ponthouin) of the Anglo-Paris Basin (Desmares et al., 2020). Its LO falls very close to the C/T boundary at Eastbourne, but its validity as biostratigraphic marker requires further investigation of its geographic distribution and synchronicity of its LO in different basins.

On a global scale, the appearance of *Praeglobotruncana*, *Dicarinella,* and *Marginotruncana* species is a long-term evolutionary phenomenon that started in the upper Albian and ended in the Santonian, and it has been related to phases of increased thermal stratification of surface waters (Premoli Silva and Sliter, 1999). Interestingly, the appearance of *P. oraviensis* in the uppermost Cenomanian is among the last speciation events known for praeglobotruncanids, although this group represented a significant component of the early–middle Turonian assemblages (e.g., Premoli Silva and Sliter, 1995, 1999). *Praeglobotruncana hilalensis* is commonly identified in the lower Turonian *H. helvetica* Zone (Petrizzo, 2000; Robaszynski et al., 2000), but it occurs from the upper Cenomanian *R. cushmani* Zone at Eastbourne (Fig. 2) and Clot Chevalier (Falzoni et al., 2016a), although it shows a scattered stratigraphic distribution and rare occurrence in this stratigraphic interval.

The appearance of *Dicarinella* is observed in the middle Cenomanian (Premoli Silva and Sliter, 1999; Fraass et al., 2015). This genus underwent a major diversification phase

during the late Cenomanian, as testified by the relatively high number of lowest occurrences (*D. hagni*, *D. imbricata*, *D. marianosi* and *D. canaliculata*) in the upper part of the *R. cushmani* Zone below the onset of OAE 2 (Premoli Silva and Sliter, 1995; Falzoni et al., 2018).

Our study suggests that the evolutionary history of the genus *Marginotruncana* started during the latest Cenomanian, contrary to what is commonly reported (e.g., Premoli Silva and Sliter, 1995, 1999; Fraass et al., 2015; Coccioni and Premoli Silva, 2015). However, *Marginotruncana* specimens are extremely rare and discontinuously present below the C/T boundary, and underwent a first major diversification phase only in the early Turonian (Premoli Silva and Sliter, 1999; Fraass et al., 2015).

5.2 Extinction of Cenomanian taxa

The record of planktonic foraminiferal extinctions at Eastbourne is compared with other low to mid-latitude sections including Pont d'Issole (Grosheny et al., 2006) and Clot Chevalier (Falzoni et al., 2016a) in SE France, Ganuza, Spain (Lamolda et al., 1997), Tarfaya, Morocco (core S57, Tsikos et al., 2004, Falzoni et al., 2018 and this study), Lar Anticline, Iran (Kalanat and Vaziri-Moghaddam, 2019), and Pueblo, Colorado (Leckie, 1985, Leckie et al. 1998; Keller and Pardo, 2004; Desmares et al., 2007, 2008; Elderbak and Leckie, 2016), with the aim to understand if extinctions were controlled by local conditions or if they resulted from wider scale environmental perturbations (Fig. 3).

The stratigraphic distribution of species in these sections is compared and traced by integrating available bio- and chemostratigraphic datums (see caption of Fig. 3 for further details). Correlation between Eastbourne and Lar Anticline (Iran) is herein reinterpreted with respect to Kalanat and Vaziri-Moghaddam (2019), according to the position of reliable

362 planktonic foraminiferal events (Falzoni et al., 2018) and because the PCE in this section
363 was recognized below the onset of the $\delta^{13}C$ excursion, implying that cooling and re-
364 oxygenation of bottom waters occurred significantly earlier in the Tethys compared to
365 basins at higher latitudes. We suggest that peak A as identified by Kalanat and Vaziri-
366 Moghaddam (2019) is actually peak B, whereas the position of peak A is not clear,
367 probably because the $\delta^{13}C$ curve is not sufficiently resolved or diagenesis masked the
368 primary signal. Nevertheless, the extinction of *Thalmanninella* species in this section is
369 unusually younger relative to the stratigraphic position of the PCE interval. Pending further
370 studies, we excluded the record of *Thalmanninella* in Iran from the discussions. All the
371 other events can be reliably correlated with Eastbourne using the position of peak B and
372 C.
373
374 5.2.1 Extinction of *Thalmanninella* species
375
376 The extinction of rotaliporids with curved and raised umbilical sutures at the beginning
377 of the last whorl (genus *Thalmanninella*) is observed within a very restricted stratigraphic
378 interval (60 cm) corresponding to the middle and upper Plenus Marl Bed 1 at Eastbourne
379 and it is correlative to the first $\delta^{13}C$ rise (Fig. 2).
380 To our knowledge, the occurrence of *T. brotzeni* in the uppermost Cenomanian at
381 Eastbourne represents one of the youngest records known for this species. This event is
382 not identified in the Vocontian Basin (Grosheny et al., 2006, 2017; Falzoni et al., 2016a),
383 Spain (Lamolda et al., 1997), Morocco (this study) and Pueblo (Leckie, 1985, Leckie et al.,
384 1998; Keller and Pardo, 2004; Desmares et al., 2007), but generally falls in older
385 stratigraphic intervals from the middle (Hasegawa, 1999; Westermann, 2010) to upper
386 Cenomanian (Leckie, 1984; Mort et al., 2007; Coccioni and Premoli Silva, 2015; Kalanat
387 and Vaziri-Moghaddam, 2019). Such discrepancies might derive from two causes: 1) *T.*

388 *brotzeni* is rare and discontinuous at the top of its stratigraphic distribution, therefore the
389 identification of its extinction level might rely on sampling resolution and size, and 2) there
390 are some inconsistencies on the published record of this species as it has been regarded
391 as a junior synonym of *T. globotruncanoides* by several authors (see discussion in
392 Petrizzo et al., 2015).

393 The extinctions of *T. deeckei* and *T. greenhornensis* are observed in the same sample
394 at Eastbourne, but the HO of the latter is consistently documented slightly above the HO of
395 the former species at low to mid-latitudes (Fig. 3). Both extinctions represent well-
396 documented isochronous events occurring slightly above the first $\delta^{13}C$ rise (Falzoni et al.,
397 2018 and this study), with three exceptions: 1) at Pueblo, where the HO of *T.*
398 *greenhornensis* is slightly delayed (above $\delta^{13}C$ peak A), 2) at Clot Chevalier, and 3) at
399 Ganuza where it falls in an earlier stratigraphic interval (Fig. 3). Its earlier disappearance in
400 the latter two localities likely results from the presence of a condensed stratigraphic
401 interval reducing the likelihood to detect rare species (Falzoni et al., 2016a) and from a
402 relatively low sampling resolution (1 sample/m), respectively.
403
404 5.2.2 Extinction of *Rotalipora* species
405
406 The extinction of rotaliporids with straight and depressed umbilical sutures (genus
407 *Rotalipora*) is observed across a 2.4 m-thick stratigraphic interval from Plenus Marl Bed 2
408 to 4 and is correlative with the first major positive $\delta^{13}C$ peak (peak A) at Eastbourne (Fig.
409 2).

410 *Rotalipora montsalvensis* is the first *Rotalipora* species that becomes extinct at
411 Eastbourne (Fig. 2). This event is not recognized in the other sections compared in Fig. 3.
412 Its extinction has been documented elsewhere in different stratigraphic intervals at the top

(González-Donoso et al. 2007) within (Tibet: Bomou et al., 2013) or below (Japan: Hasegawa, 1999) the *R. cushmani* Zone.

The extinction of *R. praemontsalvensis* slightly follows that of *R. montsalvensis* at Eastbourne (Fig. 2) and represents one of the youngest records known for this species. Specimens resembling the holotype of *R. praemontsalvensis* are documented from the top of the *R. cushmani* Zone in the Pueblo section (Fig. 3) and assigned to *Anaticinella multiloculata* s.l. (Morrow, 1934) (in Leckie, 1985), *Anaticinella planoconvexa* (Longoria, 1973) (in Caron et al., 2006), or *Rotalipora planoconvexa* (Longoria, 1973) (in Desmares et al., 2008) (see Systematic Taxonomy). This observation suggests that the extinction of *R. praemontsalvensis* might be slightly delayed (i.e., falling close to $\delta^{13}C$ peak B) in sections of the WIS.

The extinction level of *R. cushmani* is usually identified in between peak A and B (e.g., at Eastbourne [this study], Pont d'Issole [Grosheny et al., 2006] and Pueblo [Leckie, 1985, Keller and Pardo, 2004; Caron et al., 2006]) of the $\delta^{13}C$ profile (Figs. 2 and 3) and has been regarded as isochronous across several low to mid-latitude localities (Tsikos et al., 2004; Westermann et al., 2010; Falzoni et al., 2018). However, this study suggests that there are some exceptions. The HO of *R. cushmani* seems to be delayed in Spain (Lamolda et al., 1997), Morocco (Falzoni et al., 2018 and this study), and Iran (Kalanat and Vaziri-Moghaddam, 2019) (Fig. 3). The record of delayed extinction in Morocco might be biased by a possibly altered $\delta^{13}C_{org}$ profile of core S57 (Tarfaya) leading to some uncertainties in the position of peaks A and B (Falzoni et al., 2018). The delayed extinction at Ganuza seems supported by its identification above the HOs of the calcareous nannofossil species *Axopodorhabdus albianus* and *Lithraphidites acutus* (Lamolda et al., 1997), which are recognized at or above peak B in the most recent study of calcareous nannofossils at Eastbourne (Linnert et al., 2011) and at Clot Chevalier (Gale et al., 2019). However, discrepancies in the extinction levels of *A. albianus* and *L. acutus* reported in

different studies of the Eastbourne section (Paul et al., 1999; Tsikos et al., 2004; Linnert et al., 2011), possible reworking of calcareous nannofossils at Eastbourne and Clot Chevalier (Linnert et al., 2011; Gale et al., 2019), and diachronism of these events in many sections of the WIS (Corbett et al., 2014) complicate the interpretation of these data.

Finally, the HO of *R. cushmani* is recognized in an earlier stratigraphic interval at Clot Chevalier (Falzoni et al., 2016a), and it is slightly diachronous within different sections of the WIS (Leckie, 1985; Desmares et al., 2007; Lowery et al., 2014).

5.2.3 Extinction of "*Globigerinelloides*" *bentonensis*

The extinction of "*G.*" *bentonensis* is usually identified above the HO of *R. cushmani* between peaks A and B preceding the disappearance of the three other planispiral species that occur at Eastbourne (Fig. 2). This event is found in the same stratigraphic position at Clot Chevalier, and Pueblo (Fig. 3), and it has been regarded as possibly isochronous at low to mid-latitudes (Falzoni et al., 2018), with the exception of Morocco (Falzoni et al., 2018; this study), and Iran (Kalanat and Vaziri-Moghaddam, 2019), where its extinction is recognized slightly above peak B.

The extinction of "*G.*" *bentonensis* is not consistently recognized in all low to mid-latitude records, particularly when planktonic foraminifera are studied in thin section (e.g., Vocontian Basin: Grosheny et al., 2006, 2013; Tunisia: Caron et al., 2006; Tibet: Bomou et al., 2013), likely because of its rare occurrence at the top of its stratigraphic distribution.

5.3 The record of "*Globigerinelloides*", *Pseudoclavihedbergella* and *Pessagnoina simplex*

"*Globigerinelloides*" and *Pseudoclavihedbergella* species show relatively common occurrences and continuous stratigraphic distributions in the uppermost Cenomanian at Eastbourne, but they disappear from the assemblage close to peak B and C, respectively (Fig. 2). Pseudoclavihedbergellids re-occur at Eastbourne after a ~5 m-thick stratigraphic gap in their range (Fig. 2). The temporary disappearance of these taxa from the assemblage is herein referred to as eclipse (after Coccioni and Premoli Silva, 1994; Coccioni and Luciani, 2004, 2005) (Fig. 2).

The stratigraphic distribution of planispiral taxa and hedbergellids with radially elongated chambers (*Pseudoclavihedbergella* spp. and *Pessagnoina simplex*) across low to mid-latitudes is compared in Fig. 3 and discussed below.

5.3.1 The record of "*Globigerinelloides*"

The HO of "*G." bentonensis* is followed by the step-wise disappearance of three other planispiral species at Eastbourne (Fig. 2). *"Globigerinelloides" ultramicrus* disappears in Plenus Marl Bed 8 (at 14.0 m), and *"G."* cf. *bollii* and *"G." tururensis* disappear in the lowermost Ballard Cliff Mbr. (at 14.3 m and at 15.1 m, respectively) (Fig. 2). Specimens resembling *"G."* cf. *bollii* have never been illustrated in the literature from the C–T boundary interval, while *"G." tururensis* was described from the Albian–Cenomanian Gautier Fm. of Trinidad (Brönnimann, 1952) and later overlooked in the literature (see Systematic Taxonomy). Therefore, the stratigraphic range of both morphotypes is poorly constrained.

Overall, planispiral species are not documented above the HO of *"G." bentonensis* in the uppermost Cenomanian–lower Turonian in other sections of the Anglo-Paris Basin (Hart et al., 1993; Desmares et al., 2020). In the Vocontian Basin, *"G." ultramicrus* is not recognized in the stratigraphic interval from below peak B to below (Clot Chevalier: Falzoni

et al., 2016a) or above peak C (Pont d'Issole: Grosheny et al., 2006) and it is rare and of small size (<125 μm) when it reappears in the record (Fig. 3).

Planispiral species disappear from the assemblages slightly above peak B in Spain (Lamolda et al., 1997), Morocco (this study), Iran (Kalanat and Vaziri-Moghaddam, 2019), and Pueblo (Leckie, 1985; Keller and Pardo, 2004; Elderbak and Leckie, 2016) as observed at Eastbourne. However, they reappear close to peak C in Morocco and at Pueblo, but they show a scattered distribution and rare occurrence (Fig. 3).

The temporary disappearance of "*Globigerinelloides"* in the uppermost Cenomanian-lowermost Turonian is also documented in other localities (e.g., Tunisia: Nederbragt and Fiorentino, 1999; Austria: Gebhardt et al., 2010).

5.3.2 The record of *Pseudoclavihedbergella* and *Pessagnoina simplex*

Pseudoclavihedbergella simplicissima and "*Pseudoclavihedbergella*" *chevaliensis* (see Systematic Taxonomy) disappear from the assemblage slightly below the C/T boundary (at 17.5 m and at 19.1 m, respectively) at Eastbourne (Fig. 2).

Pseudoclavihedbergellids are not documented in the *W. archaeocretacea* Zone in other sections of the Anglo-Paris Basin (Hart et al., 1993; Desmares et al., 2020). In the Vocontian Basin, hedbergellids with clavate chambers disappear between peak B and C (Pont d'Issole: Grosheny et al., 2006; Clot Chevalier: Falzoni et al., 2016a; Fig. 3) and are absent from the upper *W. archaeocretacea* to lower *H. helvetica* Zone (Vergons, Les Lattes: Grosheny et al., 2006, 2017). At more tropical latitudes, they are not recognized from above (Spain: Lamolda et al., 1997) or slightly below (Tarfaya: this study; Iran: Kalanat and Vaziri-Moghaddam, 2019) peak C (Fig. 3) and in the upper *W. archaeocretacea* to lower *H. helvetica* Zone of Tunisia (Grosheny et al., 2013; Reolid et al., 2015). In the WIS, this morphogroup generally shows rare to very rare occurrence and

517 is not documented in the stratigraphic interval comprised between Bed 78 and 85 at
518 Pueblo (Leckie, 1985; Keller and Pardo, 2004; Fig. 3), corresponding to the interval
519 between peak B and C (see Elderbak and Leckie, 2016; Falzoni et al., 2018), and in the
520 middle-upper *W. archaeocretacea* Zone at Lozier Canyon (Lowery and Leckie, 2017).
521 Leckie et al. (1991) reported a gap in the stratigraphic distribution of
522 pseudoclavihedbergellids in the Black Mesa Basin (Arizona) throughout the uppermost
523 Cenomanian–lower Turonian.

524 At Eastbourne, pseudoclavihedbergellids reoccur in the assemblage at the top of the
525 section ("*P*." *chevaliensis* at 23.3 m and *P. simplicissima* at 23.9 m) after a ~5 m-thick gap
526 in their range in the upper *W. devonense* to lower *F. catinus* ammonite Zones, but
527 specimens are rare and of small size (Fig. 2). In the lower Turonian of the Vocontian
528 Basin, *Pseudoclavihedbergella simplicissima* and *Pessagnoina simplex* are found in one
529 sample only at Pont d'Issole and Vergons (Grosheny et al., 2006), but are not observed at
530 Clot Chevalier (Falzoni et al., 2016a) and Les Lattes (Grosheny et al., 2017).
531 Hedbergellids with clavate chambers re-occur in the assemblages after the gap in their
532 range in Morocco (this study) and in Iran (Kalanat and Vaziri-Moghaddam, 2019), but they
533 are never abundant (Fig. 3).

534

535

536 **5.4 Environmental causes controlling planktonic foraminiferal extinctions and**
537 **eclipses during OAE 2**

538

539 Comparison of planktonic foraminiferal records between Eastbourne and other low to
540 mid-latitude localities allows identification of similar variations in the composition of the
541 assemblages and most events are identified in the same stratigraphic order (e.g.,
542 extinction of rotaliporids, gap in the range of "*Globigerinelloides"* and hedbergellids with

543 clavate chambers) at different localities. Common patterns in the extinctions and
544 temporary absence, or crisis, of taxa suggest that these events were controlled by wide-
545 scale environmental perturbations that occurred during OAE 2, as observed for the
546 "*Heterohelix*" shift (sensu Leckie, 1985; Leckie et al., 1998).

547 The $\delta^{18}O_{carb}$ record obtained from bulk samples at Eastbourne (Tsikos et al., 2004) is
548 plotted in Fig. 3 in order to compare variations in the assemblage composition and major
549 paleoclimate trends. The $\delta^{18}O_{carb}$ record of marine carbonates is generally subject to
550 diagenetic alteration (e.g., Schrag et al., 1995), but major positive and negative $\delta^{18}O_{carb}$
551 excursions at Eastbourne correspond well to other geochemical (e.g., $\delta^{18}O$ measured on
552 macrofossil shells: Voigt et al., 2006) and paleontological evidence (e.g., occurrence of
553 boreal macrofossils: Jefferies, 1962, 1963; Gale and Christensen, 1996) for cooling and
554 warming episodes, as observed for the PCE and for the early Turonian thermal maximum,
555 suggesting it can be reliably used to identify major paleoclimate variations in this section.
556
557 5.4.1 Extinction of *Thalmanninella* and *Rotalipora*
558
559 *Thalmanninella* and *Rotalipora* are usually regarded as thermocline dwellers based on
560 analogy with the depth-ecology of modern single-keeled species, their abundance in
561 tropical pelagic settings, and few stable-isotope data that suggest adaptation to cool/deep
562 layers of the water column (e.g., Caron and Homewood, 1983; Leckie, 1987; Hart, 1999;
563 Premoli Silva and Sliter, 1999; Huber et al., 1999; Wilson and Norris, 2001; Petrizzo et al.,
564 2008; Ando et al., 2010).

565 Their global extinction at or near the onset of OAE 2 has been traditionally related to
566 the expansion of the oxygen minimum zone (OMZ), because this phenomenon likely
567 affected the survivorship and reproduction capability of deep dwellers (Leckie, 1985; Jarvis
568 et al., 1988; Oba et al., 2011; Kaiho et al., 2014; Kuhnt et al., 2017). Modern oceans are

experiencing shoaling of the OMZ as a result of climate warming, because oxygen solubility in the water decreases at increasing temperatures (e.g., Stramma et al., 2008; Gilly et al., 2013). The same scenario likely occurred at a larger scale during the maximum greenhouse phase at the C–T boundary interval, when increased sea-surface productivity might have enhanced oxygen consumption as a result of the remineralization of the organic matter (Schlanger and Jenkyns, 1976; Larson, 1991; Leckie et al., 1998, 2002; Kuypers et al., 2002; Erba, 2004; Pancost et al., 2004; Kuroda et al., 2007; Turgeon and Creaser, 2008). However, the extent of the OMZ and its variation are poorly constrained during OAE 2 (Ostrander et al., 2017), because they might have been decoupled from bottom water anoxia (Kuypers et al., 2002). Moreover, this hypothesis does not explain the record of rotaliporids in the Vocontian Basin, where they survive the deposition of the Lower Black Shale (LBS) (Grosheny et al., 2017).

An alternative explanation for the extinction of rotaliporids is a collapse in the thermal stratification of surface waters due to a major warming event that was detected at Blake Nose (western North Atlantic; Huber et al., 1999). This record, however, is condensed and incomplete (the whole *W. archaeocretaecea Zone* is only 20 cm-thick) and the topmost *R. cushmani* Zone might fall in a non-recovery interval and/or stratigraphic gap, because the extinction of *R. cushmani* and *T. greenhornensis* are found in the same sample.

Our study indicates that the extinction of *Thalmanninella* occurred synchronously at low to mid-latitudes, with the exception of the WIS, suggesting an environmental forcing with synchronous impact over a wide geographic area. The $\delta^{18}O$ record at Eastbourne indicates that *Thalmanninella* became extinct during an interval characterized by prolonged and relatively high sea-surface temperatures preceding the PCE (Fig. 3). This interval corresponds to Plenus Marl Bed 1, which contains diverse benthic communities (Hart, 1996), but includes the disappearance of certain epifaunal benthic foraminifera (Paul et al., 1999). This observation would suggest that oxygen depletion and/or increased

availability of nutrients in surface waters might have occurred in this interval. However, calcareous nannofossils and dinoflagellates indicate that sea-surface fertility reached a minimum at the top of Bed 1 (Gale et al., 2005; Pearce et al., 2009; Linnert et al., 2011), whereas macrofauna, trace fossils and sedimentary geochemistry argue against oxygen depletion at the seafloor (Gale et al., 2000).

The extinction of *Thalmanninella* in the Vocontian Basin occurs at the top of the Lower Black Shale (LBS), which was deposited during a warm interval (Grosheny et al., 2017), and it is observed within a negative $\delta^{18}O$ excursion in sections of Spain (Kaiho et al., 2014). The extinction level of *Thalmanninella* at Tarfaya corresponds to the most negative $\delta^{18}O$ values obtained for core SN°4 (Kuhnt et al., 2017).

Based on these observations, we suggest that a relatively short-term but intense warming event at the onset of OAE 2, potentially associated to a collapse in the thermal stratification of surface waters as observed at Blake Nose (Huber et al., 1999) might have contracted the ecological niches of the deep-dwelling *Thalmanninella* species and contributed to its extinction. By contrast, the HO of *T. greenhornensis* is delayed at Pueblo and falls within the “Benthonic Zone”, a re-oxygenation event of bottom waters that coincides with rapid transgression in the WIS and is correlative with the PCE (Eicher and Worstell, 1970, Eicher and Diner, 1985, Leckie, 1985; Leckie et al., 1998; Elderbak and Leckie, 2016). Disruption of the thermal stratification has been also invoked to explain the delayed extinction of the deep-dwelling *T. greenhornensis* in the WIS (Elderbak and Leckie, 2016).

The step-wise extinction of *Rotalipora* species at Eastbourne started during the first PCE pulse (HO of *R. montsalvensis*) in Plenus Marl Bed 2 and ended (HO of *R. cushmani*) in Plenus Marl Bed 4, which corresponds to the PCE coolest phase (Gale and Christensen, 1996; Jenkyns et al., 2017).

620 The HO of *R. cushmani* is also found within the PCE interval in the Vocontian Basin
621 and at Pueblo (Elderbak and Leckie, 2016; Grosheny et al., 2017; Gale et al., 2019), and it
622 occurs within a cooler interval (higher $\delta^{18}O_{carb}$ values) in Spanish sections (Kaiho et al.,
623 2014) and at Tarfaya (core SN°4: Kuhnt et al., 2017). The extinction of *R. cushmani*
624 seems slightly delayed in the latter two localities compared to Eastbourne, Pueblo and
625 sections of the Vocontian Basin (Fig. 3), potentially suggesting that the PCE is also slightly
626 delayed at lower latitudes.

627 Overall, there is strong evidence that *Rotalipora* species were negatively affected by
628 cooling during the PCE, in agreement with previous observations by Pearce et al. (2009)
629 and Jarvis et al. (2011). Nevertheless, a direct relationship between cooling and extinction
630 of *Rotalipora* does not easily match with the few oxygen-isotope data available for *R.*
631 *montsalvensis* that instead document adaptation to relatively deep/cool layers of the water
632 column in the lower Cenomanian of Blake Nose (Ando et al., 2010). Perhaps cooling might
633 have disrupted the thermal stratification of surface waters (an event consistent with
634 observations in the WIS: Elderbak and Leckie, 2016) and/or negatively affected the
635 principal food source of *Rotalipora* species. Alternatively, this group might have been more
636 thermophilic than previously thought.

637

638 5.4.2 Eclipse of planispiral taxa

639

640 The paleoecological preferences of *"Globigerinelloides"* are poorly known. No
641 geochemical data are available for "*G." ultramicrus*, while oxygen isotopes yielded by "*G."*
642 *bentonensis* suggest it inhabited the thick mixed layer during the cooler season (Petrizzo
643 et al., 2008). Moreover, planispiral taxa were scarcely tolerant to lower salinity and/or
644 higher nutrient concentrations as they decrease in abundance towards shore (Leckie et
645 al., 1998). Elderbak and Leckie (2016) identified a relationship between lithology and

646 occurrence of planispirals in the rhythmically-bedded limestone-marlstone couplets of the
647 Bridge Creek Limestone Member at Pueblo, with "*Globigerinelloides"* being absent in the
648 limestone beds that were deposited during phases of reduced stratification and reinforced
649 northward migration of warm Tethyan waters into the WIS.

650 Overall, previous studies suggest that planispiral taxa were generally adapted to cool
651 waters during times of enhanced thermal stratification. These paleoecological preferences
652 might potentially explain the temporary crisis of *"Globigerinelloides"* that started almost
653 synchronously at low to mid-latitudes (Fig. 3). In fact, the eclipse of planispirals began at
654 the onset of rising sea-surface temperatures after the PCE, but it is also concomitant with
655 the acme of calcareous dinoflagellate cysts (calcispheres: Gale et al., 2000; Pearce et al.,
656 2009) at Eastbourne, the acme of radiolaria in the Vocontian Basin, and the onset of the
657 "*Heterohelix*" shift at Pueblo (Leckie, 1985; Leckie et al., 1998), in Morocco (Keller et al.,
658 2008; Falzoni et al., 2018), and Iran (Kalanat and Vaziri-Moghaddam, 2019). These events
659 have been generally associated with increased vertical mixing and surface waters
660 productivity, although the paleoecology of calcispheres and the interpretation of sea-
661 surface fertility at Eastbourne are controversial (Wendler et al., 2002; Erba, 2004; Gale et
662 al., 2000; Pearce et al., 2009; Linnert et al., 2011). Caron et al. (2006) reported levels with
663 common calcispheres spread throughout the C–T boundary interval at Pueblo and Wadi
664 Bahloul, but they do not document any discernable calcisphere acme, therefore the
665 calcisphere record in these two sections is not comparable with Eastbourne.

666 Based on the above, we suggest that three different causes might have contributed to
667 the eclipse of planispiral taxa at the C/T boundary: 1) average increase of sea-surface
668 temperatures after the PCE, 2) reduced thermal stratification, and 3) increased sea-
669 surface productivity. However, discrimination among these causes is currently not possible
670 due to the limited knowledge of the paleoecology of planispiral species.

671

672

673 5.4.3 Eclipse of hedbergellids with clavate chambers

674

675 Hedbergellids with clavate chambers were found in relatively proximal environments
676 with distributions and relative abundances similar to "*Globigerinelloides*", thus they were
677 interpreted as relatively shallow dwellers (Leckie, 1987; Leckie et al., 1998; Hart, 1999).
678 However, the few stable-isotope data available for this morphogroup suggest a
679 thermocline habitat during the Albian-early Cenomanian and in open ocean settings (i.e.,
680 Blake Nose: Norris and Wilson, 1998; Leckie et al., 2002; Petrizzo et al., 2008; Ando et al.,
681 2010). Most importantly, they are particularly common and diverse at the onset and during
682 the recovery phase of Cretaceous OAEs (but rare or absent in organic-rich lithologies) and
683 have been interpreted to be adapted to oxygen-poor nutrient-rich environments as their
684 Cenozoic homeomorphs (e.g., Magniez-Jannin, 1998; Premoli Silva and Sliter, 1999;
685 Coccioni and Luciani, 2004, 2005; Coccioni et al., 2006; Coxall et al., 2007), although
686 temperature, salinity and type of food might have controlled their distribution (Coccioni et
687 al., 2006; Coxall et al., 2007). Accordingly, the abundance of species with clavate
688 chambers has been suggested as a proxy for the strength of OAE-related environmental
689 perturbations (Coccioni et al., 2006) or for the expansion of the OMZ during greenhouse
690 climate modes (Coxall et al., 2007).

691 Our study reveals that the eclipse of hedbergellids with clavate chambers occurred
692 almost synchronously at low to mid-latitudes during the terminal phase of OAE 2. At
693 Eastbourne, *P. simplicissima* disappears in an interval where other intermediate and deep
694 dwellers (*Praeglobotruncana*, *Dicarinella* and *Marginotruncan*a) are rare and low in
695 diversity (Fig. 2). At Tarfaya (this study), Iran (Kalanat and Vaziri-Moghaddam, 2019) and
696 Pueblo (Leckie et al., 1998; Keller and Pardo, 2004) hedbergellids with clavate chambers
697 are mainly replaced by biserial taxa ("*Heterohelix*" shift). Moreover, the record in the

Vocontian Basin supports the lack of correlation between organic-rich lithologies and distribution of hedbergellids with clavate chambers (Grosheny et al., 2006; Falzoni et al., 2016a), and Kalanat and Vaziri-Moghaddam (2019) found common specimens only in samples with low TOC content in the Lar Anticline section (Iran).

Based on these observations, we suggest that hedbergellids with clavate chambers clearly suffered when sea-surface productivity exceeded a critical threshold and/or when reduced thermal stratification contracted the ecological niches available for deep dwellers, implying that the abundance of clavate forms cannot be used to reliably trace the expansion of the OMZ during OAE 2. In fact, the clavate forms were replaced by other taxa (e.g., biserials or radiolaria) during intervals of high sea-surface productivity and reduced thermal stratification

5.5 A planktonic foraminiferal PCE fauna?

A number of planktonic foraminiferal extinctions (e.g., *Rotalipora* spp. and *"G." bentonensis*) fall within the PCE interval in several low to mid-latitude sections including Eastbourne (Fig. 3). However, these extinctions involve presumed cool/deep dwellers that are not expected to suffer cold sea-surface temperatures. For this reason, a direct cause-effect relationship between cooling during the PCE and changes in the taxonomic composition of planktonic foraminiferal assemblages has never been proved, although this event had certainly influenced the composition of several Northern Hemisphere marine (particularly benthic) communities.

Desmares et al. (2016, 2020) and Grosheny et al. (2017) identified an increased proportion of the left- to right-coiled *Muricohedbergella delrioensis* specimens within assemblages of the PCE interval at Pueblo, and in sections of the Vocontian and Anglo-

Paris Basin. This variation in the coiling direction of *M. delrioensis* has been suggested to be a proxy of cooling sea-surface temperatures in the upper Cenomanian in analogy with some living species (e.g., Ericson, 1959). This hypothesis could not be tested at Eastbourne, because of the high morphologic variability of muricate hedbergellids that complicated the discrimination between *M. delrioensis* s.s. and similar morphotypes, and its complex taxonomic history (two designated neotypes: Longoria, 1974 and Masters, 1976) having different morphological features; see Petrizzo and Huber, 2006).

Nevertheless, two planktonic foraminiferal species show restricted stratigraphic distributions and/or remarkable increase in their abundance in selected intervals at Eastbourne (Fig. 2) suggesting a possible relationship with the PCE interval: 1) *Muricohedbergella kyphoma* occurs very rarely in two samples at the base of the section (at 0.2 and 0.8 m), but it becomes common to very common in Plenus Marl Beds 4 and 5 (11.2 to 12.2 m); 2) *Praeglobotruncana plenusiensis* n. sp. shows a stratigraphic distribution limited to Plenus Marl Bed 2 and 4 (9.2 to 11.8 m).

Muricohedbergella kyphoma was described from the *W. archaeocretacea* Zone of Japan (Hasegawa, 1999) and might have been misidentified with the very similar *M. planispira* in previous studies at Dover (Jarvis et al., 1988) and Eastbourne (Paul et al., 1999; Keller et al., 2001), all documenting occurrence or increased abundance of *M. planispira* in the middle Plenus Marl. The stratigraphic distribution of *M. kyphoma* in Japan cannot be precisely established due to the rare occurrence of planktonic foraminifera across the C/T boundary and unavailability of a highly-resolved carbon isotope record (Hasegawa, 1995, 1999). However, if *M. kyphoma* is a cool water taxon associated with the uppermost Cenomanian cool snap, its occurrence in the *W. archaeocretacea* Zone of Japan might represent the first evidence for the PCE in the Pacific Ocean and suggests that this event might be more global in nature. This observation is consistent with results

749 by Sinninghe Damsté et al. (2010) suggesting that the PCE was driven by a drop in the
750 atmosphere pCO_2 levels and thus represented a global phenomenon.

751 *Praeglobotruncana plenusiensis* is herein described as a new species (see Systematic
752 Taxonomy). Despite its rare occurrence at Eastbourne, it shows remarkably distinctive
753 taxonomic features and a large test size. No other specimens with these morphological
754 features were previously illustrated in the literature, with the possible exception of a
755 specimen in Leckie (1985) from the Pueblo section (WIS) approximately found at the same
756 stratigraphic interval. Further documentation of *P. plenusiensis* in other localities is
757 required to establish a possible relationship with episodes of sea-surface cooling,
758 however, its restricted range in beds associated with the PCE macrofossil fauna would
759 support this hypothesis.

760

761

762 **6. Conclusions**

763

764 The stratigraphically complete and microfossil-rich Cenomanian–Turonian transition at
765 Eastbourne enables the detailed documentation of a sequence of planktonic foraminiferal
766 events that can be correlated among the most complete OAE 2 sequences.

767 A pulse in the diversification of double-keeled taxa is observed in the interval
768 preceding the onset of OAE 2. The overlying stratigraphic interval is characterized by the
769 step-wise extinction of *Thalmanninella* and *Rotalipora* species, and of *"G." bentonensis*.
770 These events are followed by the eclipse of planispiral taxa during the latest Cenomanian,
771 and later, of hedbergellids with radially elongated chambers during the early Turonian.
772 This sequence of events is consistently found in all low to mid-latitude sections with a
773 complete record across the C/T boundary, suggesting that variations in the assemblages

774 were likely controlled by wide-scale environmental perturbations that involved at least the
775 North European Basins, the North and Central Atlantic and Tethyan Ocean.

776 Our study suggests that the extinction of *Thalmanninella* and *Rotalipora* that have
777 been commonly attributed to the expansion of the OMZ at the onset of OAE 2 might have
778 been controlled by opposite climate forcing. In fact, the extinction of *Thalmanninella* is
779 generally documented within a warming event potentially associated with the disruption of
780 thermally stratified waters, with the exception of the WIS, where this event is delayed. By
781 contrast, the extinction of *Rotalipora* is identified within the PCE, but further investigations
782 are required to understand whether cooling was the primary cause for its extinction, as
783 previous studies have suggested that rotaliporids were adapted to cool/deep layers of the
784 water column.

785 We suggest that the eclipse of "*Globigerinelloides"* might have been caused by the
786 onset of warming that led to the early Turonian thermal maximum and/or enhanced sea-
787 surface productivity and reduced thermal stratification. Increased mixing might also have
788 reduced the ecological niches available for the deep-dwelling hedbergellids with clavate
789 chambers that were presumably less tolerant to high sea-surface productivity compared to
790 biserial taxa.

791 Finally, we highlight that the stratigraphic ranges of *Muricohedbergella kyphoma* and
792 *Praeglobotruncana plenusiensis* n. sp. at Eastbourne parallel that shown by Boreal
793 macrofossils and correspond to relatively high $\delta^{18}O$ values during the PCE, representing
794 the first evidence for a planktonic foraminiferal PCE fauna. Both taxa were likely cool/deep
795 dwellers and might be used as proxies for constraining the PCE interval in pelagic
796 sequences and in the absence of geochemical data.

797

798

799 **7. Systematic taxonomy**

800

801 Below are provided emended descriptions, discussions of synonymies and taxonomic
802 and/or biostratigraphic remarks for relevant species and morphotypes of uncertain
803 taxonomic position mentioned in the text and in the figures. Two *Praeglobotruncana*
804 species occurring at Eastbourne are described as new.

805

806 Genus *Thalmanninella* Sigal, 1948

807 *Type species. Thalmanninella brotzeni* Sigal, 1948, p. 102, pl. 1, fig. 5A–C.

808

809

810 *Thalmanninella* cf. *brotzeni* Sigal, 1948

811 (Fig. 4, 1A–C, 2A–C, 3A–C)

812

813 *Description*. Medium to large-sized trochospiral test, moderately high to high
814 trochospire; subcircular peripheral outline, asymmetrical lateral profile with convex spiral
815 side and flat to slightly convex umbilical side; single-keeled throughout the last whorl; six to
816 eight chambers in the last whorl, slowly increasing in size as added. Spiral side with
817 crescentic to petaloid chambers, sutures curved and raised. Umbilical side with
818 subrectangular to trapezoidal chambers; umbilical sutures curved and raised to depressed
819 at the end of the last whorl. Umbilical area relatively small, about 1/3 of the maximum
820 diameter; small-sized supplementary apertures umbilical in position.

821 *Distinguishing features*. Specimens assigned to *T.* cf. *brotzeni* (Fig. 4, 1A–C, 2A–C,
822 3A–C) differ from *T. brotzeni* (Fig. 4, 4A–C, 5A–C) and *T. greenhornensis* (Fig. 4, 6A–C,
823 7A–C) by having a higher trochospire. Moreover, they differ from *T. greenhornensis* by
824 possessing petaloid to subcircular chambers on the spiral side and from *T. deeckei* (Fig. 4,
825 8A–C) by possessing a spiroconvex rather than biconvex to umbilico-convex lateral profile.

826 *Remarks*. Morphotypes assigned to *T.* cf. *brotzeni* are rare in the assemblage but they
827 show stable morphological features throughout their stratigraphic range at Eastbourne.
828 The features of the umbilical side (i.e., shape of chambers and sutures) would suggest a
829 phyletic relationship with *T. brotzeni*, but further studies are required to understand if these
830 high-spired morphotypes fall in its range of variability or if they represent a distinct taxon.
831
832
833 *Thalmanninella* cf. *greenhornensis* (Morrow, 1934)
834 (Fig. 4, 9A–C, 10A–C)
835
836 *Description*. Medium to large-sized trochospiral test; subcircular peripheral outline,
837 symmetrical lateral profile with convex spiral and umbilical sides; single-keeled throughout
838 the last whorl; six to seven chambers in the last whorl, slowly growing in size as added.
839 Spiral side with subtriangular chambers, sutures curved and raised. Umbilical side with
840 subrectangular to trapezoidal chambers; umbilical sutures curved and raised to straight
841 and depressed at the end of the last whorl. Umbilical area representing about 1/2 to 1/3 of
842 the maximum diameter; small-sized supplementary apertures umbilical in position.
843 *Distinguishing features*. It resembles *T. greenhornensis* (Fig. 4, 6A–C, 7A–C) in the
844 taxonomically relevant features of the umbilical side and lateral profile, but differs by
845 having a lower number of chambers in the last whorl (6 to 7 rather than 8 to 10) that are
846 typically subtriangular and more elongated rather than crescentic as in its holotype (Fig. 4,
847 6A–C). It differs from *T.* cf. *brotzeni* (Fig. 4, 1A–C, 2A–C, 3A–C) and *T. brotzeni* (Fig. 4,
848 4A–C, 5A–C) by possessing subtriangular-shaped chambers, a slow rate of chamber size
849 increase in the last whorl and by having a rounded rather than suboval peripheral outline.
850 *Remarks*. This morphotype is relatively rare in the assemblage, but it shows the same
851 abundance as *T. greenhornensis* s.s. and is found in samples where the latter species

852 does not occur. Moreover, it shows consistent and stable morphological features
853 throughout its stratigraphic distribution. Further studies are required to establish if it
854 represents a valid species or an ecophenotype with restricted geographic distribution
855 and/or biostratigraphic value.
856
857
858 Genus *Rotalipora* Brotzen, 1942
859 *Type species. Rotalipora turonica* Brotzen, 1942, p. 32, fig. 10.
860
861 *Rotalipora montsalvensis* Mornod, 1950
862 (Fig. 5, 1A–C, 2A–C, 3A–C)
863
864 1950 *Globotruncana (Rotalipora) montsalvensis* Mornod, p. 580, pl. 4, fig. 1A–C
865 (middle Cenomanian, Montsalvens Chain, Switzerland)
866 1950 *Globotruncana (Rotalipora) montsalvensis minor* Mornod, p. 580, pl. 2, fig. 2A–C
867 (middle Cenomanian, Montsalvens Chain, Switzerland)
868 1954 *Rotalipora turonica thomei* Hagn and Zeil, p. 28–29, pl. 1 (upper Cenomanian,
869 Bayerishen Alpen, Germany)
870 2006 *Rotalipora montsalvensis* Mornod in Caron and Spezzaferri, p. 377, pl. 2, figs.
871 1A–C and 3A–C (middle Cenomanian, Montsalvens Chain, Switzerland)
872
873 *Distinguishing features*. *Rotalipora montsalvensis* (Fig. 5, 1A–C, 2A–C, 3A–C) is
874 differentiated from *R. cushmani* (holotype in Fig. 5, 4A–C) by having a less-developed and
875 thinner keeled periphery, less-ornamented chambers on the umbilical and spiral sides and
876 by the absence of umbilical triangular thickenings on all the chambers of the last whorl.
877 Transitional specimens (Fig. 5, 3A–C) between *R. montsalvensis* and *R. cushmani* are

878 characterized by having a well-developed peripheral keel and thickenings on a few
879 chambers of the last whorl and are commonly observed throughout the Grey Chalk and
880 Plenus Marl Mbs.

881 *Remarks*. *Rotalipora montsalvensis* was described and illustrated with a single-keeled
882 periphery barely developed throughout the last whorl, straight umbilical sutures with
883 sutural supplementary apertures and straight to curved and weakly raised to depressed
884 spiral sutures (see holotype Fig. 4, 1A–C). The variety *R. montsalvensis minor* was
885 differentiated from *R. montsalvensis* s.s. by its smaller test size and the occurrence of two
886 to three supplementary apertures between the ultimate two chambers (Mornod, 1950).
887 This variety is herein regarded as junior synonym of *R. montsalvensis* in agreement with
888 González-Donoso et al. (2007). The description and illustration of *Rotalipora turonica*
889 *thomei* with a thin single-keeled periphery and absence of shell ornamentation on the
890 umbilical side suggest that this species falls in the range of variability of *R. montsalvensis*
891 in agreement with González-Donoso et al. (2007).

892

893

894 *Rotalipora praemontsalvensis* Ion, 1976

895 (Fig. 5, 5A–C, 6A–C, 7A–C, 8A–C)

896

897 1973 Not *Pseudoticinella planoconvexa* Longoria, p. 422–423, pl. 2, figs. 6–9 (upper
898 Cenomanian, Eagle Ford Group, Britton Clay, Texas)

899 1976 *Rotalipora praemontsalvensis praemontsalvensis* Ion, pp. 43–44, pl. 1, figs. 1–4
900 (middle Cenomanian, western Carpathians, Romania)

901 1976 *Rotalipora praemontsalvensis lobata* Ion, pp. 44, pl. 2, figs. 1–4 (middle
902 Cenomanian, western Carpathians, Romania)

1976 *Rotalipora praemontsalvensis altispira* Ion, pp. 44–45, pl. 2, figs. 5–7 (middle Cenomanian, western Carpathians, Romania)

1985 *Anaticinella multiloculata* s.l. Morrow, in Leckie, p. 149, pl. 4, figs. 3–4, 7–8 (upper Cenomanian, Bridge Creek Limestone Mbr., Pueblo, Colorado)

2006 *Anaticinella planoconvexa* Longoria, in Caron et al., p. 184, fig. 7, n. 4 (upper Cenomanian, Hartland Shale Mbr., Pueblo, Colorado)

2008 *Rotalipora planoconvexa* Longoria, in Desmares et al., p. 96, pl. 1, fig. 4A–D (upper Cenomanian, Hartland Shale and Bridge Creek Limestone Mbr., Pueblo, Colorado)

Emended description. Medium to large-sized trochospiral test, low to moderately high trochospire; subcircular peripheral outline, nearly symmetrical lateral profile with variably convex spiral and umbilical sides; usually single-keeled in the first two chambers of the last whorl, pinched to rounded in the other chambers; usually five to seven chambers in the last whorl, moderately increasing in size as added. Spiral side with petaloid to subcircular chambers, sutures slightly curved and depressed; sutures of the inner whorl might be very weakly keeled. Umbilical side with subglobular to subtriangular chambers; umbilical sutures straight to weakly curved and depressed. Umbilical area relatively small, 1/3 to 1/4 of the maximum diameter; supplementary apertures variably developed in the specimens, usually sutural in position.

Distinguishing features. *Rotalipora praemontsalvensis* (Fig. 5, 5A–C, 6A–C, 7A–C, 8A–C) differs from *R. montsalvensis* (Fig. 5, 1A–C, 2A–C, 3A–C) by having more inflated chambers on the umbilical and spiral sides and a less developed peripheral keel, which is present in some but not all chambers of the last whorl or may be completely absent. It differs from the holotype of *Thalmanninella multiloculata* (Fig. 5, 9A–C) by having petaloid to subcircular rather than subrectangular to subtrapezoidal chambers on the spiral side,

928 fewer chambers in the last whorl and a smaller umbilical area. Moreover, the
929 supplementary apertures are usually sutural rather than umbilical in position.

930 *Remarks*. Ion (1976) described three subspecies of *R. praemontsalvensis* (i.e.,
931 *praemontsalvensis*, *lobata* and *altispira*). These subspecies were differentiated according
932 to the number and morphology of the chambers in the last whorl and development of the
933 keeled periphery, which is absent in the subspecies *lobata*, present on the first chamber of
934 the last whorl in *altispira* and on the first 1–3 chambers of the last whorl in
935 *praemontsalvensis* (Ion, 1976). All three morphotypes occur at Eastbourne and are
936 included in the range of variability of *R. praemontsalvensis*.

937 *Rotalipora praemontsalvensis* was described from middle Cenomanian assemblages.
938 González-Donoso et al. (2007) extended its distribution to the upper *R. cushmani* Zone in
939 agreement with its range at Eastbourne. Other specimens assigned to *Anaticinella*
940 *multiloculata* s.l. (Leckie, 1985), *Anaticinella planoconvexa* (Caron et al., 2006) or
941 *Rotalipora planoconvexa* (Desmares et al., 2008) and identified at the top of the *R.*
942 *cushmani* Zone in the Pueblo section might fall in the range of variability of *R.*
943 *praemontsalvensis*. These morphotypes were interpreted as likely deriving from *R.*
944 *cushmani* through the loss of the peripheral keel and development of inflated chambers at
945 the onset of OAE 2, as observed in the *T. greenhornensis-T. multiloculata* phyletic lineage.
946 In our opinion, however, the species *planoconvexa* Longoria (1973) is not phyletically
947 related to *R. cushmani*, but it is more likely a junior synonym or closely related to
948 *multiloculata* Morrow (1934), as suggested by González-Donoso et al. (2007). In fact, the
949 holotype of *planoconvexa* (Fig. 5, 10A–C) differs from the holotype of *multiloculata* (Fig. 5,
950 9A–C) only by its higher trochospire and by having 6 rather than 8 chambers in the last
951 whorl increasing more slowly in size, i.e., morphological differences that would support the
952 accommodation of both taxa in the genus *Thalmanninella*. Accordingly, both type
953 specimens have the same wall texture (smooth with scattered pustules), straight to slightly

954 curved spiral sutures, distinctly curved and depressed umbilical sutures, supplementary
955 apertures umbilical in position, a rather large umbilical area, and were selected from
956 coeval assemblages of the WIS.
957
958
959 Genus "*Globigerinelloides*" Cushman and Ten Dam, 1948
960 *Type species.* "*Globigerinelloides*" *algerianus* Cushman and Ten Dam, 1948, p. 43, pl.
961 8, figs. 4–6.
962 The genus is quoted in the text and figures because it is polyphyletic and under
963 taxonomic revision (see Petrizzo et al., 2017).
964
965
966 "*Globigerinelloides*" cf. *bollii* Pessagno, 1967
967 (Fig. 6, 1A–C)
968
969 *Description*. Medium to small-sized planispiral test; subcircular to suboval peripheral
970 outline, symmetrical lateral profile; six to eight subglobular chambers in the last whorl,
971 slowly growing in size as added. Chambers are subglobular to slightly reniform in edge
972 view. Sutures straight and depressed. Primary aperture equatorial, opening at the base of
973 the final chamber with a low arch; umbilicus ½ to 1/3 of the maximum diameter. Wall finely
974 perforate and slightly pustulose in the earlier chambers.
975 *Distinguishing features*. Specimens assigned to "*G.*" cf. *bollii* (Fig. 6, 1A–C) resemble
976 the holotype of "*G." bollii* (Fig. 6, 2A–C) but differs by having slightly more globular and
977 inflated chambers. It differs from "*G." bentonensis* (Fig. 6, 3A–C) by having globular rather
978 than reniform chambers and a more compressed edge view. It differs from *"G." ultramicrus*

(Fig. 6, 4A–C) by usually showing fewer chambers increasing more rapidly in size in the last whorl and a more lobate and less circular peripheral outline.

Remarks. "*Globigerinelloides" bollii* was described from the Santonian–Campanian of Texas (Pessagno, 1967) and later identified in coeval assemblages (Exmouth Plateau: Petrizzo, 2000; Canada: Georgescu, 2006; Texas: Gale et al., 2008; Umbria–Marche Basin and Shatsky Rise: Petrizzo et al., 2011). Petrizzo et al. (2017) reported "*G." bollii* from the uppermost Coniacian–Santonian of Tanzania, while Coccioni and Premoli Silva (2015) identified the LO of "*G." bollii* in the middle Turonian *Dicarinella primitiva-Marginotruncana sigali* Zone in the Bottaccione-Contessa composite section. However, "*G*." *bollii* has never been recognized in assemblages older than the Turonian and *"G."* cf. *bollii* is not recorded across the C/T boundary at Eastbourne, thus we cannot totally exclude that their range is separated by a short stratigraphic gap. For this reason, the validity of *G."* cf. *bollii* as a distinct species and its phyletic relationship with the Turonian–Campanian morphotypes should be verified by further studies.

"*Globigerinelloides*" *tururensis* (Brönnimann, 1952)

(Fig. 6, 5A–C, 6A–B, 7A–B, 8A–C)

1952 *Globigerinella tururensis* Brönnimann, p. 52, fig. 27 1A–B (upper Albian–Cenomanian, Gautier Fm., Trinidad)

? 1959 *Planomalina alvarezi* Eternod Olvera, p. 91–92, pl. 4, fig. 5–7 (Campanian–Maastrichtian, Mendez Fm. Tampico, Mexico)

1997 *Globigerinelloides bentonensis* Morrow in Lamolda et al., p. 340, fig. 5Q–R (upper Cenomanian, Ganuza section, Spain)

2015 *Globigerinelloides eaglefordensis* Moreman in Eldrett, p. 337, pl. 1, n. 5–10 (upper Cenomanian, Eagle Ford Group, Iona-1 core, Texas)

Distinguishing features. "*Globigerinelloides" tururensis* (Fig. 6, 5A–C, 6A–B, 7A–B, 8A–C) differs from all other co-occurring planispiral species, including "*G." bentonensis* (Fig. 6, 3A–C), by having a subrectangular rather than circular peripheral outline, a more rapid chamber size increase rate particularly at the end of the final whorl, resulting in a very large subtrapezoidal ultimate chamber in equatorial view. Moreover, it differs from "*G." bentonensis* (Fig. 6, 3A–C) by having a more axially compressed edge view due the presence of a less reniform and inflated last chamber, which can be observed in the "*G." tururensis* type specimen illustrated by drawing (Fig. 6, 6A–B). It differs from "*G." ultramicrus* (Fig. 6, 4A–C) by usually possessing fewer chambers in the last whorl. It can be differentiated from "*G."* cf. *bollii* (Fig. 6, 1A–C) because the latter species shows globular chambers and a more lobate equatorial periphery.

Remarks. *"Globigerinelloides" tururensis* was described from late Albian–Cenomanian assemblages of the Gautier Formation (Trinidad) yielding *Thalmanninella appenninica* (Brönnimann, 1952; Bolli, 1959; Kugler and Bolli, 1967) and later overlooked, despite its diagnostic morphological features (moderately compressed lateral profile in edge view and large subtrapezoidal ultimate chamber) were clearly illustrated by Brönnimann (1952) (see holotype in Fig. 6, 5A–C and the additional specimen figured by Brönnimann, 1952, here reillustrated in Fig. 6, 6A–B). Specimens assigned to *"G." tururensis* in this study (Fig. 6, 7A–B, 8A–C) strictly resemble its holotype (Fig. 6, 5A–C) and the specimen figured by Brönnimann (1952) (Fig. 6, 6A–B). Possible transitional specimens between "*"G." tururensis* and *"G." bentonensis* are observed at Eastbourne and show a moderately inflated ultimate chamber and a similar wall texture (i.e., finely pustulose), and suggest that these species are phyletically related. However, we regard both taxa as distinct species

according to the distinguishing features listed above and to the morphological variability observed within the *"Globigerinelloides"* population at Eastbourne. In other studies, specimens of *"G." tururensis* might have been assigned to other species co-occurring with *"G." bentonensis* and *"G." ultramicrus*, such as "*G." caseyi* and "*G." eaglefordensis* (e.g., Luciani and Cobianchi, 1999; Hasegawa, 1999; Coccioni and Luciani, 2004; Eldrett et al., 2015). However, these identifications require revision, because the holotype of "*G." caseyi* was regarded as a junior synonym of "*G." bentonensis* (Petrizzo and Huber, 2006), while the holotype of "*G." eaglefordensis* is a benthic specimen (Moullade et al., 2002).

Specimens assigned to *"G." tururensis* might also fall in the range of variability of "*G." alvarezi* (holotype in Fig. 6, 9A–C). The latter species was described from Campanian–Maastrichtian assemblages of Mexico and recognized in several middle Turonian–Maastrichtian sequences from low to high latitudes (Eastern Pacific Ocean: Sliter, 1972; Umbria–Marche Basin: Premoli Silva and Sliter, 1995; Coccioni and Premoli Silva, 2015; Tanzania: Petrizzo et al., 2017; Southern High Latitudes: Huber, 1992). To our knowledge, "*G." alvarezi* has never been identified or illustrated from stratigraphic sequences older than the middle Turonian, while *"G." tururensis* has never been recognized above the Cenomanian (Brönnimann, 1952; Bolli, 1959; Kugler and Bolli, 1967). Because *"G." tururensis* disappears few meters below the C/T boundary at Eastbourne, we cannot totally exclude a short stratigraphic gap separating the ranges of *"G." tururensis* and "*G." alvarezi* and that both taxa represent valid species. However, their morphological similarities would support the accommodation of these taxa in the same long-ranging species in case no stratigraphic gap will be documented by future studies.

Genus *Pseudoclavihedbergella* Georgescu, 2009

Type species. Hedbergella amabilis Loeblich and Tappan, 1961, p. 274, pl. 3, figs. 1–7 and 9.

Pseudoclavihedbergella simplicissima (Magné and Sigal, 1954)

(Fig. 7, 1A–C, 2A–D, 3A–D, 4A–B, 5A–D, 6A–D)

1954 *Hastigerinella simplicissima* Magné and Sigal, p. 487, pl. 14, figs. 11A–C (lower Cenomanian, Tunisia)

1961 *Hedbergella amabilis* Loeblich and Tappan, p. 274, pl. 3, figs. 1–7 and 9 (Cenomanian, Britton Clay, Eagle Ford Group, Texas)

Emended description. Small to medium size low trochospiral test; strongly lobate equatorial periphery; four to six, often five chambers in the last whorl. Symmetrical and rounded, never pinched, lateral profile. First chambers of the last whorl globular, then globular to subcylindrical and radially elongated and often tilted with regard to a plane perpendicular to the coiling axis. The radial elongation and the chamber size increase rate are highly variable among specimens but chambers never develop bulbous distal projections. Umbilical and spiral sutures straight and depressed. Umbilicus small, 1/3 to 1/4 of the maximum diameter, primary aperture extraumbilical, opening at the base of the final chamber with a moderately high arch covered by a thick lip. Wall texture finely pustulose in the earlier chambers to smooth at the end of the final whorl and macroperforate (pore diameter >2.5 µm sensu Huber and Leckie, 2011), with pore density usually decreasing throughout the last whorl; an imperforate peripheral band is observed in several specimens.

Distinguishing features. *Pseudoclavihedbergella simplicissima* (Fig. 7, 1A–C, 2A–D, 3A–D, 4A–B, 5A–D, 6A–D) differs from the holotype of *Pessagnoina simplex* Morrow (1934) (Fig. 7, 7A–C) by having a less radially elongated ultimate chamber and a smoother wall texture. However, the reliability of these morphological features to differentiate the latter species should be verified by further studies because no specimens resembling the holotype of *P. simplex* occur at Eastbourne (see discussion below on the classification at genus level); it differs from *Muricohedbergella flandrini* (Porthault, 1970) by having a rounded rather than pinched lateral profile.

Remarks. *Pseudoclavihedbergella simplicissima* and *P. amabilis* (holotype: Fig. 7, 3A–C; paratype: Fig. 7, 4A–B) are low-trochospiral hedbergellids having radially elongated chambers in the ultimate whorl and co-occurring in Albian–Cenomanian assemblages. Loeblich and Tappan (1961) described *P. amabilis* likely unaware of the species described by Magné and Sigal (1954) and a number of its paratypes (e.g., Fig. 7, 4A–B) closely resemble the type specimens of *P. simplicissima* (e.g., Fig. 7, 2A–D). Previous authors have discussed their possible synonymy and reached different conclusions: Masters (1977) and Leckie (1984) regarded *P. amabilis* as a junior synonym of *P. simplicissima*, while Georgescu (2009) considered the former as a taxonomically distinct species according to the occurrence of a generally larger pore size (1.8 to 5.0 μm vs. 0.9 to 2.2 μm) and more chambers in the last whorl that are more radially elongated compared to *P. simplicissima*. However, the latter study was not based on the examination of *P. simplicissima* type specimens. Observation of its holotype (Fig. 7, 1A–C) and topotype (Fig. 7, 2A–D) and comparison with the holotype (Fig. 7, 3A–D) and one of the paratypes (Fig. 7, 4A–B) of *P. amabilis* suggest that the number of chambers in the ultimate whorl is identical (5) in both species. Moreover, all type specimens share the same taxonomically relevant features including the chamber shape (i.e., subglobular at the beginning of the last whorl with the ultimate chambers that may become subcilindrical and slightly to

moderately elongated), the low trochospire, the dimensions of the umbilical area, and the position and features of the primary aperture. Most importantly, the high-resolution image of the wall texture of the topotype of *P. simplicissima* (Fig. 7, 2D) indicates that the pore size ranges from 4 to 5 μm and therefore is comparable to the pore diameter yielded by specimens assigned to *P. amabilis*, including its holotype (Georgescu, 2009). This latter specimen shows a higher pore density (see Fig. 7, 3D) compared to *P. simplicissima*. However, we believe that pore density is not taxonomically significant in this group, as we have observed a decrease in pore density within the same specimen through ontogeny and a variation in pore density among different specimens having similar shell morphology, as already observed in the population of *P. amabilis* (Georgescu, 2009) and in other Cretaceous hedbergellids (e.g., *Hedbergella infracretacea* and *Muricohedbergella planispira*: Huber and Leckie, 2011). As a consequence, we regard *P. amabilis* as a junior synonym of *P. simplicissima.*

Classification at genus level. *Pseudoclavihedbergella simplicissima* and *P. amabilis* have been generally accommodated in the genus *Clavihedbergella* Banner and Blow (1959), according to the presence of radially elongated chambers in its type species *C. subcretacea* (Tappan, 1943). However, Georgescu (2009) suggested that *C. subcretacea* has a smooth wall texture and is phyletically related to the ticinellid group, while the finely pustulose species *amabilis* and *simplicissima* belong to a different lineage evolved from *M. delrioensis*. Accordingly, Georgescu (2009) erected the new genus *Pseudoclavihedbergella* to include the *amabilis-simplicissima* morphogroup, both species being characterized by a slightly pustulose wall texture and by petaloid chambers with elongation axis perpendicular to or at a high angle to the previous whorl. We follow this classification at the genus level pending further studies on the taxonomy and phylogeny of hedbergellids with radially elongated chambers.

1131 Georgescu (2009) also erected the genus *Pessagnoina* to accommodate the species
1132 *simplex* Morrow (1934) and *moremani* Cushman (1931) suggested to evolve from *P.*
1133 *simplicissima* through the gradual development of more radially elongated chambers (*P.*
1134 *simplex*) and bulbous distal projections (*P. moremani*). Georgescu (2009) differentiated
1135 *Pessagnoina* from *Pseudoclavihedbergella* by the absence of an imperforate peripheral
1136 band and occurrence of smaller-sized pores in the former genus. However, the chamber
1137 elongation, the pore diameter and the imperforate peripheral band are unstable characters
1138 within the population of *P. simplicissima* and the primary type specimens of *P.*
1139 *simplicissima* and *P. amabilis* do not show an imperforate peripheral band. Moreover, no
1140 specimens with elongated chambers as observed in the holotype of *P. simplex* were
1141 identified at Eastbourne, preventing evaluation of the morphologic variability in *P. simplex*-
1142 like morphotypes within the assemblage. As a consequence, the synonymy between *P.*
1143 *simplicissima* and *P. simplex* and the validity of *Pessagnoina* cannot be verified in this
1144 study.
1145
1146
1147 *"Pseudoclavihedbergella" chevaliensis* Falzoni et al., 2016a
1148 (Fig. 7, 8A–C, 9A–C)
1149
1150 2016a *"Pseudoclavihedbergella" chevaliensis* Falzoni et al., p. 88, fig. 12, 3A–C, 4A–
1151 C, 5A–D (lower Turonian, Clot Chevalier, Vocontian Basin, SE France)
1152
1153 *Remarks*. *"Pseudoclavihedbergella" chevaliensis* (Fig. 7, 8A–C) was described from
1154 the Vocontian Basin and its LO was identified in the *W. archaeocretacea* Zone about 4 m
1155 above the C/T boundary (Falzoni et al., 2016a). Specimens strictly resembling its holotype
1156 (Fig. 7, 9A–C) are rare at Eastbourne but are found at the base of the section, suggesting

that (a) its LO falls in an older stratigraphic interval in the Anglo-Paris Basin and that (b) this species was not endemic to the Vocontian Basin.

Classification at genus level. *"Pseudoclavihedbergella" chevaliensis* was tentatively assigned to the genus *Pseudoclavihedbergella* Georgescu (2009) according to the features of the wall texture (smooth and macroperforate) resembling that yielded by the *P. simplicissima* morphogroup (Falzoni et al., 2016a). However, the genus *Pseudoclavihedbergella* was erected to exclusively accommodate specimens with radially elongated chambers in the ultimate whorl, a feature that is not observed in *"P." chevaliensis.* For the time being, we retain the original generic assignment of *chevaliensis* pending further studies on well-preserved specimens from other localities. As a consequence, the genus is quoted in the text.

Genus *Muricohedbergella* Huber and Leckie, 2011

Type species. Globigerina cretacea var. *delrioensis* Carsey, 1926, p. 43, fig. 16.

Muricohedbergella kyphoma (Hasegawa, 1999)

(Fig. 8, 1A–C, 2A–C, 3A–E, 4A–C, 5A–C)

1999 *Hedbergella kyphoma* Hasegawa, p. 181, fig. 5, n. 1–4 (lower Turonian, Takinosawa Fm., Japan)

Distinguishing features. *Muricohedbergella kyphoma* (Fig. 8, 1A–C, 2A–C, 3A–E, 4A–C, 5A–C) differs from *M. planispira* (Fig. 8, 6A–C) by usually possessing more chambers in the last whorl that are subtriangular on the umbilical side and reniform and occasionally

elongated in the direction of coiling on the spiral side. Moreover, the chamber size increase rate is slower and more irregular in *M. kyphoma*, while the inner whorl is more depressed in *M. planispira*. The wall texture is macroperforate (pore diameter >2.5 μm) and slightly to moderately pustulose in both species. It differs from *"P." chevaliensis* (Fig. 7, 8A–C, 9A–C) by being less compressed in lateral view, by having a less lobate equatorial periphery and by typically having subtriangular rather than subglobular chambers on the umbilical side. Moreover, the wall texture of "*P." chevaliensis* is smoother and shows larger pores. *Muricohedbergella kyphoma* differs from both species by usually being larger in size. The holotype of *Globigerina loetterli* Nauss (1947) is poorly preserved (see Georgescu, 2010) hampering a detailed morphological comparison with *M. kyphoma*. However, the latter species differs from the holotype of *G. loetterli* by having a lower trochospire, subrectangular rather than subcircular chambers on the spiral side and subtriangular rather than globular chambers on the umbilical side.

Remarks. *Muricohedbergella kyphoma* was described from the *W. archaeocretacea* Zone of Japan (Hasegawa, 1999) and never recognized in other localities. At Eastbourne, *M. kyphoma* commonly occurs in the Plenus Marl Bed 4 in the interval corresponding to the topmost *R. cushmani* Zone to lowermost *W. archaeocretacea* Zone (i.e., 11.2 to 12.2 m above the base of the section). An increase in abundance of *M. kyphoma* slightly above the extinction level of *R. cushmani* was also reported in Japan (Hasegawa, 1999).

Genus *Whiteinella* Pessagno, 1967

Type species. Whiteinella archaeocretacea Pessagno, 1967, pl. 54, figs. 22–24.

Whiteinella cf. *baltica* Douglas and Rankin, 1969

(Fig. 8, 7A–C, 8A–C)

Distinguishing features. The very slow chamber increase rate and arrangement in the ultimate whorl strictly resemble that shown by the type specimens of *W. baltica*. However, *W.* cf. *baltica* (Fig. 8, 7A–C, 8A–C) differs from *W. baltica* by having a higher trochospire. It differs from the holotype of *Whiteinella paradubia* (Fig. 8, 9A–C) by having fewer chambers (4 to 4.5 rather than 6 or more) in the last whorl.

Remarks. Specimens assigned to *Whiteinella* cf. *baltica* are frequent at Eastbourne and show a continuous stratigraphic distribution.

Genus *Praeglobotruncana* Bermudez, 1952

Type species. Globorotalia delrioensis Plummer, 1931, p. 199, pl. 13, fig. 2.

Praeglobotruncana gungardensis n. sp.

(Fig. 9, 1A–C, Holotype, 2A–C, Paratype A, 3A–C, Paratype B)

Description. Medium to large-sized, low trochospiral test; circular to suboval outline, moderately to strongly asymmetrical profile with flat to moderately convex spiral side, and moderately to strongly convex umbilical side; equatorial periphery moderately lobate, 5.5 to 7 chambers in the last whorl. Spiral side with petaloid chambers increasing slowly and sometimes irregularly in size as added; chamber surface is slightly inflated and moderately pustulose to smooth at the end of the last whorl; spiral sutures are curved to straight and generally depressed with the exception of the last 2 chambers of the penultimate and first 1 to 3 chambers of the last whorl, which usually show weakly raised spiral sutures marked

by aligned pustules. Umbilical side with subglobular to subtriangular chambers and straight and depressed sutures; umbilical area about 1/3 of the maximum diameter; primary aperture extraumbilical-umbilical. Relatively wide imperforate peripheral band marked by randomly distributed to partially aligned pustules usually disappearing toward the end of the last whorl; ultimate chambers usually tilted toward the umbilical area. Wall texture macroperforate.

Distinguishing features. *Praeglobotruncana gungardensis* (Fig. 9, 1A–C, 2A–C, 3A–C) resembles *Praeglobotruncana rillella* (Fig. 9, 4A–C) but differs by having a more symmetric lateral profile due to a moderately convex rather than flat spiral side and usually a larger umbilical area. It differs from *P. compressa* (Fig. 9, 5A–C) by having more chambers in the last whorl (5.5 to 7 rather than 4 to 4.5) that grow less rapidly in size, a higher trochospire and a larger umbilical area. It is differentiated from the other *Praeglobotruncana* species by the strongly convex umbilical side. It differs from *Helvetoglobotruncana praehelvetica* (Fig. 9, 6A–C) by having a smoother wall texture, a slightly raised inner whorl and a more biconvex lateral profile.

Remarks. This species shows stable and distinctive morphological features and occurs frequently in the Grey Chalk. It is also identified in the Plenus Marl and White Chalk, where it is less common.

Type locality. Gun Gardens, Eastbourne, SE England (Anglo-Paris Basin). Holotype and Paratype A from sample GC-340 (2.6 m), Paratype B from sample GC-180 (4.2 m).

Type level. Upper Cenomanian (*R. cushmani* Zone).

Repository. Holotype (Micro-Unimi n. 2059; Fig. 9, 1A–C), Paratype A (Micro-Unimi n. 2060; Fig. 9, 2A–C), Paratype B (Micro-Unimi n. 2061; Fig. 9, 3A–C) deposited in the Micropaleontological Collection, Università degli Studi di Milano, Dipartimento di Scienze della Terra “A. Desio”, Italy.

Maximum diameter. Holotype = 480 µm; Paratype A = 410 µm, Paratype B = 390 µm.

Praeglobotruncana plenusiensis n. sp.

(Fig. 9, 7A–C, Holotype, 8A–C, Paratype)

? 1985 *Praeglobotruncana praehelvetica* Trujillo in Leckie, p. 147, pl. 2, n. 2–3 (upper Cenomanian, Bridge Creek Limestone, Pueblo, Colorado)

Description. Medium to large-sized low trochospiral test; suboval outline, strongly asymmetrical profile with flat spiral side and strongly convex umbilical side; equatorial periphery moderately lobate, 4 to 5 chambers in the last whorl. Spiral side with crescent-shaped to petaloid chambers growing slowly in size as added; chamber surface is flat and smooth; spiral sutures are curved, marked by aligned pustules to keeled throughout the penultimate and ultimate whorl with the exception of the suture between the last two chambers, which is weakly raised to depressed. Umbilical side with subglobular to subtrapezoidal chambers and straight and depressed sutures; umbilical area relatively small about 1/3 to 1/4 of the maximum diameter; primary aperture extraumbilical-umbilical. Lateral profile with a thick imperforate peripheral band that is shifted toward the spiral side and disappears toward the end of the last whorl; the imperforate peripheral band is marked by pustules that are randomly distributed along the equatorial periphery. The last chamber is typically inflated in edge view and forms an angle of nearly 90° to the imperforate peripheral band. Wall texture macroperforate.

Distinguishing features. *Praeglobotruncana plenusiensis* (Fig. 9, 7A–C, 8A–C) differs from the holotype of *P. rillella* (Fig. 9, 4A–C) by possessing fewer chambers in the last whorl and raised spiral sutures. Moreover, the imperforate peripheral band is usually thicker and shifted toward the spiral side when the specimens are observed in lateral view.

It is distinguished from *P. gungardensis* n. sp. (Fig. 9, 1A–C, 2A–C, 3A–C) by having a thicker imperforate peripheral band, raised spiral sutures and a distinct plano-convex rather than biconvex lateral profile. It differs from *H. praehelvetica* (Fig. 9, 6A–C) by possessing a smoother wall texture and a thick imperforate peripheral band composed of coarse and randomly distributed pustules. By contrast, the single-keeled periphery in the *H. praehelvetica-H. helvetica* lineage is very thin and usually not visible in edge view (see the *Helvetoglobotruncana* type material and pristinely preserved specimens from Tanzania in Huber and Petrizzo, 2014).

Remarks. No other morphotypes with these morphological features were previously illustrated in the literature, with the possible exception of the spiral and lateral views of a specimen from the Pueblo section that was assigned to *Praeglobotruncana praehelvetica* (= *Helvetoglobotruncana praehelvetica*) (Leckie, 1985) (Fig. 9, 9A–B). This specimen, however, more likely belongs to the *Praeglobotruncana* lineage according to the features of its lateral profile (i.e., thick imperforate peripheral band) and to the genus level classification given by Leckie (1985).

Type locality. Gun Gardens, Eastbourne, SE England (Anglo-Paris Basin). Holotype from sample PM+520 (11.2 m) and Paratype A from sample PM+580 (11.8 m).

Type level. Upper Cenomanian (top *R. cushmani* to base *W. archaeocretacea* Zone).

Repository. Holotype (Micro-Unimi n. 2062; Fig. 9, 7A–C), Paratype (Micro-Unimi n. 2063; Fig. 9, 8A–C) deposited in the Micropaleontological Collection, Università degli Studi di Milano, Dipartimento di Scienze della Terra “A. Desio”, Italy.

Maximum diameter. Holotype = 475 µm; Paratype = 470 µm.

Genus *Dicarinella* Porthault, 1970

Type species. Globotruncana indica Jacob and Sastry, 1950, p. 267, fig. 2.

Dicarinella falsohelvetica Desmares, 2020

(Fig. 9, 10A–C; Fig. 10, 1A–C, 2A–C)

2020 *Dicarinella falsohelvetica* Desmares, p. 9, fig. 7, n. 5A–C (lowermost Turonian, Craie à *Terebratella carantonensis*, Mézières-sur-Ponthouin, France)

Distinguishing features. *Dicarinella falsohelvetica* (Fig. 9, 10A–C; Fig. 10, 1A–C, 2A–C) differs from *D. marianosi* (senior synonym of *D. elata* after Huber et al., 2017) by having a thick imperforate peripheral band separating two widely-spaced keels. By contrast, the holotype of *D. marianosi* (Fig. 10, 3A–C) possesses a thick single-keeled periphery with no imperforate peripheral band, although specimens with two very closely-spaced keels joining at the end of the last whorl were also considered to fall in its range of variability (Huber et al., 2017). In addition, *D. falsohelvetica* is distinguished from *D. marianosi* by having slightly inflated spiral chambers at the beginning of the last whorl, a flatter spiral side, a more pustulose test surface and a smaller umbilical area. It differs from *Dicarinella* cf. *primitiva* (Fig. 10, 4A–C, 5A–C) by having a larger and more umbilico-convex test, more chambers in the last whorl and keels that do not merge at the end of the last whorl. It differs from *P. plenusiensis* (Fig., 9, 7A–C, 8A–C) by having a larger umbilical area, keeled spiral sutures throughout the last whorl and two distinct keels rather than a thick imperforate peripheral band with pustules randomly distributed along the equatorial periphery. Nevertheless, *P. plenusiensis* and *D. falsohelvetica* share other morphological features (i.e., the strongly umbilico-convex profile, spiral petaloid chambers, and depressed umbilical sutures) suggesting that these species might be phylogenetically related.

Genus *Marginotruncana* Hofker, 1956

Type species. Rosalina marginata Reuss, 1845, p. 36, pl. 8, figs. 54A–B, pl. 13, figs. 68A–B.

The type species of *Marginotruncana* selected by Hofker (1956) is *marginata* Reuss (1845). However, Neagu (2012) pointed out that the type specimens of *marginata* illustrated by Reuss (1845, 1854) possess depressed umbilical sutures. Accordingly, Neagu (2012) assigned *marginata* to the genus *Dicarinella*. Nevertheless, the type species of *Marginotruncana* has never been replaced.

Marginotruncana caronae Peryt, 1980

(Fig. 10, 6A–C, 7A–C, 8A–C)

1980 *Marginotruncana caronae* Peryt, p. 60. Pl. 15, figs. 1A–C (upper Turonian, Poland)

2016a *Marginotruncana caronae* Peryt in Falzoni et al., p. 86, fig. 11, n. 1–2 (upper Cenomanian–lower Turonian, Clot Chevalier, Vocontian Basin, SE France)

2017 *Marginotruncana caronae* Peryt in Huber et al., p. 39, pl. 4, n. 5–9 (upper Turonian, TDP Site 31, Tanzania)

Distinguishing features. It differs from *Dicarinella takayanagii* by having raised spiral sutures throughout the final whorl and from *Marginotruncana pseudolinneiana* by possessing an inflated ultimate chamber on the umbilical side, less widely-spaced keels,

and weakly raised umbilical sutures. Specimens here assigned to *M. caronae*, as well as those illustrated in previous studies (Falzoni et al., 2016a; Huber et al., 2017), differ from its holotype by having a flat to weakly inflated chamber surface on the spiral side.

Remarks. The lateral and spiral sides of specimens assigned to *M. caronae* (Fig. 10, 6A–C, 7A–C, 8A–C) show very stable morphological features, while differences are observed on the umbilical side. Most specimens show depressed umbilical sutures with the exception of the last formed chamber, which may be bordered by a curved and raised suture. These morphotypes resemble that illustrated by Falzoni et al. (2016a) from a coeval stratigraphic interval of the Vocontian Basin. However, few specimens identified in the White Chalk possess distinctly curved and moderately raised umbilical sutures on several chambers and more closely resemble the *M. caronae* morphotypes illustrated by Huber et al. (2017) from the Turonian of Tanzania. Because specimens with raised umbilical sutures are found in a younger stratigraphic interval (Turonian), we suggest that the development of this feature might be acquired through gradual evolutionary steps.

Marginotruncana cf. *sigali* (Reichel, 1950)

(Fig. 10, 9A–C)

Distinguishing features. *Marginotruncana* cf. *sigali* (Fig. 10, 9A–C) resembles the holotype of *M. sigali* (Fig, 10, 10A–C) by having crescentic to subpetaloid chambers and raised sutures on the spiral side, U-shaped and mostly raised sutures on the umbilical side and a biconvex lateral profile. It differs from the holotype by having a thick imperforate peripheral band with pustules randomly distributed along the equatorial periphery rather than a single keel.

Remarks. Specimens with these morphological features were documented from the lowermost Turonian *W. archaeocretacea* Zone of the Vocontian Basin (Falzoni et al., 2016a) and interpreted as possible ancestor of *M. sigali*. Interestingly, *M.* cf. *sigali* occurs at Eastbourne in the *R. cushmani* Zone and it is not identified in the overlying stratigraphic interval. For this reason, the phyletic relationship with *M. sigali* requires further study.

Acknowledgements

The authors are indebted to the editor Eduardo A. M. Koutsoukos and to the reviewers R. Mark Leckie and Brian T. Huber for their fruitful and thoughtful comments that greatly improved the quality of this manuscript. Annachiara Bartolini (Muséum National d'Histoire Naturelle, MNHN, Paris, France) is warmly thanked for the help provided during the study of planktonic foraminiferal primary types deposited at the MNHN. Agostino Rizzi (CNR, Italy) and Sylvain Pont (MNHN, France) are acknowledged for their kind assistance at the Scanning Electron Microscope. This study was funded by a post-doctoral fellowship at the University of Milan to FF and by the Italian Ministry of Education and Research (MIUR), projects PRIN 2010X3PP8J_001 and PRIN 2017RX9XXXY E. Erba scientific coordinator. Research activity at the MNHN was supported by a SYNTHESYS Project (http://www.synthesys.info/) of the European Community Research Infrastructure Action (FP7 "Capacities" Program) to FF.

References

1414 Ando, A., Huber, B.T., MacLeod, K.G., 2010. Depth-habitat reorganization of planktonic
1415 foraminifera across the Albian/Cenomanian boundary. Paleobiology 36, 357–373.
1416 doi:10.1666/09027.1.
1417 Banner, B.T., Blow, W.H., 1959. The classification and stratigraphical distribution of the
1418 Globigerinaceae. Palaeontology 2, 1–27.
1419 Barclay R.S., McElwain J.C., Sageman B.B., 2010. Carbon sequestration activated by a
1420 volcanic CO_2 pulse during Ocean Anoxic Event 2. Nature Geoscience 3, 205–208.
1421 Bermudez, P.J., 1952. Estudio sistematico de los foraminiferos Rotaliformes. Boletin de
1422 Geologia Ministerio de Minas e Venezuela 2, 1–153.
1423 Bolli, H.M., 1959. Planktonic foraminifera from the Cretaceous of Trinidad, B.W.I. Bulletins
1424 of American Paleontology 39, 257–277.
1425 Bomou, B., Adatte, T., Tantawy, A.A., Mort, H., Fleitmann, D., Huang, Y., Föllmi, K.B.,
1426 2013. The expression of the Cenomanian–Turonian oceanic anoxic event in Tibet.
1427 Palaeogeography, Palaeoclimatology, Palaeoecology 369, 466–481.
1428 Boudinot, F.G., Dildar, N., Leckie, R.M., Parker, A., Jones, M.M., Sageman, B.B.,
1429 Bralower, T.J., Sepúlveda, J., 2020. Neritic ecosystem response to Oceanic Anoxic
1430 Event 2 in the Cretaceous Western Interior Seaway, USA. Palaeogeography,
1431 Palaeoclimatology, Palaeoecology 546, 109673.
1432 Brönnimann, P., 1952. Globigerinidae from the Upper Cretaceous (Cenomanian–
1433 Maestrichtian) of Trinidad, B.W.I. Bulletins of American Paleontology 34, 5–71.
1434 Brotzen, F., 1942. Die Foraminiferengattung *Gavellinella* nov. gen. und die Systematik der
1435 Rotaliformes. Sveriges Geologiska Undersökning, Ser. C, 36, 1–60.
1436 Caron, M., Homewood, P., 1983. Evolution of early planktic foraminifers. Marine
1437 Micropaleontology 7, 453-462. doi:10.1016/0377-8398(83)90010-5.

1438 Caron, M., Spezzaferri, S., 2006. Scanning electron microscope documentation of the lost
1439 holotypes of Mornod, 1949: *Thalmanninella reicheli* and *Rotalipora montsalvensis*. The
1440 Journal of Foraminiferal Research 36, 374–378.
1441 Caron, M., Dall'Agnolo, S., Accarie, H., Barrera, E., Kauffman, E.G., Amédro, F.,
1442 Robaszynski, F., 2006. High-resolution stratigraphy of the Cenomanian–Turonian
1443 boundary interval at Pueblo (USA) and Wadi Bahloul (Tunisia): stable isotope and bio-
1444 events correlation. Géobios 39, 171–200.
1445 Carsey, D.O., 1926. Foraminifera of the Cretaceous of Central Texas. University of Texas
1446 Bulletin, 2612, p. 1–56.
1447 Coccioni, R., Luciani, V., 2004. Planktonic foraminifera and environmental changes across
1448 the Bonarelli Event (OAE2, latest Cenomanian) in its type area: a high resolution study
1449 from the Tethyan reference Bottaccione section (Gubbio, central Italy). Journal of
1450 Foraminiferal Research 34, 109–129.
1451 Coccioni, R., Luciani, V., 2005. Planktonic foraminifers across the Bonarelli Event (OAE2,
1452 latest Cenomanian): the Italian record. Palaeogeography, Palaeoclimatology,
1453 Palaeoecology 224, 167–185.
1454 Coccioni, R., Premoli Silva, I., 1994. Planktonic foraminifera from the Lower Cretaceous of
1455 Rio Argos sections (southern Spain) and biostratigraphic implications. Cretaceous
1456 Research 15, 645–687.
1457 Coccioni, R., Premoli Silva, I., 2015. Revised Upper Albian–Maastrichtian planktonic
1458 foraminiferal biostratigraphy and magneto-stratigraphy of the classical Tethyan Gubbio
1459 section (Italy). Newsletters on Stratigraphy 48, 47–90.
1460 Coccioni, R., Luciani, V., Marsili, A., 2006. Cretaceous oceanic anoxic events and radially
1461 elongated chambered planktonic foraminifera: Paleoecological and paleoceanographic
1462 implications. Palaeogeography, Palaeoclimatology, Palaeoecology 235, 66–92.

1463 Corbett, M.J., Watkins, D.K., Pospichal, J.J., 2014. A quantitative analysis of calcareous
1464 nannofossil bioevents of the Late Cretaceous (Late Cenomanian–Coniacian) Western
1465 Interior Seaway and their reliability in established zonation schemes. Marine
1466 Micropaleontology 109, 30–45.
1467 Coxall, H.K., Wilson, P.A., Pearson, P.N., Sexton, P.F., 2007. Iterative evolution of digitate
1468 planktonic foraminifera. Paleobiology 33, 495–516.
1469 Cushman, J.A., 1931. *Hastigerinella* and other interesting foraminifera from the Upper
1470 Cretaceous of Texas. Contributions from the Cushman Foundation for Foraminiferal
1471 Research 7, 83–90.
1472 Cushman, J. A., Ten Dam, A., 1948. *Globigerinelloides*, a new genus of the
1473 Globigerinidae. Contributions from the Cushman Laboratory for Foraminiferal
1474 Research 24, 42–43.
1475 Desmares, D., Grosheny, D., Beaudoin, B., Gardin, S., Gauthier-Lafaye, F., 2007. High
1476 resolution stratigraphic record constrained by volcanic ashes layers at the
1477 Cenomanian-Turonian boundary in the Western Interior Basin, USA. Cretaceous
1478 Research 28, 561–582.
1479 Desmares, D., Grosheny, D., Beaudoin, B., 2008. Ontogeny and phylogeny of Upper
1480 Cenomanian rotaliporids (Foraminifera). Marine Micropaleontology 69, 91–105.
1481 Desmares, D., Crognier, N., Bardin, J., Testé, M., Beaudoin, B., Grosheny, D., 2016. A
1482 new proxy for Cretaceous paleoceanographic and paleoclimatic reconstructions:
1483 Coiling direction changes in the planktonic foraminifera *Muricohedbergella*
1484 *delrioensis*. Palaeogeography, Palaeoclimatology, Palaeoecology 445, 8–17.
1485 Desmares, D., Testé, M., Broche, B., Tremblin, M., Gardin, S., Villier, L., Masure, E.,
1486 Grosheny, D., Morel, N., Raboeuf, P., 2020. High-resolution biostratigraphy and
1487 chemostratigraphy of the Cenomanian stratotype area (Le Mans, France). Cretaceous
1488 Research 106, 104198, 1–15.

1489 Douglas, R.G., 1969. Upper Cretaceous planktonic foraminifera in northern California; Part
1490 1, Systematics. Micropaleontology 15, 151–209.
1491 Douglas, R.G., Rankin C., 1969. Cretaceous planktonic foraminifera from Bornholm and
1492 their zoogeographic significance. Lethaia 2, 185–217.
1493 Eicher, D.L., Diner, R., 1985. Foraminifera as indicators of water mass in the Cretaceous
1494 Greenhorn Sea, Western Interior. In: Pratt, L.M., Kauffman, E.G., Zelt, F.B. (Eds.),
1495 Fine-grained Deposits and Biofacies of the Cretaceous Western Interior Seaway:
1496 Evidence of Cyclic Sedimentary Processes, Field Trip Guidebook, Society of
1497 Economic Paleontologists and Mineralogists 4, 60–71.
1498 Eicher, D.L., Worstell, P., 1970. Cenomanian and Turonian foraminifera from the Great
1499 Plains, United States. Micropaleontology 16, 269–324.
1500 Elderbak, K., Leckie, R.M., 2016. Paleocirculation and foraminiferal assemblages of the
1501 Cenomanian–Turonian Bridge Creek Limestone bedding couplets: Productivity vs.
1502 dilution during OAE2. Cretaceous Research 60, 52–77.
1503 Eldrett, J.S., Ma, C., Bergman, S.C., Lutz, B., Gregory, F.J., Dodsworth, P., Phipps, M.,
1504 Hardas, P., Minisini, D., Ozkan, A., Ramezani, J., Bowring, S.A., Kamo, S.L.,
1505 Ferguson, K., Macaulay, C., Kelly, A.E., 2015. An astronomically calibrated
1506 stratigraphy of the Cenomanian, Turonian and earliest Coniacian from the Cretaceous
1507 Western Interior Seaway, USA: Implications for global chronostratigraphy. Cretaceous
1508 Research 56, 316–344.
1509 Eldrett, J.S., Dodsworth, P., Bergman, S.C., Wright, M., Minisini, D., 2017. Water-mass
1510 evolution in the Cretaceous Western Interior Seaway of North America and equatorial
1511 Atlantic. Climate of the Past 13, 855–878.
1512 Erba E., 2004. Calcareous nannofossils and Mesozoic oceanic anoxic events. Marine
1513 Micropaleontology 52, 85–106.

1514 Erbacher, J., Thurow, J., Littke, R., 1996. Evolution patterns of radiolaria and organic
1515 matter variations: a new approach to identify sea-level changes in mid-Cretaceous
1516 pelagic environments. Geology 24, 499–502.
1517 Ericson, D.B., 1959. Coiling direction of Globigerina pachyderma as a climatic index.
1518 Science 130, 219–220.
1519 Eternod Olvera, Y., 1959. Foraminiferos del Cretacico Superior de la Cuenca de Tampico-
1520 Tuxpan, Mexico. Boletin Association Mexicana de Geologos Petroleros 11, 63–134.
1521 Falzoni, F., Petrizzo, M.R., Jenkyns, H.C., Gale, A.S., Tsikos, H., 2016a. Planktonic
1522 foraminiferal biostratigraphy and assemblage composition across the Cenomanian–
1523 Turonian boundary interval at Clot Chevalier (Vocontian Basin, SE France).
1524 Cretaceous Research, 59, 69–97.
1525 Falzoni, F., Petrizzo, M.R., Clarke, L.J., MacLeod, K.G., Jenkyns, H.C., 2016b. Long-term
1526 Late Cretaceous oxygen- and carbon-isotope trends and planktonic foraminiferal
1527 turnover: A new record from the southern midlatitudes. GSA Bulletin 128, 1725–1735.
1528 Falzoni F., Petrizzo M.R., Caron M., Leckie R.M., Elderbak K., 2018. Age and
1529 synchronicity of planktonic foraminiferal bioevents across the Cenomanian-Turonian
1530 boundary interval (Late Cretaceous). Newsletters on Stratigraphy 51, 343–380.
1531 Forster A., Schouten S., Moriya K., Wilson P.A., Sinninghe Damsté, J.S., 2007. Tropical
1532 warming and intermittent cooling during the Cenomanian/Turonian oceanic anoxic
1533 event 2: Sea surface temperature records from the equatorial Atlantic.
1534 Paleoceanography, 22, PA1219, doi:10.1029/2006PA001349.
1535 Fraass, A.J., Kelly, D.C., Peters, S.E., 2015. Macroevolutionary history of the planktic
1536 foraminifera. Annual Review of Earth and Planetary Sciences 43, 139–166.
1537 Gale, A.S., 1996. Turonian correlation and sequence stratigraphy of the Chalk in southern
1538 England. Geological Society, London, Special Publication 103, 177–195.

1539 Gale, A.S., Christensen, W.K., 1996. Occurrence of the belemnite *Actinocamax plenus* in
1540 the Cenomanian of SE France and its significance. Bulletin of the Geological Society
1541 of Denmark 43, 68–77.
1542 Gale A.S., Jenkyns H.C., Kennedy W.J., Corfield, R.M., 1993. Chemostratigraphy versus
1543 biostratigraphy: data from around the Cenomanian–Turonian boundary. Journal of the
1544 Geological Society 150, 29–32.
1545 Gale, A.S., Smith, A.B., Monks, N.E.A., Young, J.A., Howard, A., Wray, D.S., Huggett,
1546 J.M., 2000. Marine biodiversity through the Late Cenomanian–Early Turonian:
1547 palaeoceanographic controls and sequence stratigraphic biases. Journal of the
1548 Geological Society 157, 745–757.
1549 Gale, A.S., Kennedy, W.J., Voigt, S., Walaszczyk, I., 2005. Stratigraphy of the Upper
1550 Cenomanian–Lower Turonian Chalk succession at Eastbourne, Sussex, UK:
1551 Ammonites, inoceramid bivalves and stable carbon isotopes. Cretaceous Research
1552 26, 460–487.
1553 Gale, A.S., Hancock, J.M., Kennedy, W.J., Petrizzo, M.R., Lees, J.A., Walaszczyk, I.,
1554 Wray, D.S., 2008. An integrated study (geochemistry, stable oxygen and carbon
1555 isotopes, nannofossils, planktonic foraminifera, inoceramid bivalves, ammonites and
1556 crinoids) of the Waxahachie Dam Spillway section, north Texas: a possible boundary
1557 stratotype for the base of the Campanian Stage. Cretaceous Research 29, 131–167.
1558 Gale A.S., Jenkyns H.C., Tsikos H., van Breugel Y., Sinninghe Damsté J.S., Bottini C.,
1559 Erba E., Russo F., Falzoni F., Petrizzo M.R., Dickson A.J., Wray D.S., 2019. High-
1560 resolution bio- and chemostratigraphy of an expanded record of Oceanic Anoxic Event
1561 2 (Late Cenomanian-Early Turonian) at Clot Chevalier, near Barrême, SE France
1562 (Vocontian Basin, SE France). Newsletters on Stratigraphy 52, 97–129. Doi:
1563 10.1127/nos/2018/0445.

1564 Gebhardt, H., Friedrich, O., Schenk, B., Fox, L., Hart, M.B., and Wagreich, M., 2010.
1565 Paleoceanographic changes at the northern Tethyan margin during the Cenomanian–
1566 Turonian Oceanic Anoxic Event (OAE-2): Marine Micropaleontology 77, 25–45.
1567 Georgescu, M.D., 2006. Santonian–Campanian planktonic foraminifera in the New Jersey
1568 coastal plain and their distribution related to the relative sea-level changes. Canadian
1569 Journal of Earth Sciences 43, 101–120.
1570 Georgescu, M.D., 2009. Upper Albian-lower Turonian non-schackoinid planktic
1571 foraminifera with elongate chambers: morphology reevaluation, taxonomy and
1572 evolutionary classification. Revista Española de Micropaleontología 41, 255–294.
1573 Georgescu, M.D., 2010. Evolutionary classification of the Upper Cretaceous (Turonian–
1574 lower Campanian) planktic foraminifera with incipient meridional
1575 ornamentation. Journal of Micropalaeontology 29, 149–161.
1576 Gilly, W.F., Beman, J.M., Litvin, S.Y., Robison, B.H., 2013. Oceanographic and biological
1577 effects of shoaling of the oxygen minimum zone. Annual review of marine science 5,
1578 393–420.
1579 González-Donoso, J.M., Linares, D., Robaszynski, F., 2007. The rotaliporids, a
1580 polyphyletic group of Albian-Cenomanian planktonic foraminifera: Emendation of
1581 genera. Journal of Foraminiferal Research 37, 175–186.
1582 Grosheny, D., Beaudoin, B., Morel, L., Desmares, D., 2006. High-resolution
1583 biostratigraphy and chemostratigraphy of the Cenomanian–Turonian Boundary Event
1584 in the Vocontian Basin, S-E France. Cretaceous Research 27, 629–640.
1585 Grosheny, D., Ferry, S., Jati, M., Ouaja, M., Bensalah, M., Atrops, F., Chikhi-Aouimeur, F.,
1586 Benkerouf-Kechid, F., Negra, H., Salem, H. A., 2013. The Cenomanian–Turonian
1587 boundary on the Saharan Platform (Tunisia and Algeria). Cretaceous Research 42,
1588 66–84.

1589 Grosheny, D., Ferry, S., Lecuyer, C., Thomas, A., Desmares, D., 2017. The Cenomanian–
1590 Turonian Boundary Event (CTBE) on the southern slope of the Subalpine Basin (SE
1591 France) and its bearing on a probable tectonic pulse on a larger scale. Cretaceous
1592 Research 72, 39–65.
1593 Hagn, H., Zeil, W., 1954. Globotruncanen aus dem Ober-Cenoman und Unter-Turon der
1594 Bayerischen Alpen. Eclogae Geologicae Helvetiae 47, 1–60.
1595 Hart, M.B., 1996. Recovery of the food chain after the Late Cenomanian extinction
1596 event. Geological Society, London, Special Publications 102, 265–277.
1597 Hart, M.B., 1999. The evolution and biodiversity of Cretaceous planktonic Foraminiferida.
1598 Geobios 32, 247–255.
1599 Hart, M.B., Leary, P.N., 1989. The stratigraphic and palaeogeographic setting of the late
1600 Cenomanian ‘anoxic’ event. Journal of the Geological Society 146, 305–310.
1601 Hart, M.B., Dodsworth, P., Duane, A.M., 1993. The late Cenomanian event in eastern
1602 England. Cretaceous Research 14, 495–508.
1603 Hart, M.B., Monteiro, J.F., Watkinson, M.P., Price, G.D., 2002. Correlation of events at the
1604 Cenomanian/Turonian boundary: Evidence from Southern England and Colorado. In:
1605 Wagreich, M. (Ed.), Aspects of Cretaceous Stratigraphy and Palaeobiogeography.
1606 Schriftenreihe der erdwissenschaftliche Kommission der Österreichische Akademie
1607 der Wissenschaften, Wien, 15: 35–46, Verlag der Österreichische Akademie der
1608 Wissenschaften, Wien.
1609 Hasegawa, T., 1995. Correlation of the Cenomanian/Turonian boundary between Japan
1610 and Western Interior of the United States. Journal of the Geological Society of Japan
1611 101, 2–12.
1612 Hasegawa, T., 1999. Planktonic foraminifera and biochronology of the Cenomanian-
1613 Turonian (Cretaceous) sequence in the Oyubari area, Hokkaido, Japan.
1614 Paleontological Research 3, 173–192.

1615 Hay, W.W., DeConto, R., Wold, C.N., Wilson, K.M., Voigt, S., Schulz, M., Wold-Rossby,
1616 A., Dullo, W.C., Ronov, A.B., Balukhovsky, A.N., Soeding, E., 1999. Alternative global
1617 Cretaceous paleogeography. In: Barrera, E., Johnson, C.C. (Eds.), The Evolution of
1618 the Cretaceous Ocean/climate System. Special Papers of the Geological Society of
1619 America 332, 1–47.
1620 Haynes, S.J., Huber, B.T., Macleod, K.G., 2015. Evolution and phylogeny of mid-
1621 Cretaceous (Albian–Coniacian) biserial planktic foraminifera. Journal of Foraminiferal
1622 Research 45, 42–81.
1623 Heimhofer, U., Wucherpfennig, N., Adatte, T., Schouten, S., Schneebeli-Hermann, E.,
1624 Gardin, S., Keller, G., Kentsch, S., Kujau, A., 2018. Vegetation response to
1625 exceptional global warmth during Oceanic Anoxic Event 2. Nature Communications 9,
1626 1–8, DOI: 10.1038/s41467-018-06319-6.
1627 Hofker, J., 1956. Die Globotruncanen von Nord-west Deustchland und Holland. Neues
1628 Jahrbuch für Geologie und Paläontologie Abh 103, 312–340.
1629 Huber, B.T., 1992. Upper Cretaceous planktic foraminiferal biozonation for the Austral
1630 Realm. Marine Micropaleontology 20, 107–128.
1631 Huber, B.T., Leckie, R.M., 2011. Planktic foraminiferal species turnover across deep-sea
1632 Aptian/Albian boundary sections. Journal of Foraminiferal Research 41, 53–95.
1633 Huber, B.T., Petrizzo, M.R., 2014. Evolution and taxonomic study of the Cretaceous
1634 planktic foraminiferal genus *Helvetoglobotruncana* Reiss, 1957. Journal of
1635 Foraminiferal Research 44, 40–57.
1636 Huber, B.T., Leckie, R.M., Norris, R.D., Bralower, T.J., CoBabe, E., 1999. Foraminiferal
1637 assemblage and stable isotopic change across the Cenomanian-Turonian boundary in
1638 the subtropical North Atlantic. Journal of Foraminiferal Research 29, 392–417.
1639 Huber, B.T., Petrizzo, M.R., Young, J.R., Falzoni, F., Gilardoni, S.E., Bown, P.R., Wade,
1640 B.S., 2016. Pforams@ microtax. Micropaleontology 62, 429–438.

1641 Huber, B.T., Petrizzo, M.R., Watkins, D.K., Haynes, S.J., MacLeod, K.G., 2017.
1642 Correlation of Turonian continental margin and deep-sea sequences in the subtropical
1643 Indian Ocean sediments by integrated planktonic foraminiferal and calcareous
1644 nannofossil biostratigraphy. Newsletters on Stratigraphy 50, 141–185.
1645 Huber, B.T., MacLeod, K.G., Watkins, D.K., Coffin, M.F., 2018. The rise and fall of the
1646 Cretaceous Hot Greenhouse climate. Global and Planetary Change 167, 1–23.
1647 Jacob, K., Sastry, M.V.A., 1950. On the occurrence of *Globotruncana* in Uttatur stage of
1648 the trichinopoly Cretaceous, South India. Current Science, 16, 266–268.
1649 Ion, J., 1976. A propos de la souche des Rotalipores, *Rotalipora praemontsalvensis* n. sp.:
1650 Dări de Seamă ale Şedinţelor, Institutul de Geologie şi Geofizică Bucharest 62, 39–46.
1651 Jarvis, I., Carson, G.A., Cooper, M.K.E., Hart, M.B., Leary, P.N., Tocher, B.A., Horne, D.,
1652 Rosenfeld, A., 1988. Microfossil assemblages and the Cenomanian–Turonian (Late
1653 Cretaceous) oceanic anoxic event. Cretaceous Research 9, 3–103.
1654 Jarvis, I., Gale, A.S., Jenkyns, H.C., Pearce, M.A., 2006. Secular variation in Late
1655 Cretaceous carbon isotopes: A new $\delta^{13}C$ carbonate reference curve for the
1656 Cenomanian–Campanian (99.6–70.6 Ma). Geological Magazine 143, 561–608.
1657 Jarvis, I., Lignum, J.S., Gröcke, D.R., Jenkyns, H.C., Pearce, M.A., 2011. Black shale
1658 deposition, atmospheric CO_2 drawdown, and cooling during the Cenomanian–
1659 Turonian Oceanic Anoxic Event. Paleoceanography 26, PA3201,
1660 doi:10.1029/2010PA002081.
1661 Jeans, C.V., Long, D., Hall, M.A., Bland, D.J., Cornford, C., 1991. The geochemistry of the
1662 Plenus Marls at Dover, England: evidence of fluctuating oceanographic conditions and
1663 of glacial control during the development of the Cenomanian–Turonian $\delta^{13}C$
1664 anomaly. Geological Magazine 128, 603–632.
1665 Jefferies, R.P.S., 1962. The palaeoecology of the *Actinocamax plenus* subzone (lowest
1666 Turonian) in the Anglo-Paris Basin. Palaeontology 4, 609–647.

1667 Jefferies, R.P.S., 1963. The stratigraphy of the *Actinocamax plenus* subzone (Turonian) in
1668 the Anglo-Paris Basin. Proceedings of the Geologists' Association 74, 1-33.
1669 Jenkyns, H.C., 2010. Geochemistry of oceanic anoxic events, Geochemistry, Geophysics,
1670 Geosystems 11, Q03004, doi:10.1029/2009GC002788.
1671 Jenkyns, H.C., Dickson, A.J., Ruhl, M., Boorn, S.H., 2017. Basalt-seawater interaction, the
1672 Plenus Cold Event, enhanced weathering and geochemical change: Deconstructing
1673 Oceanic Anoxic Event 2 (Cenomanian–Turonian, Late Cretaceous). Sedimentology
1674 64, 16–43.
1675 Jiménez Berrocoso, Á., Huber, B.T., MacLeod, K.G., Petrizzo, M.R., Lees, J.A., Wendler,
1676 I., Coxall, H., Mweneinda, A.K., Falzoni, F., Birch, H., Haynes, S. J., Bown, P.R.,
1677 Robinson, S.A., Singano, J.M., 2015. The Lindi Formation (upper Albian–Coniacian)
1678 and Tanzania Drilling Project Sites 36–40 (Lower Cretaceous to Paleogene):
1679 Lithostratigraphy, biostratigraphy and chemostratigraphy. Journal of African Earth
1680 Sciences 101, 282–308.
1681 Kaiho, K., Katabuchi, M., Oba, M., Lamolda, M., 2014. Repeated anoxia–extinction
1682 episodes progressing from slope to shelf during the latest Cenomanian. Gondwana
1683 Research 25, 1357–1368.
1684 Kalanat, B., Vaziri-Moghaddam, H., 2019. The Cenomanian/Turonian boundary interval
1685 deep-sea deposits in the Zagros Basin (SW Iran): Bioevents, carbon isotope record
1686 and palaeoceanographic model. Palaeogeography, Palaeoclimatology,
1687 Palaeoecology 533, 109238.
1688 Keller, G., Pardo, A., 2004. Age and paleoenvironment of the Cenomanian-Turonian
1689 global stratotype section and point at Pueblo, Colorado. Marine Micropaleontology 51,
1690 95–128.
1691 Keller, G., Han, Q., Adatte, T., Burns, S., 2001. Paleoenvironment of the Cenomanian-
1692 Turonian transition at Eastbourne, England. Cretaceous Research 22, 391–422.

Keller, G., Adatte, T., Berner, Z., Chellai, E.H., Stueben, D., 2008. Oceanic events and biotic effects of the Cenomanian-Turonian anoxic event, Tarfaya Basin, Morocco. Cretaceous Research 29, 976–994.

Kennedy, W.J., Walaszczyk, I., Cobban, W.P., 2005. The Global Boundary Stratotype Section and Point for the base of the Turonian Stage of the Cretaceous: Pueblo, Colorado, USA. Episodes 28, 93–104.

Kopaevich, L., Vishnevskaya, V., 2016. Cenomanian–Campanian (Late Cretaceous) planktonic assemblages of the Crimea–Caucasus area: Palaeoceanography, palaeoclimate and sea level changes. Palaeogeography, Palaeoclimatology, Palaeoecology 441, 493–515.

Kugler, H.G., Bolli, H.M., 1967. Cretaceous biostratigraphy in Trinidad, WI. Asociación Venezolana de Geología, Minería y Petróleo 10, 209–236.

Kuhnt, W., Holbourn, A.E., Beil, S., Aquit, M., Krawczyk, T., Flögel, S., Chellai, E.H., Jabour, H., 2017. Unraveling the onset of Cretaceous Oceanic Anoxic Event 2 in an extended sediment archive from the Tarfaya-Laayoune Basin, Morocco. Paleoceanography 32, 923–946.

Kuroda J., Ogawa N.O., Tanimizu M., Coffin M.F., Tokuyama H., Kitazato H., Ohkouchi N., 2007. Contemporaneous massive subaerial volcanism and Late Cretaceous Oceanic Anoxic Event 2. Earth and Planetary Science Letters 256, 211–223.

Kuypers M.M.M., Pancost R.D., Nijenhuis I.A., Sinninghe Damstè J.S., 2002. Enhanced productivity led to increased organic carbon burial in the euxinic North Atlantic basin during the late Cenomanian oceanic anoxic event. Paleoceanography 17, 3–13.

Lamolda, M.A., Gorostidi, A., Paul, C.R.C., 1994. Quantitative estimates of calcareous nannofossil changes across the Plenus Marls (latest Cenomanian), Dover, England: implications for the generation of the Cenomanian-Turonian Boundary Event. Cretaceous Research 15, 143–164.

1719 Lamolda, M.A., Gorostidi, A., Martínez, R., López, G., Peryt, D., 1997. Fossil occurrences
1720 in the Upper Cenomanian–Lower Turonian at Ganuza, northern Spain: An approach to
1721 Cenomanian/Turonian boundary chronostratigraphy. Cretaceous Research 18, 331–
1722 353.
1723 Larson R.L., 1991. Latest pulse of the Earth: Evidence for a mid-Cretaceous super plume.
1724 Geology 19, 547–550.
1725 Leary P.N., Carson G.A., Cooper M.K.E., Hart M.B., Horne D., Jarvis I., Rosenfeld A.,
1726 Tocher B.A., 1989. The biotic response to the late Cenomanian oceanic anoxic event;
1727 integrated evidence from Dover, SE England. Journal of the Geological Society 146,
1728 311–317.
1729 Leckie, R.M., 1984. Mid-Cretaceous planktonic foraminiferal biostratigraphy off central
1730 Morocco. Deep Sea Drilling Project Leg 79, Sites 545 and 547. In: Hinz, K., Winterer
1731 E.L. et al. (Eds.), Initial Reports of the Deep Sea Drilling Project 79, U.S. Government
1732 Printing Office, Washington, D.C., 579– 620.
1733 Leckie, R.M., 1985. Foraminifera of the Cenomanian–Turonian boundary interval,
1734 Greenhorn Formation, Rock Canyon Anticline, Pueblo, Colorado. In: Pratt, L.M.,
1735 Kauffman, E.G., Zelt, F.B. (Eds.), Fine-grained Deposits and Biofacies of the
1736 Cretaceous Western Interior Seaway: Evidence of Cyclic Sedimentary Processes,
1737 Field Trip Guidebook, Society of Economic Paleontologists and Mineralogists 4, 139–
1738 149.
1739 Leckie, R.M., 1987. Paleoecology of mid-Cretaceous planktonic foraminifera: A
1740 comparison of open oceans and epicontinental sea assemblages. Micropaleontology
1741 33, 164–176.
1742 Leckie, R.M., Schmidt, M.G., Finkelstein, D., Yuretich, R., 1991. Paleoceanographic and
1743 paleoclimatic interpretations of the Mancos Shale (Upper Cretaceous), Black Mesa
1744 Basin, Arizona. In: Nations, J.D., Eaton, J.G. (Eds.), Stratigraphy, Depositional

1745 Environments, and Sedimentary Tectonics of the Western Margin, Cretaceous
1746 Western Interior Seaway, Geological Society of America Special Paper, 260, 139–152.
1747 Leckie, R.M., Yuretrich, R.F., West, O.L.O., Finkelstein, D., Schmidt, M., 1998.
1748 Paleoceanography of the southwestern Western Interior Sea during the time of the
1749 Cenomanian–Turonian boundary (Late Cretaceous). In: Dean, W., Arthur, M.A. (Eds.),
1750 Stratigraphy and Paleoenvironments of the Cretaceous Western Interior Seaway.
1751 SEPM Concepts in Sedimentology and Paleontology 6, 101–126.
1752 Leckie, R.M., Bralower, T.J., Cashman, R., 2002. Oceanic anoxic events and plankton
1753 evolution: Biotic response to tectonic forcing during the mid-Cretaceous.
1754 Paleoceanography 17, doi: 10.1029/2001PA000623.
1755 Linnert, C., Mutterlose, J., Mortimore, R., 2011. Calcareous nannofossils from Eastbourne
1756 (southeastern England) and the paleoceanography of the Cenomanian–Turonian
1757 Boundary interval. Palaios 26, 298–313.
1758 Lirer, F., 2000. A new technique for retrieving calcareous microfossils from lithified lime
1759 deposits. Micropaleontology 46, 365–369.
1760 Loeblich A.R., Tappan H., 1961. Cretaceous planktonic foraminifera; part 1, Cenomanian.
1761 Micropaleontology 7, 257–304.
1762 Longoria, J.F., 1973. *Pseudoticinella*, a new genus of planktonic foraminifera from the
1763 early Turonian of Texas. Revista Española de Micropaleontología 5, 417–423.
1764 Longoria, J.F., 1974. Stratigraphic, morphologic and taxonomic studies of Aptian
1765 planktonic foraminifera: Revista Española de Micropaleontología, Numero
1766 Extraordinario, 5–107.
1767 Lowery, C.M., Leckie, R.M., 2017. Biostratigraphy of the Cenomanian-Turonian Eagle
1768 Ford Shale of South Texas. Journal of Foraminiferal Research 47, 105–128.
1769 Lowery, C.M., Corbett, M.J., Leckie, R.M., Watkins, D., Miceli Romero, A., Pramudito, A.,
1770 2014. Foraminiferal and nannofossil paleoecology and paleoceanography of the

1771 Cenomanian–Turonian Eagle Ford Shale of southern Texas. Palaeogeography,
1772 Palaeoclimatology, Palaeoecology 413, 49–65.
1773 Luciani, V., Cobianchi, M., 1999. The Bonarelli Level and other black shales in the
1774 Cenomanian-Turonian of the northeastern Dolomites (Italy): calcareous nannofossil
1775 and foraminiferal data. Cretaceous Research 20, 135–167.
1776 MacLeod K.G., Jiménez Berrocoso Á., Huber B.T., Wendler I.E., 2013. A stable and hot
1777 Turonian without glacial $\delta^{18}O$ excursions is indicated by exquisitely preserved
1778 Tanzanian foraminifera. Geology 41, 1083–1086, doi:/10.1130/G34510.1.
1779 Magné, J., Sigal, J., Cheylan, G., 1954. Description des espèces nouvelles; 1–
1780 Foraminifères. Résultats géologiques et micropaléontologiques du sondage d'El
1781 Krachem (Hauts Plateaux algérois) 3, 480–489.
1782 Magniez-Jannin, F. 1998. L'élongation des loges chez les foraminifères planctoniques du
1783 Crétacé inférieur: une adaptation à la sous-oxygénation des eaux? (Chamber
1784 elongation in Early Cretaceous planktonic foraminifera: an adaptive response to
1785 oxygen depleted water?). Comptes Rendus de l'Académie des Sciences, ser. II,
1786 Sciences de lat Terre et des Planètes 326, 207–213.
1787 Masters, B.A., 1976. Planktic foraminifera from the Upper Cretaceous Selma Group,
1788 Alabama. Journal of Paleontology 50, 318–330.
1789 Masters, B.A., 1977. Mesozoic planktonic foraminifera. A world-wide review and analysis.
1790 In: Ramsay, A.T.S. (Eds.) Oceanic Micropaleontology 1, 301–732. Academic Press,
1791 London.
1792 Mornod, L., 1950. Les Globorotalidés du Crétacé supérieur du Montsalvens (Préalpes
1793 fribourgeoises). Eclogae geologicae Helvetiae 42, 573–596.
1794 Morrow, A.L., 1934. Foraminifera and Ostracoda from the Upper Cretaceous of Kansas. J.
1795 Paleontol. 8, 186–205.

1796 Mort, H., Jacquat, O., Adatte, T., Steinmann, P., Föllmi, K., Matera, V., Berner, Z., Stüben,
1797 D., 2007. The Cenomanian/Turonian anoxic event at the Bonarelli Level in Italy and
1798 Spain: enhanced productivity and/or better preservation? Cretaceous Research 28,
1799 597–612.
1800 Moullade, M., Bellier, J.P., Tronchetti, G., 2002. Hierarchy of criteria, evolutionary
1801 processes and taxonomic simplification in the classification of Lower Cretaceous
1802 planktonic foraminifera. Cretaceous Research 23, 111–148.
1803 Nauss, A.W., 1947. Cretaceous microfossils of the Vermilion area, Alberta. Journal of
1804 Paleontology 329–343.
1805 Nederbragt, A.J., Fiorentino, A., 1999. Stratigraphy and palaeoceanography of the
1806 Cenomanian–Turonian Boundary Event in Oued Mellegue, north-western Tunisia.
1807 Cretaceous Research 20, 47–62.
1808 Norris, R.D., Wilson, P.A., 1998. Low-latitude sea-surface temperatures for the mid-
1809 Cretaceous and the evolution of planktic foraminifera. Geology 26, 823–826.
1810 O'Brien C.L., Robinson S.A., Pancost R.D., Sinninghe Damsté J.S., Schouten S., Lunt
1811 D.J., Alsenz H., Bornemann A., Bottini C., Brassell, S.C., Farnsworth A., Forster A.,
1812 Huber B.T., Inglis G.N., Jenkyns H.C., Linnert C., Littler K., Markwick P., McAnena A.,
1813 Mutterlose J., Naafs B.D.A., Püttmann W., Sluijs A., van Helmond A.G.M.N., Vellekoop
1814 J., Wagner T., Wrobel N.E., 2017. Cretaceous sea-surface temperature evolution:
1815 Constraints from TEX_{86} and planktonic foraminiferal oxygen isotopes. Earth Science
1816 Reviews 172, 224–247.
1817 O'Connor, L.K., Jenkyns, H.C., Robinson, S.A., Remmelzwaal, S.R., Batenburg, S.J.,
1818 Parkinson, I.J., Gale, A.S., 2020. A re-evaluation of the Plenus Cold Event, and the
1819 links between CO_2, temperature, and seawater chemistry during OAE 2.
1820 Paleoceanography and Paleoclimatology 35, e2019PA003631, doi:
1821 10.1029/2019PA003631.

1822 Oba, M., Kaiho, K., Okabe, T., Lamolda, M.A., Wright, J.D., 2011. Short-term euxinia
1823 coinciding with rotaliporid extinctions during the Cenomanian-Turonian transition in the
1824 middle-neritic eastern North Atlantic inferred from organic compounds. Geology *39*,
1825 519–522.
1826 Ostrander, C.M., Owens, J.D., Nielsen, S.G., 2017. Constraining the rate of oceanic
1827 deoxygenation leading up to a Cretaceous Oceanic Anoxic Event (OAE-2:~94
1828 Ma). Science Advances 3, e1701020.
1829 Pancost R.D., Crawford N., Magness S., Turner A., Jenkyns H.C., Maxwell J.R., 2004.
1830 Further evidence for the development of photic-zone euxinic conditions during
1831 Mesozoic oceanic anoxic events. Journal of the Geological Society 161, 353–364.
1832 Paul, C.R.C., Lamolda, M.A., Mitchell, S.F., Vaziri, M.R., Gorostidi, A., Marshall, J.D.,
1833 1999. The Cenomanian–Turonian boundary at Eastbourne (Sussex, UK): a proposed
1834 European reference section. Palaeogeography, Palaeoclimatology, Palaeoecology
1835 150, 83–121.
1836 Pearce, M.A., Jarvis, I., Tocher, B.A., 2009. The Cenomanian–Turonian boundary event,
1837 OAE2 and palaeoenvironmental change in epicontinental seas: new insights from the
1838 dinocyst and geochemical records. Palaeogeography, Palaeoclimatology,
1839 Palaeoecology 280, 207–234.
1840 Peryt, D., 1980. Planktic foraminifera zonation of the Upper Cretaceous in the Middle
1841 Vistula river Valley, Poland. Paleontologia Polonica 41, 1–96.
1842 Pessagno, E.A., Jr., 1967. Upper Cretaceous planktonic foraminifera from the western
1843 Gulf coastal Plain. Paleontographica Americana 5, 245–445.
1844 Petrizzo, M.R., 2000. Upper Turonian-lower Campanian planktonic foraminifera from
1845 southern mid-high latitudes (Exmouth Plateau, NW Australia): biostratigraphy and
1846 taxonomic notes. Cretaceous Research 21, 479–505.

1847 Petrizzo, M.R., 2001. Late Cretaceous planktonic foraminifera from Kerguelen Plateau
1848 (ODP Leg 183): new data to improve the Southern Ocean biozonation. Cretaceous
1849 Research 22, 829–855.
1850 Petrizzo, M.R., Huber, B.T., 2006. Biostratigraphy and taxonomy of Late Albian planktonic
1851 foraminifera from ODP Leg 171B (western north Atlantic Ocean). Journal of
1852 Foraminiferal Research 36, 165–189.
1853 Petrizzo, M.R., Huber, B.T., Wilson, P.A., MacLeod, K.G., 2008. Late Albian
1854 paleoceanography of the western subtropical North Atlantic. Paleoceanography 23,
1855 PA1213. doi:10.1029/2007PA001517.
1856 Petrizzo, M.R., Falzoni, F., Premoli Silva, I., 2011. Identification of the base of the lower-to-
1857 middle Campanian *Globotruncana ventricosa* Zone: Comments on reliability and
1858 global correlations. Cretaceous Research 32, 387–405.
1859 Petrizzo, M.R., Caron, M., Premoli Silva, I., 2015. Remarks on the identification of the
1860 Albian/Cenomanian boundary and taxonomic clarification of the planktonic foraminifera
1861 index species *globotruncanoides*, *brotzeni* and *tehamaensis*. Geological
1862 Magazine 152, 521–536.
1863 Petrizzo, M.R., Jiménez Berrocoso, Á., Falzoni, F., Huber, B.T., MacLeod, K.G., 2017. The
1864 Coniacian–Santonian sedimentary record in southern Tanzania (Ruvuma Basin, East
1865 Africa): Planktonic foraminiferal evolutionary, geochemical and palaeoceanographic
1866 patterns. Sedimentology 64, 252–285.
1867 Plummer, H.J., 1931. Some Cretaceous foraminifera in Texas. University of Texas Bulletin
1868 3101, 109–203.
1869 Porthault, B., 1970. Le Sénonien inférieur de Puget-Théniers (Alpes-Maritimes) et sa
1870 microfaune. In: Donze, P., Thomel, G., de Villoutreys, O. (Eds.), Géobios 3, 41–106.

1871 Premoli Silva, I., Sliter, W.V., 1995. Cretaceous planktonic foraminiferal biostratigraphy
1872 and evolutionary trends from the Bottaccione section, Gubbio, Italy. Palaeontographia
1873 Italica 81, 2–90.
1874 Premoli Silva, I., Sliter, W.V., 1999. Cretaceous paleoceanography: Evidence from
1875 planktonic foraminiferal evolution. In: Barrera, E., Johnson, C.C., (Eds.), The Evolution
1876 of the Cretaceous Ocean-Climate System. Special Papers of the Geological Society of
1877 America 332, 301–328, doi:10.1130/0-8137-2332-9.301.
1878 Reichel, M., 1950. Observations sur les *Globotruncana* du gisement de la Breggia
1879 (Tessin). Eclogae Geologicae Helveticae 42, 596–617.
1880 Reolid, M., Sánchez-Quiñónez, C.A., Alegret, L., Molina, E., 2015. Palaeoenvironmental
1881 turnover across the Cenomanian-Turonian transition in Oued Bahloul, Tunisia:
1882 foraminifera and geochemical proxies. Palaeogeography, Palaeoclimatology,
1883 Palaeoecology 417, 491–510. doi:10.1016/j.palaeo.2014.10.011.
1884 Reuss, A.E., 1845. Die Versteinerungen der böhmischen Kreide-Formation. E.
1885 Schweizebart, Stuttgart, 1–58.
1886 Robaszynski, F., Caron, M., 1995. Foraminiféres planctoniques du Crétacé: commentaire
1887 de la zonation Europe-Méditerranée. Bulletin de la Société Géologique de France 166,
1888 681–692.
1889 Robaszynski, F., González-Donoso, J.M., Linares, D., Amèdro, F., Caron, M., Dupuis, C.,
1890 D'Hondt, A.V., Gartner, S., 2000. Le Crétacé supérieur de la région de Kalaat Senan,
1891 Tunisie Centrale. Litho-biostratigraphie intégrée: zones d'ammonites, de foraminifères
1892 planctoniques et de nannofossiles du Turonien supérieur au Maastrichtien: Bulletin
1893 des Centres de Recherche et d'Exploration-Production d'Elf-Aquitaine 22, 359–490.
1894 Scheibnerova, V., 1960. Poznamky rodu *Praeglobotruncana* Bermudez z kysuckych
1895 vrstiev bradloveho pasma. Geol. Sb. Bratislava 11, 85–90.

1896 Scheibnerova, V., 1962. Stratigrafia strednej a vrchnej kriedy tetydní oblasti na zaklade
1897 globotruncanid. Geologica Carpathica 13, 219–226.
1898 Schlanger, S.O., Jenkyns, H.C., 1976. Cretaceous oceanic anoxic events: Causes and
1899 consequences. Geologie en Mijnbouw 55, 179–184.
1900 Schlanger, S.O., Arthur, M.A., Jenkyns, H.C., Scholle, P.A., 1987. The Cenomanian-
1901 Turonian Oceanic Anoxic Event, I. Stratigraphy and distribution of organic carbon-rich
1902 beds and the marine $\delta^{13}C$ excursion. Geological Society, London, Special Publications
1903 26, 371–399.
1904 Scholle, P.A., Arthur, M.A., 1980. Carbon isotope fluctuations in Cretaceous pelagic
1905 limestones: Potential stratigraphic and petroleum exploration tool. AAPG Bulletin 64,
1906 67–87.
1907 Schrag D.P., DePaolo, D.J., Richter, F.M., 1995. Reconstructing past sea surface
1908 temperatures: correcting for diagenesis of bulk marine carbonate. Geochimica et
1909 Cosmochimica Acta 59, 2265–2278.
1910 Sigal, J., 1948. Notes sur les genres de foraminiferes *Rotalipora* Brotzen, 1942 et
1911 *Thalmanninella* (Famille des Globorotaliidae). Revue de l'Institut Francais du Petrole
1912 et Annales des Combustible Liquides, 3, 95–103.
1913 Sigal, J., 1952. Aperçu stratigraphique sur la Micropaléontologie du Crétacé. Alger, 19th
1914 Int. Geol. Congr., Monographies Régionales, 1st ser., Algérie 26, 1–45.
1915 Sinninghe Damsté, J.S., Kuypers, M.M., Pancost, R.D., Schouten, S., 2008. The carbon
1916 isotopic response of algae, (cyano)bacteria, archaea and higher plants to the late
1917 Cenomanian perturbation of the global carbon cycle: Insights from biomarkers in black
1918 shales from the Cape Verde Basin (DSDP Site 367). Organic Geochemistry 39, 1703–
1919 1718.
1920 Sinninghe Damsté, J.S., van Bentum, E.C., Reichart, G.J., Pross, J., Schouten, S., 2010.
1921 A CO_2 decrease-driven cooling and increased latitudinal temperature gradient during

1922 the mid-Cretaceous Oceanic Anoxic Event 2. Earth and Planetary Science Letters
1923 293, 97–103.
1924 Sliter, W.V., 1972. Cretaceous foraminifera-depth habitats and their origin. Nature 239,
1925 514-515. doi:10.1038/239514a0.
1926 Stramma, L., Johnson, G.C., Sprintall, J., Mohrholz, V., 2008. Expanding oxygen-minimum
1927 zones in the tropical oceans. Science 320, 655–658.
1928 Tappan, H., 1943. Foraminifera from the Duck Creek formation of Oklahoma and
1929 Texas. Journal of Paleontology 17, 476–517.
1930 Trujillo, E.F., 1960. Upper Cretaceous foraminifera from near Redding, Shasta County,
1931 California. Journal of Paleontology 34, 290–346.
1932 Tsikos, H., Jenkyns, H.C., Walsworth-Bell, B., Petrizzo, M.R., Forster, A., Kolonic, S.,
1933 Erba, E., Premoli Silva, I., Baas, M., Wagner, T., Sinninghe Damsté, J.S., 2004.
1934 Carbon-isotope stratigraphy recorded by the Cenomanian–Turonian Oceanic Anoxic
1935 Event: Correlation and implications based on three localities. Journal of the Geological
1936 Society of London 161, 711–719.
1937 Turgeon, S.C., Creaser, R.A., 2008. Cretaceous Oceanic Anoxic Event 2 triggered by a
1938 massive magmatic episode. Nature, 454, 323–326, doi:10.1038/nature07076.
1939 van Helmond, N.A., Sluijs, A., Papadomanolaki, N., Plint, A.G., Gröcke, D., Pearce, M.A.,
1940 Eldrett, J.S., Trabucho-Alexandre, J., Walaszczyk, I., van de Schootbrugge, B.,
1941 Brinkhuis, H., 2016. Equatorward phytoplankton migration during a cold spell within
1942 the Late Cretaceous super-greenhouse. Biogeosciences 13, 2859–2872.
1943 Voigt S., Gale A.S., Voigt T., 2006. Sea-level change, carbon cycling and palaeoclimate
1944 during the Late Cenomanian of northwest Europe; an integrated palaeoenvironmental
1945 analysis. Cretaceous Research 27, 836–858.
1946 Voigt, S., Erbacher, J., Mutterlose, J., Weiss, W., Westerhold, T., Wiese, F., Wilmsen, M.,
1947 Wonik, T., 2008. The Cenomanian – Turonian of the Wunstorf section – (North

Germany): Global stratigraphic reference section and new orbital time scale for Oceanic Anoxic Event 2. Newsletters on Stratigraphy 43, 65–89.

Wendler, J., Gräfe, K.U., Willems, H., 2002. Palaeoecology of calcareous dinoflagellate cysts in the mid-Cenomanian Boreal Realm: implications for the reconstruction of palaeoceanography of the NW European shelf sea. Cretaceous Research 23, 213–229.

Westermann, S., Caron, M., Fiet, N., Fleitmann, D., Matera, V., Adatte, T., Föllmi, K.B., 2010. Evidence for oxic conditions during oceanic anoxic event 2 in the northern Tethyan pelagic realm. Cretaceous Research 31, 500–514.

Wilmsen, M., 2003. Sequence stratigraphy and palaeoceanography of the Cenomanian Stage in northern Germany. Cretaceous Research 24, 525–568.

Wilmsen, M., Niebuhr, B., Chellouche, P., 2010. Occurrence and significance of Cenomanian belemnites in the lower Danubian Cretaceous Group (Bavaria, southern Germany). Acta Geologica Polonica 60, 231–241.

Wilson, P.A., Norris, R.D., 2001. Warm tropical ocean surface and global anoxia during the mid-Cretaceous period. Nature 412, 425–429.

Taxonomic Appendix

Remarks on selected species mentioned in the text and in the figures but not discussed in the taxonomy section are provided below with the author(s) and year of description to better clarify the species concept applied in this study. The author(s) and year of description of all other species mentioned in this study but not included in the list below can be found in the database “pf@mikrotax” available at http://www.mikrotax.org/pforams/index.html (see Huber et al., 2016).

The taxonomy of biserial species follows Haynes et al. (2015). The term “*Heterohelix*” shift is maintained herein to be consistent with previous authors, however the genus

"*Heterohelix*" is quoted in the text and figures, because all biserial species occurring across the C/T boundary are currently accommodated in other genera (e.g., *Protoheterohelix* and *Planoheterohelix*).

Dicarinella hagni (Scheibnerova, 1962)

Morphotypes resembling the holotype of *Dicarinella roddai* Hasegawa (1999) are included in the range of variability of *D. hagni* due to the identification of many specimens with transitional morphological features.

Dicarinella marginata (Reuss, 1845)

The species concept follows the revision by Neagu (2012).

Dicarinella cf. *primitiva* (Dalbiez, 1955)

The specimens here assigned to *D.* cf. *primitiva* are distinguished from the closely resembling *D. hagni* (Scheibnerova, 1962) by possessing a planoconvex profile with a distinctly flat spiral side and keels joining at the end of the final whorl as observed in the holotype of *D. primitiva* and following the species concept by Falzoni et al. (2016a). However, the holotype of *D. primitiva* was illustrated only in lateral view, therefore a complete evaluation of its original species concept requires further study.

Helvetoglobotruncana cf. *praehelvetica* (Trujillo, 1960)

The species concept follows Falzoni et al. (2018).

Muricohedbergella delrioensis (Carsey, 1926)

Morphotypes falling in the range of variability of the neotype by Masters (1976) and of the neotype by Longoria (1974) have been included in the range of variability of M. *delrioensis* in agreement with Petrizzo and Huber (2006).

Captions

Fig. 1. Paleogeographic reconstruction for the late Cenomanian (94 Ma), with location of Eastbourne and of the other sections discussed in this study (after Hay et al., 1999).

Fig. 2. Stratigraphic distribution and relative abundance of planktonic foraminiferal species at Gun Gardens, Eastbourne (SE England). Lithostratigraphy and carbon-isotope profile after Tsikos et al. (2004), position of peaks A, B and C after Jarvis et al. (2006) and Voigt et al. (2008) (see Falzoni et al., 2018 for discussion). Age/Stage and ammonite stratigraphy after Gale et al. (2005). Plenus Cold Event (PCE) interval after Jenkyns et al. (2017). The stratigraphic distribution of cool-water taxa potentially associated with the PCE is highlighted (see text for further details). Eclipse = temporary disappearance of selected taxa (sensu Coccioni and Premoli Silva, 1994; Coccioni and Luciani, 2004, 2005). Abbreviation: *Thalm.* = *Thalmanninella*.

Fig. 3. Stratigraphic distribution and abundance of some planktonic foraminiferal species in selected mid-low latitude localities. Lithostratigraphy, oxygen- and carbon-isotope record of the Eastbourne section after Tsikos et al. (2004), peaks A, B and C after Jarvis et al. (2006) and Voigt et al. (2008), early Turonian thermal maximum and calcisphere acme at Eastbourne after Pearce et al. (2009). Plenus Cold Event (PCE) interval after Jenkyns et al. (2017). Age/Stage and ammonite stratigraphy after Gale et al. (2005). Correlation of sections with Eastbourne is according to published bio-, chemo- and litho-stratigraphic datums by Kennedy et al. (2005), Gale et al. (2005, 2019), Jarvis et al. (2011), Falzoni et al. (2016a), and Grosheny et al. (2017). Correlation with Ganuza is based on the $\delta^{13}C$ profile by Kaiho et al. (2014) and calcareous nannofossils events by

Lamolda et al. (1997). Planktonic foraminifera of Eastbourne and Morocco (Tarfaya, Core S57) after Tsikos et al. (2004), Falzoni et al. (2018) and this study; Pont d'Issole: Grosheny et al. (2006) and Jarvis et al. (2011); Clot Chevalier: Falzoni et al. (2016a) and this study; Spain, Ganuza: Lamolda et al. (1997); Iran, Lar Anticline: Kalanat and Vaziri-Moghaddam (2019); Pueblo: Leckie (1985), Leckie et al. (1998), Keller and Pardo (2004), Caron et al. (2006), Desmares et al. (2007, 2008), and Elderbak and Leckie (2016). Relative abundances of species are not available for Pont d'Issole and Ganuza. The specimen illustrated as *"G." bentonensis* by Lamolda et al. (1997) does not possess a reniform ultimate chamber in edge view and more likely falls in the range of variability of *"G." tururensis*. For this reason, the range of *"G." bentonensis* at Ganuza is reported as *"Globigerinelloides"* spp. The "*Heterohelix*" shift corresponds to the interval where the abundance of biserial taxa is equal or exceeds the 50% of the assemblage >63 μm according to its original definition (Leckie, 1985; Leckie et al., 1998).

Fig. 4. *Thalmanninella* specimens from the Eastbourne section and holotypes of the species discussed in the text. Scale bar = 100 μm. 1A–C, *Thalmanninella* cf. *brotzeni,* sample GC-420 (1.8 m); 2A–C, *Thalmanninella* cf. *brotzeni*, sample GC-200 (4.0 m); 3A–C, *Thalmanninella* cf. *brotzeni*, sample PM+120 (7.2 m); 4A–C, *Thalmanninella brotzeni* Sigal (1948), holotype (MNHN-F-F60843); 5A–C, *Thalmanninella brotzeni*, sample GC-180 (4.2 m); 6A–C, *Thalmanninella greenhornensis*, (Morrow, 1934), holotype (USNM PAL 75378); 7A–C, *Thalmanninella greenhornensis*, sample GC-260 (3.4 m); 8A–C, *Thalmanninella deeckei*, sample GC-340 (2.6 m); 9A–C, *Thalmanninella* cf. *greenhornensis*, sample GC-520 (0.8 m); 10A–C, *Thalmanninella* cf. *greenhornensis*, sample GC-480 (1.2 m).

Fig. 5. *Rotalipora* specimens from the Eastbourne section and holotypes of the species discussed in the text. Scale bar = 100 µm. 1A–C, *Rotalipora montsalvensis* (Mornod, 1950), holotype (NMB-C39014); 2A–C, *Rotalipora montsalvensis*, sample GC-340 (2.6 m); 3A–C, *Rotalipora montsalvensis*, sample PM+320 (9.2 m); 4A–C, *Rotalipora cushmani* (Morrow, 1934), holotype (USNM PAL 75377); 5A–C, *Rotalipora praemontsalvensis praemontsalvensis* Ion (1976), holotype (100636a); 6A–C, *Rotalipora praemontsalvensis altispira* Ion (1976), holotype (100636d); 7A–C, *Rotalipora praemontsalvensis*, sample PM+240 (8.4 m); 8A–C, *Rotalipora praemontsalvensis*, sample GC-480 (1.2 m); 9A–C, *Globorotalia multiloculata* Morrow (1934), holotype (USNM PAL 75379); 10A–C, *Pseudoticinella planoconvexa* Longoria (1973), holotype.

Fig. 6. *"Globigerinelloides"* specimens from the Eastbourne section and type specimens of the species discussed in the text. Scale bar = 100 µm. 1A–C, "*Globigerinelloides*" cf. *bollii*, sample GC-600 (0 m); 2A–C, "*Globigerinelloides*" *bollii* Pessagno (1967), holotype (USNM MO 689272); 3A–C, *"Globigerinelloides" bentonensis*, sample GC-560 (0.4 m); 4A–C, *"Globigerinelloides" ultramicrus*, sample GC-560 (0.4 m); 5A–C, *"Globigerinelloides" tururensis* (Brönnimann, 1952), holotype (USNM PAL 370092); 6A–B, *"Globigerinelloides" tururensis*, type specimen figured by Brönnimann (1952); 7A–B, *"Globigerinelloides" tururensis*, sample GC-560 (0.4 m); 8A–C, *"Globigerinelloides" tururensis*, sample GC-500 (1.0 m); 9A–C, *"Globigerinelloides" alvarezi* (Eternod Olvera, 1959), holotype (USNM PAL 528215).

Fig. 7. *Pseudoclavihedbergella* specimens from the Eastbourne section and type specimens of the species discussed in the text. Scale bar = 100 µm unless differently specified. 1A–C, *Pseudoclavihedbergella simplicissima* (Magné and Sigal, 1954), holotype (MNHN-F-F60880); 2A–D, *Pseudoclavihedbergella simplicissima* (Magné and Sigal,

1954), topotype (MNHN-F-F60880), 2D: scale bar = 20 μm; 3A–D, *Pseudoclavihedbergella amabilis* (Loeblich and Tappan, 1961), holotype (USNM PAL 371424), 3D: scale bar = 20 μm; 4A–B, *Pseudoclavihedbergella amabilis* (Loeblich and Tappan, 1961), paratype (USNM PAL 371425); 5A–D, *Pseudoclavihedbergella simplicissima*, sample GC-600 (0 m), 5D: scale bar = 20 μm; 6A–D, *Pseudoclavihedbergella simplicissima*, sample GC-340 (2.6 m), 6D: scale bar = 50 μm; 7A–C, *Pessagnoina simplex* (Morrow, 1934), holotype (USNM PAL 75376); 8A–C, *"Pseudoclavihedbergella" chevaliensis*, sample GC-560 (0.4 m); 9A–C, *"Pseudoclavihedbergella" chevaliensis* Falzoni et al. (2016a), holotype (Micro-Unimi n. 1988).

Fig. 8. *Muricohedbergella* and *Whiteinella* specimens from the Eastbourne section and type specimens of the species discussed in the text. Scale bar = 100 μm unless differently specified. 1A–C, *Muricohedbergella kyphoma* (Hasegawa, 1999), holotype (IGPS n. 102504); 2A–C, *Muricohedbergella kyphoma* (Hasegawa, 1999), paratype (IGPS n. 102507); 3A–E, *Muricohedbergella kyphoma,* sample PM+520 (11.2 m), 3D: scale bar = 50 μm, 3E: scale bar = 20 μm; 4A–C, *Muricohedbergella kyphoma*, sample PM+520 (11.2 m); 5A–C, *Muricohedbergella kyphoma*, sample PM+580 (11.8 m); 6A–C, *Muricohedbergella planispira* (Tappan, 1940), holotype (USNM CC 25113); 7A–C, *Whiteinella* cf. *baltica*, sample GC-600 (0 m); 8A–C, *Whiteinella* cf. *baltica*, sample GC-100 (5.0 m); 9A–C, *Whiteinella paradubia*, (Sigal, 1952), holotype (MNHN-F-F60808).

Fig. 9. *Praeglobotruncana* and *Dicarinella* specimens, and holotypes of the species discussed in the text. Scale bar = 100 μm. 1A-C, *Praeglobotruncana gungardensis* n. sp., holotype, sample GC-340 (2.6 m) (Micro-Unimi n. 2059); 2A–C, *Praeglobotruncana gungardensis*, n. sp., paratype A, sample GC-340 (2.6 m) (Micro-Unimi n. 2060); 3A–C,

Praeglobotruncana gungardensis, n. sp., paratype B, sample GC-180 (4.2 m) (Micro-Unimi n. 2061); 4A–C, *Praeglobotruncana rillella* Desmares (2020), holotype (P6M4360); 5A–C, *Praeglobotruncana compressa*, sample GC-340 (2.6 m); 6A–C, *Helvetoglobotruncana praehelvetica* (Trujillo, 1960), holotype (UCMP 48790); 7A-C, *Praeglobotruncana plenusiensis* n. sp., holotype, sample PM+520 (11.2 m) (Micro-Unimi n. 2062); 8A–C, *Praeglobotruncana plenusiensis* n. sp., paratype, sample PM+580 (11.8 m) (Micro-Unimi n. 2063); 9A–B, specimen illustrated by Leckie (1985) from the upper Cenomanian of the Pueblo section and possibly falling in the range of variability of *P. plenusiensis*; 10A–C, *Dicarinella falsohelvetica*, sample WC+360 (17.5 m).

Fig. 10. *Dicarinella* and *Marginotruncana* specimens from the Eastbourne section, and holotype of the species discussed in the text. Scale bar = 100 µm. 1A–C, *Dicarinella falsohelvetica*, sample WC+360 (17.5 m); 2A–C, *Dicarinella falsohelvetica* Desmares (2020), holotype (P6M4365); 3A–C, *Dicarinella marianosi* (Douglas, 1969), holotype (UCMP 49003 – CWRUH 013); 4A–C, *Dicarinella* cf. *primitiva*, sample PM+620 (12.2 m); 5A–C, *Dicarinella* cf. *primitiva*, sample PM+620 (12.2 m); 6A–C, *Marginotruncana caronae*, sample GC-540 (0.6 m); 7A–C, *Marginotruncana caronae*, sample WC+100 (14.9 m); 8A–C, *Marginotruncana caronae*, sample WC+1120 (25.1 m); 9A–C, *Marginotruncana* cf. *sigali*, sample GC-520 (0.8 m); 10A–C *Marginotruncana sigali* (Reichel, 1950), holotype.

Appendix A. Supplementary data. Semiquantitative abundances of the planktonic foraminiferal species identified at Eastbourne. Abbreviations: GC = Grey Chalk; PM = Plenus Marl; WC = White Chalk; VR = Very rare (1-2 specimens); R = rare (3-5 specimens); F = frequent (5-15% of the assemblage); C = common (15-30% of the assemblage); VC = very common (> 30% of the assemblage).

Highlights

- Extinctions and eclipses of certain taxa are synchronous at mid-low latitudes
- Extinction of *Thalmanninella* observed during a warming event at the onset of OAE 2
- Extinction of *Rotalipora* occurred within the Plenus Cold Event
- Eclipse of planispirals and pseudoclavihedbergellids follows increased fertility
- First evidence for a planktonic foraminiferal Plenus Cold Event fauna

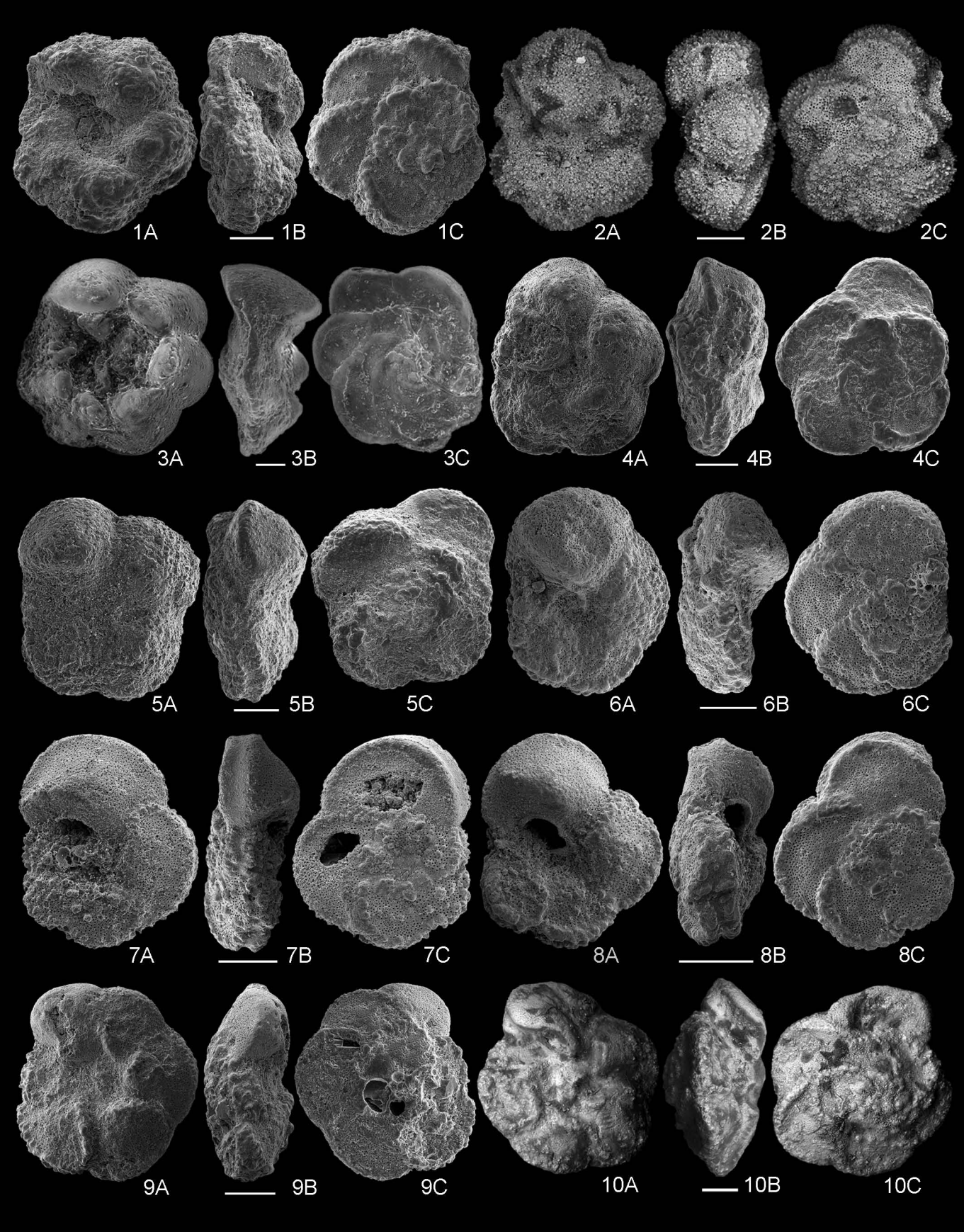
1A
1B
1C
2A
2B
2C
3A
3B
3C
4A
4B
4C
5A
5B
5C
6A
6B
6C
7A
7B
7C
8A
8B
8C
9A
9B
9C
10A
10B
10C

Fig. 1

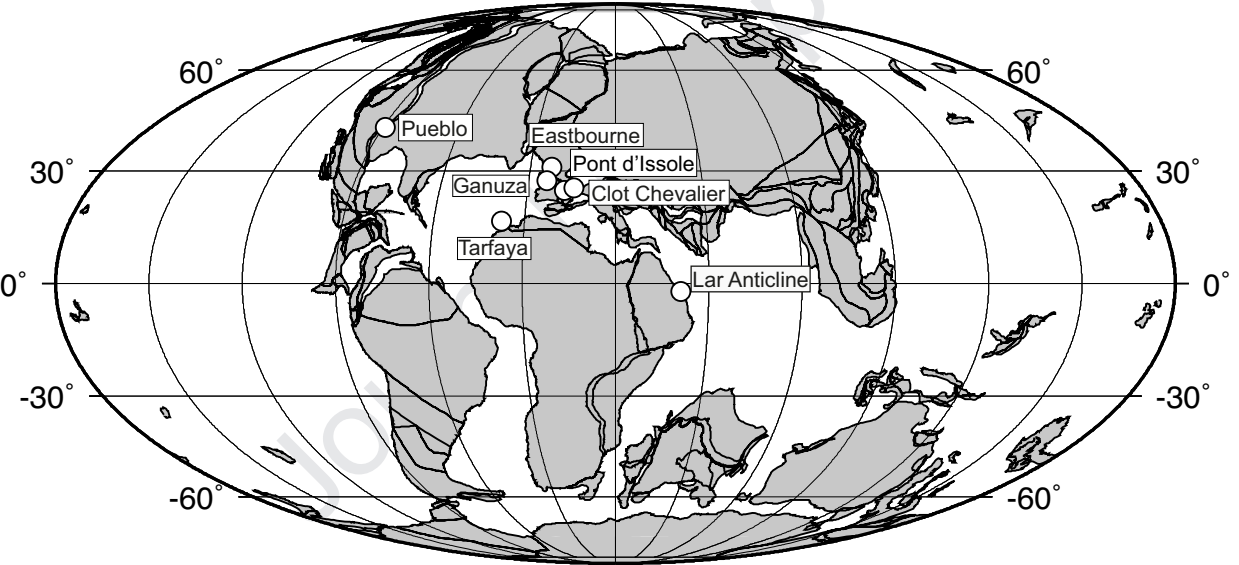
60°
60°
30°
30°
0°
0°
-30°
-30°
-60°
-60°
Pueblo
Eastbourne
Pont d'Issole
Ganuza
Clot Chevalier
Tarfaya
Lar Anticline

Fig. 2

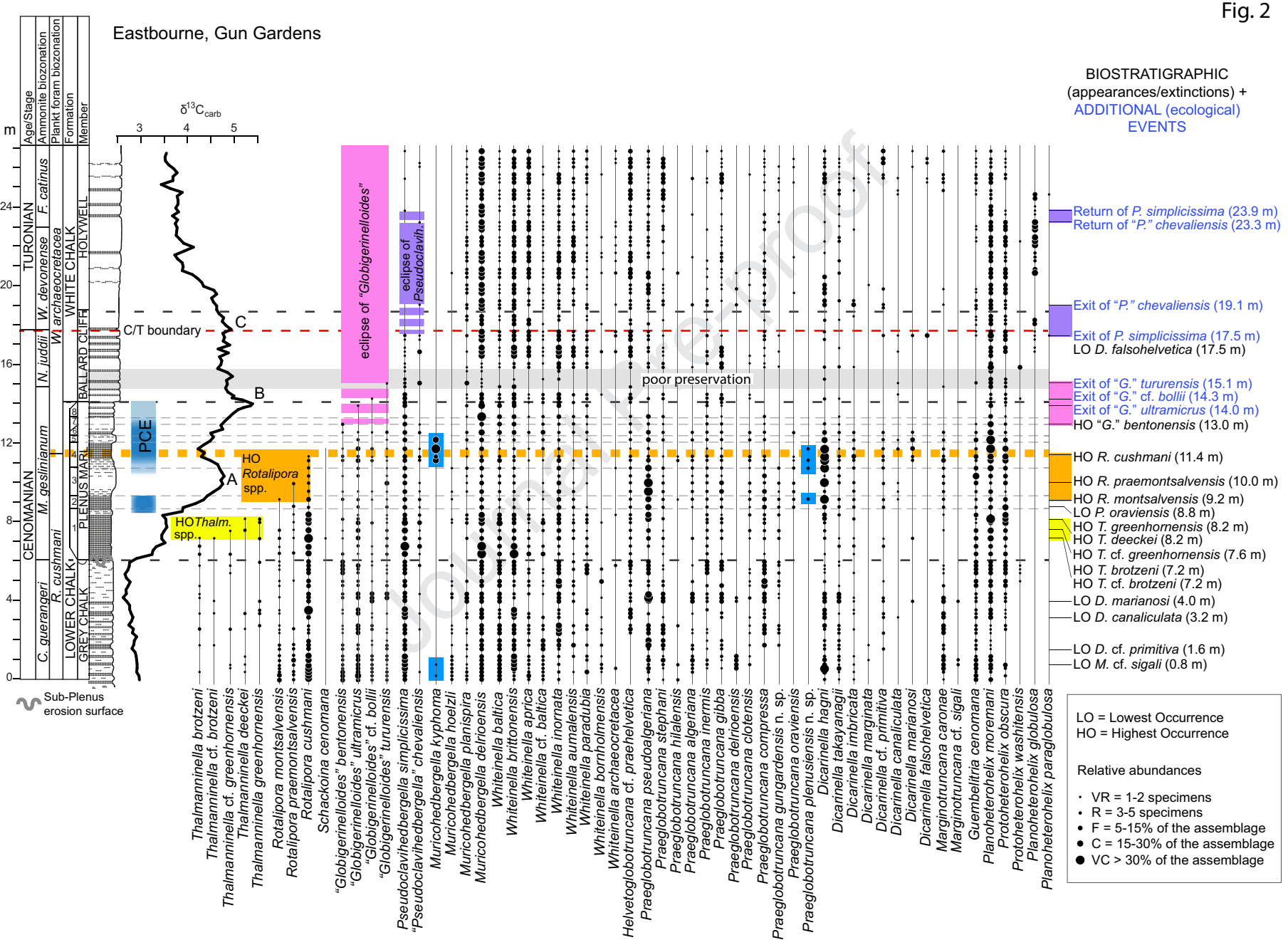

landscape -horizontal

Fig. 2

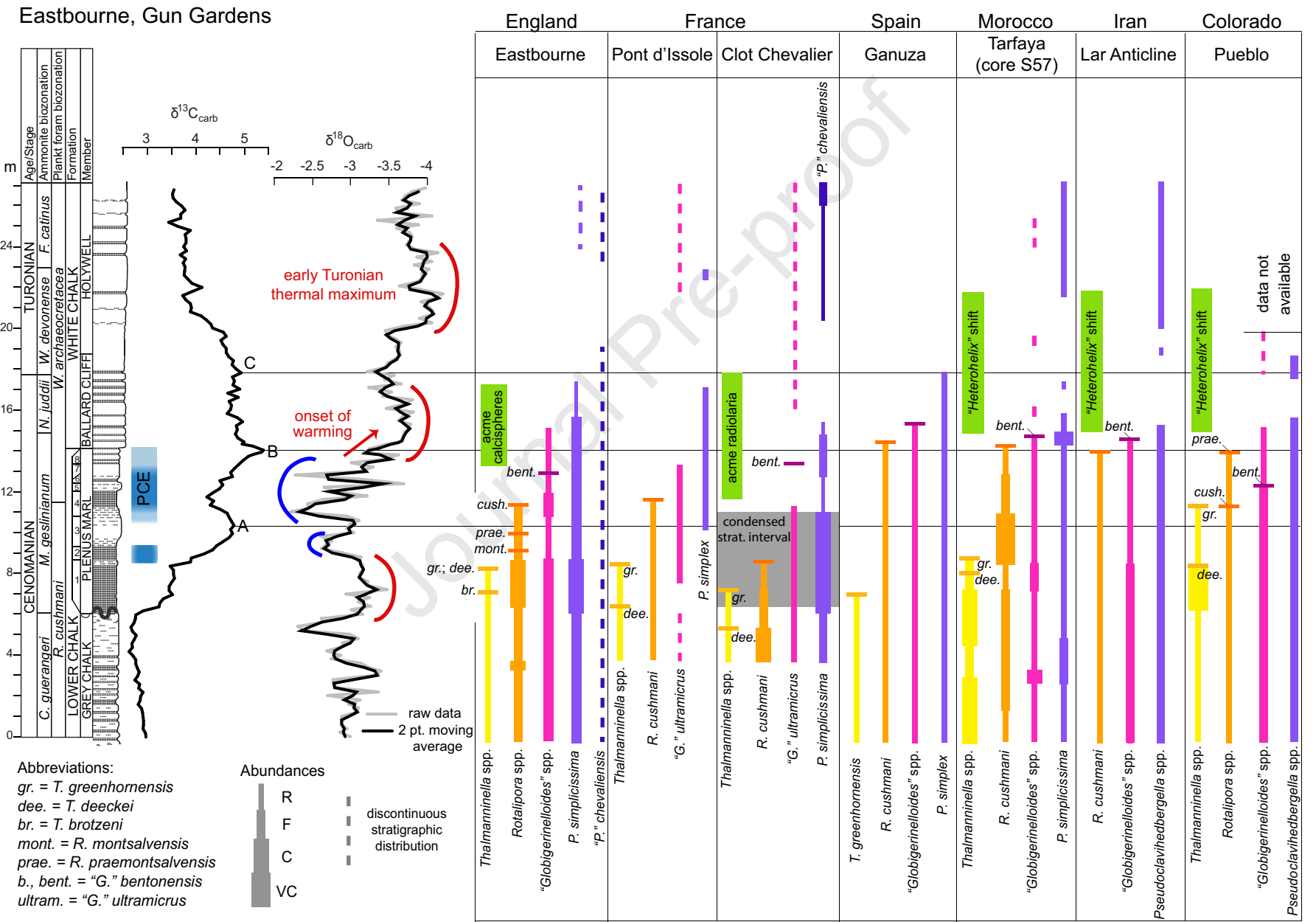

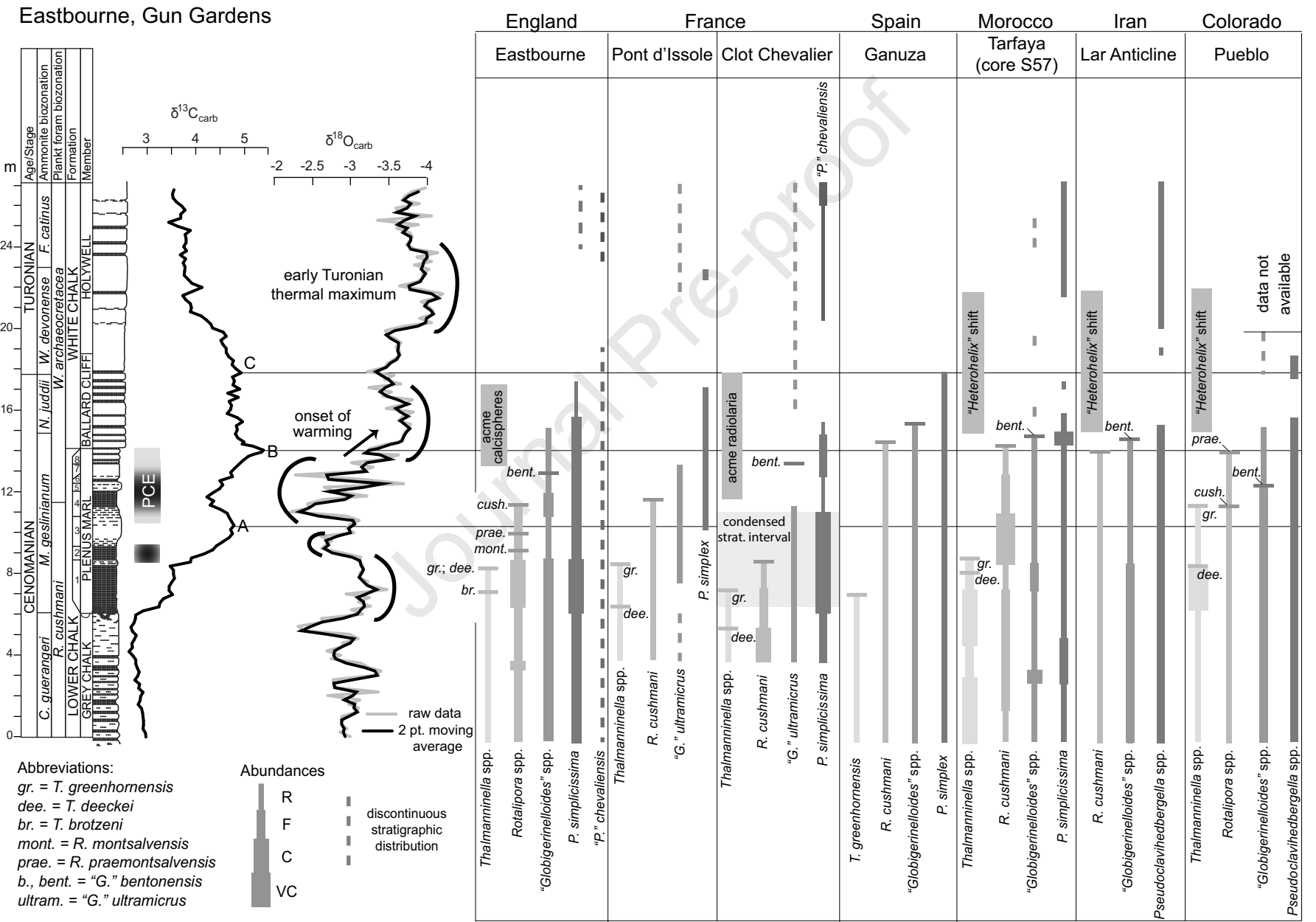

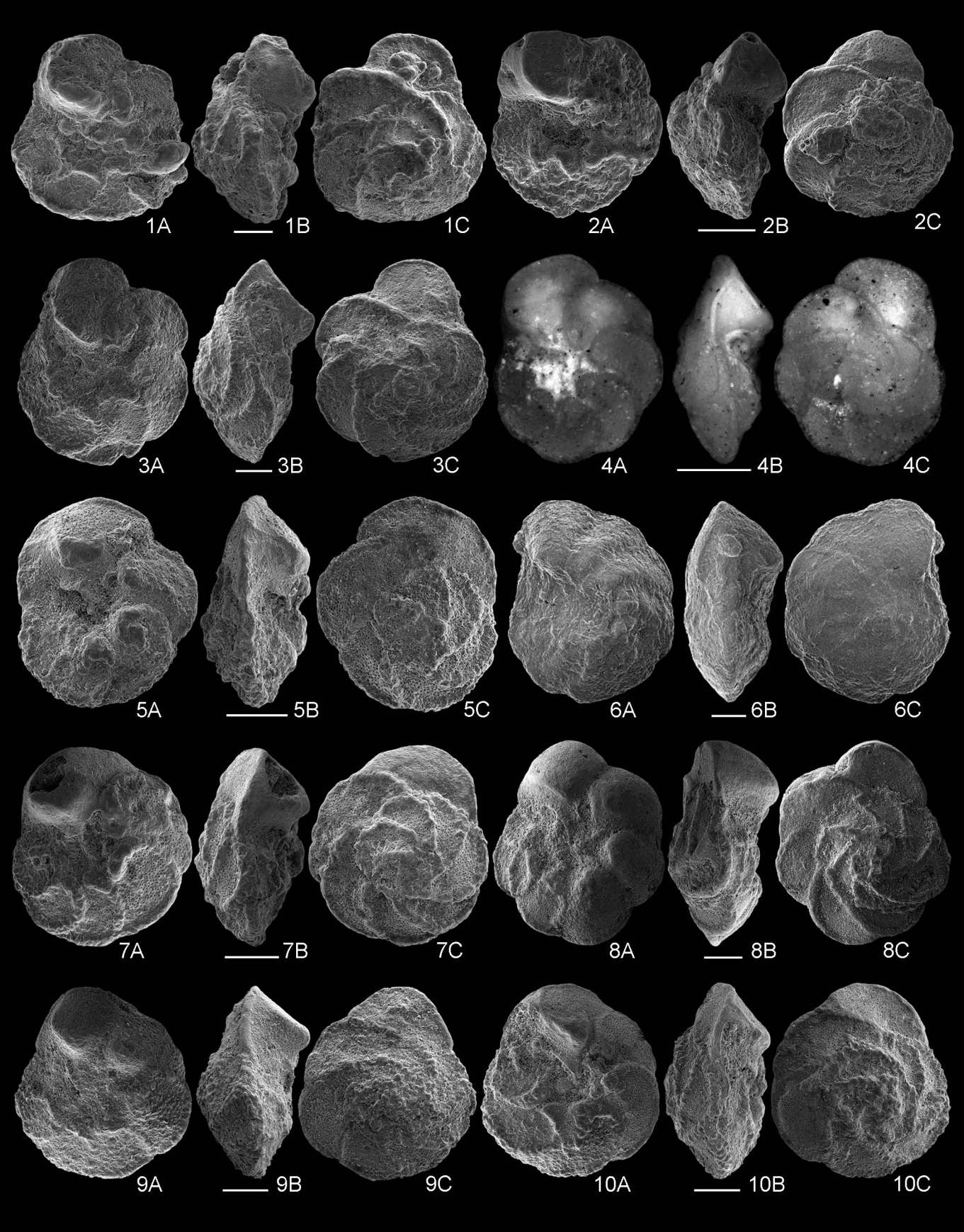
1A
1B
1C
2A
2B
2C
3A
3B
3C
4A
4B
4C
5A
5B
5C
6A
6B
6C
7A
7B
7C
8A
8B
8C
9A
9B
9C
10A
10B
10C

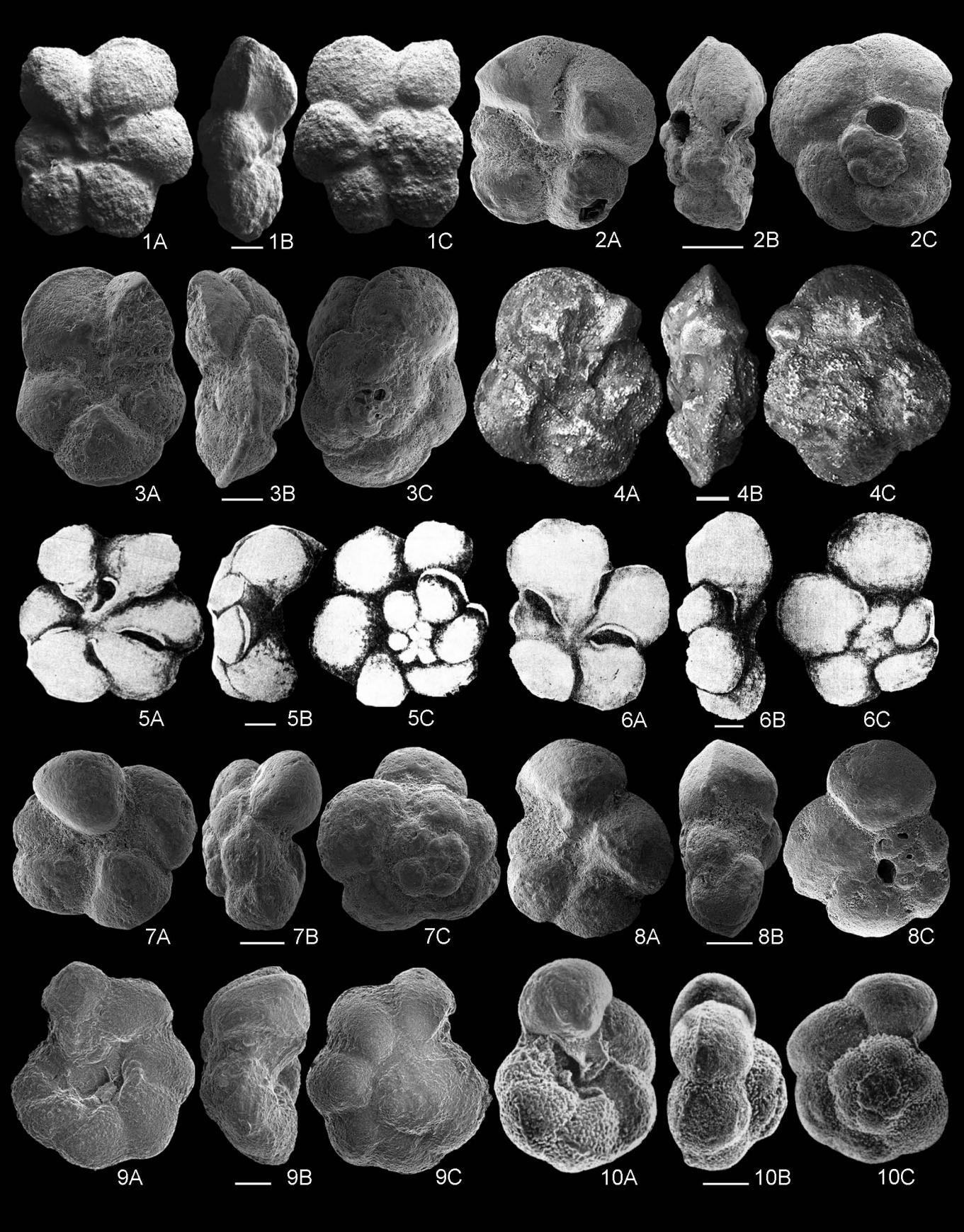
1A
1B
1C
2A
2B
2C
3A
3B
3C
4A
4B
4C
5A
5B
5C
6A
6B
6C
7A
7B
7C
8A
8B
8C
9A
9B
9C
10A
10B
10C

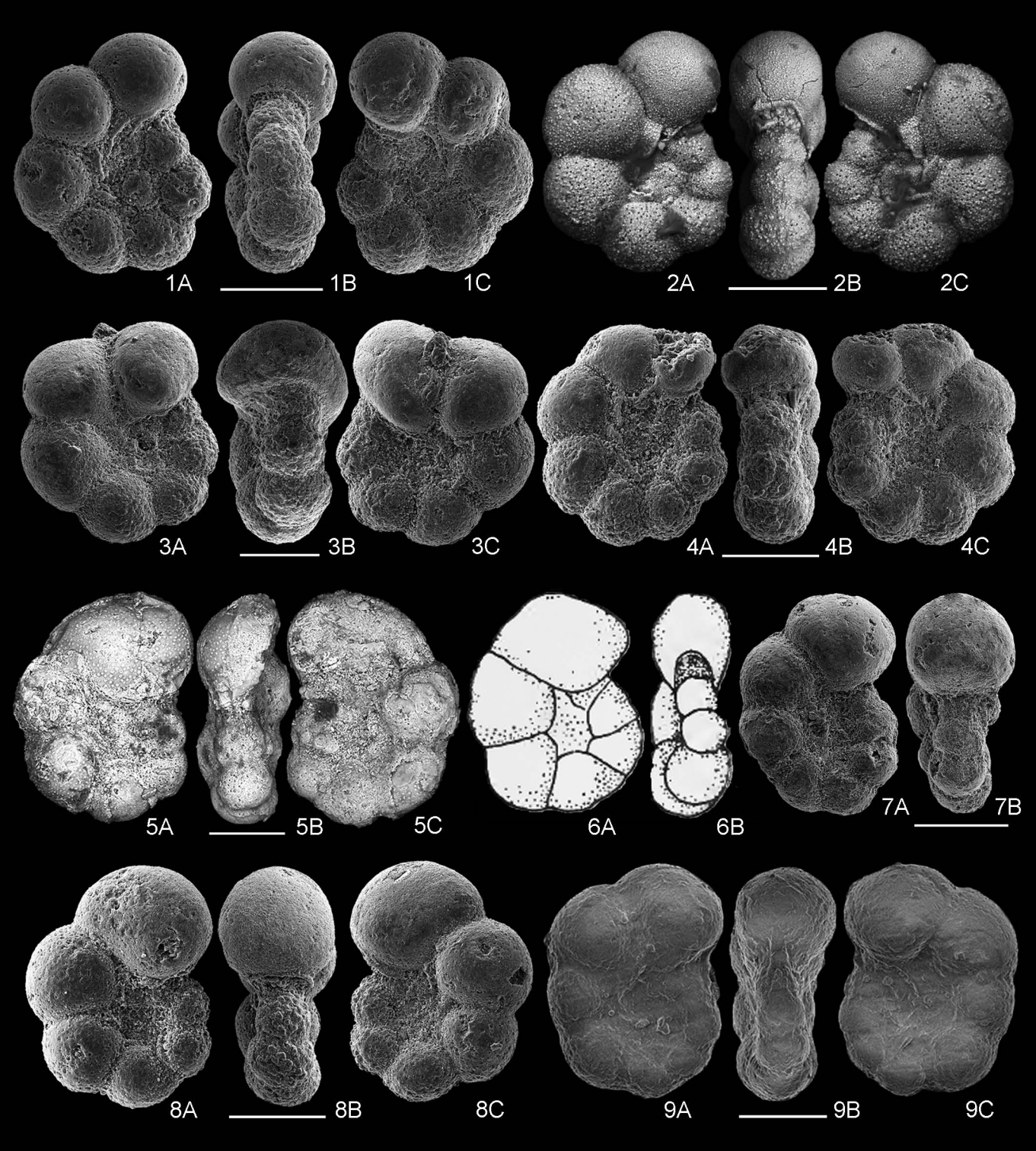
1A
1B
1C
2A
2B
2C
3A
3B
3C
4A
4B
4C
5A
5B
5C
6A
6B
7A
7B
8A
8B
8C
9A
9B
9C

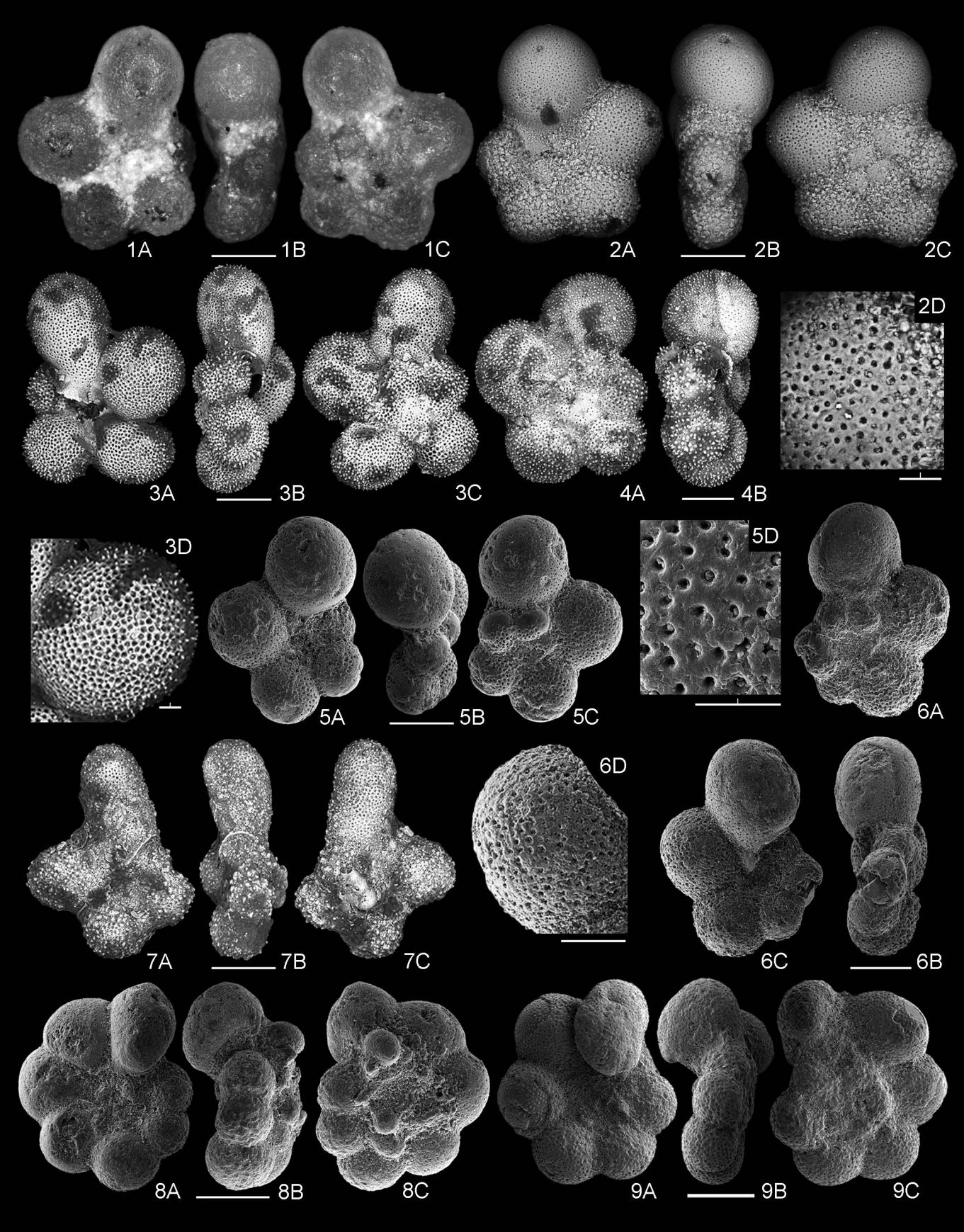
1A
1B
1C
2A
2B
2C
3A
3B
3C
4A
4B
2D
3D
5A
5B
5C
5D
6A
7A
7B
7C
6D
6C
6B
8A
8B
8C
9A
9B
9C

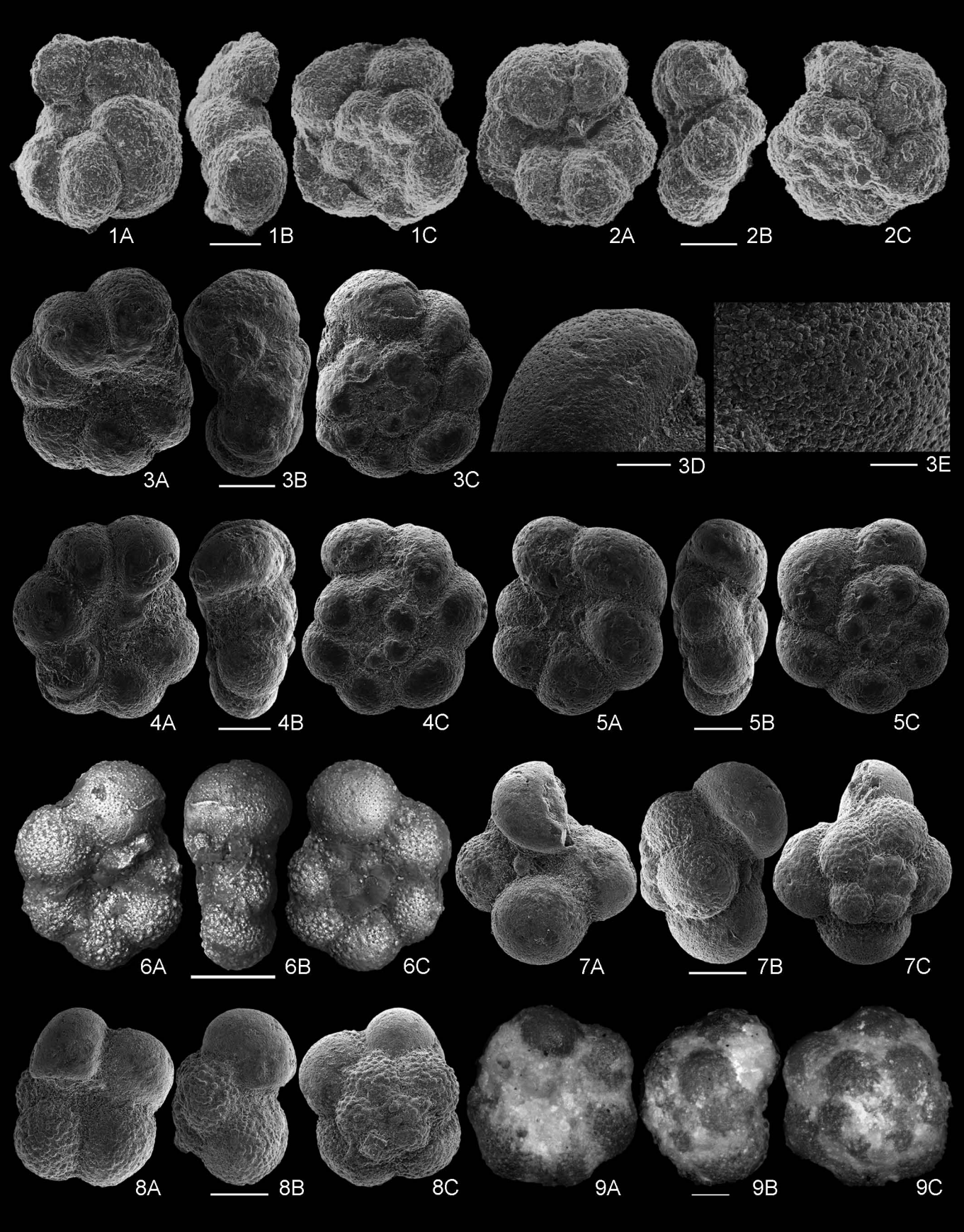
1A
1B
1C
2A
2B
2C
3A
3B
3C
3D
3E
4A
4B
4C
5A
5B
5C
6A
6B
6C
7A
7B
7C
8A
8B
8C
9A
9B
9C

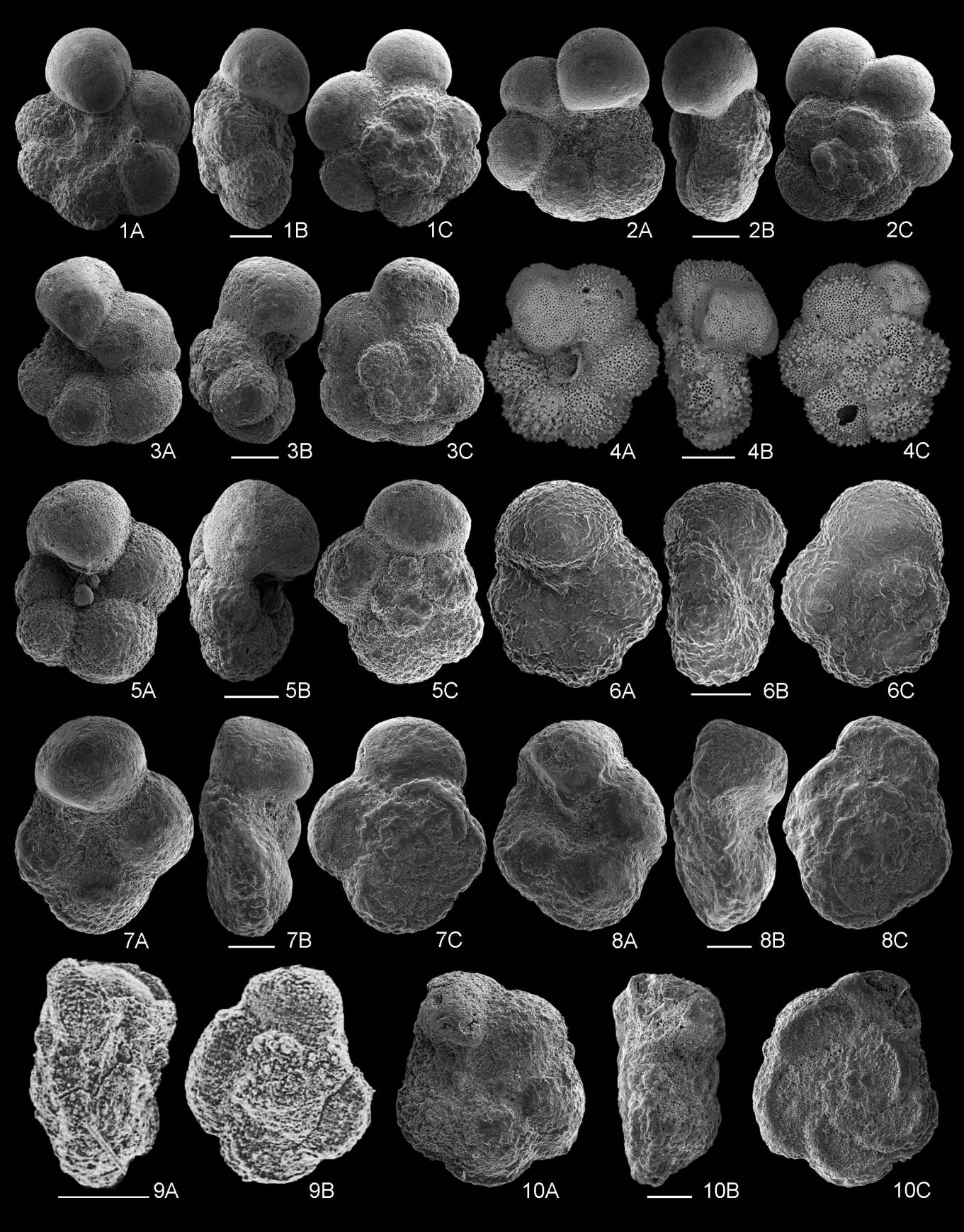
1A
1B
1C
2A
2B
2C
3A
3B
3C
4A
4B
4C
5A
5B
5C
6A
6B
6C
7A
7B
7C
8A
8B
8C
9A
9B
10A
10B
10C

All authors have contributed to the manuscript and have approved the final version of the manuscript.
Falzoni: Conceptualization, Methodology, Investigation, Writing - Original Draft, Writing - Review & Editing, Visualization.
Petrizzo: Supervision, Investigation, Writing - Review & Editing.

Declaration of interests

☐× The authors declare that they have no known competing financial interests or personal relationships that could have appeared to influence the work reported in this paper.

☐The authors declare the following financial interests/personal relationships which may be considered as potential competing interests: